Title

Bridging the Gap in Distributed Energy Resource Operations: Advancements in Tariff Designs and Load Optimization for Congestion Management

Author

Phanivong, Phillippe

Publication Date

2023

Peer reviewed|Thesis/dissertation

Bridging the Gap in Distributed Energy Resource Operations: Advancements in Tariff Designs and Load Optimization for Congestion Management

by

Phillippe K. Phanivong

A dissertation submitted in partial satisfaction of the

requirements for the degree of

Doctor of Philosophy

in

Energy and Resources

in the

Graduate Division

of the

University of California, Berkeley

Committee in charge:

Professor Duncan Callaway, Chair
Professor Dan Kammen
Alexandra von Meier

Summer 2023

Bridging the Gap in Distributed Energy Resource Operations: Advancements in Tariff Designs and Load Optimization for Congestion Management

Abstract

Bridging the Gap in Distributed Energy Resource Operations: Advancements in Tariff Designs and Load Optimization for Congestion Management

by

Phillippe K. Phanivong

Doctor of Philosophy in Energy and Resources

University of California, Berkeley

Professor Duncan Callaway, Chair

Customers are adopting new technologies, fundamentally changing their relationship with the electrical grid. These technologies, known as distributed energy resources (DERs), allow customers to control their consumption. They give customers the flexibility to purchase energy when prices are lower and sometimes sell electricity back to the grid when prices are high. While DERs can benefit the individual customer and potentially contribute to decarbonization, they also require electrical utility companies to change how they operate the grid, especially in the distribution system. This dissertation examines the relationship between DER operations and the electrical distribution system. We first explore how "business as usual" approaches to DERs could negatively impact the grid. Specifically, how current electricity tariffs provide an incentive structure for customers to optimize their DERs and how their optimized consumption could lead to congestion issues on the distribution system. Then, we explore data-driven tools for addressing this congestion. We collect data from simulated smart meters and develop a voltage estimator to manage congestion through a centralized optimized DER dispatch approach. Finally, we propose an electricity tariff design that provides the benefits of centralized congestion management, but instead through price signals sent to customers.

In Chapter 1, we explore the relationship between current electricity tariffs and future DER operations. We model commercial customers optimizing their electric vehicle (EV) charging under different Pacific Gas and Electric (PG&E) tariffs, including a new tariff (BEV tariff) with a novel subscription-based power charge. We model customers optimizing their load across different seasons to capture the prices in each tariff and compare the total annual costs. Once we calculate the optimal charging strategy for each customer, we model them in an open-source grid simulation software using a feeder model based on a PG&E distribution feeder, measuring voltage and wholesale energy costs. We find that undervoltage would occur in our distribution feeder under all four tariffs we examine. This result indicates that

current tariff designs are insufficient for congestion management, and additional measures are required. We also find that customers could see nearly a 15% reduction in costs by switching from one tariff to another. This cost savings for the customer is also reflected in a potentially problematic revenue gap for the utility when customers change tariffs. Finally, we show that subscription-based tariffs are less efficient than traditional demand charge-based tariffs, but the lower prices in the BEV tariff mask its inefficiency.

In Chapter 2, we explore ways to add a voltage constraint to the same EV charging coordination problem as Chapter 1 for distribution system operators (DSOs) to perform direct, centralized control of DERs. This chapter presents a novel three-phase data-driven linear voltage magnitude estimator based on past smart meter and substation data. This estimator is trained offline solely on data readily available for the distribution system operator and reduces the size of the voltage constraint by only estimating voltage at customer service connections. We show that our voltage estimator can prevent undervoltage in the EV charging coordination problem and is faster and more accurate than three-phase linearized voltage approximations, requiring less computational memory and no knowledge of the distribution system network connectivity.

In Chapter 3, we examine price-signal control methods for congestion management of DERs. We describe a new pricing scheme for day-ahead congestion management of DERs, referred to as Load Responsive Prices (LRPs). Using the LRP method, we can determine the optimal load profile of customers from offline analyses and then use day-ahead prices (potentially taken from the wholesale market) to calculate prices that customers can independently optimize for without additional communication from the DSO beyond the prices themselves. We find that customers optimizing using LRPs consume the same way as customers following direct load control methods but without knowing the load levels the system operator requires. We end the chapter with a discussion of various implementation considerations. We discuss ways to reduce customer cost increases, methods for addressing incorrect forecasts, and other important issues for practitioners.

We conclude with a summary of findings, policy recommendations, and future research directions.

Dedicated in memory of Sheila Warshaw, Ted Corley, Charles Wagner, Andrew Urbats, Richard Tillery, and Birdie Benator.

Contents

Contents **ii**

List of Figures **iv**

List of Tables **v**

Introduction **1**
Background and motivation 1
Purpose of this Research 3
Overview of Chapters 5

1 The impacts of retail tariff design on electric vehicle charging for commercial customers **8**
1.1 Introduction 8
1.2 Methodology 11
1.3 Results 20
1.4 Discussion 28
1.5 Conclusion 31

2 Data-Driven Linear Three-Phase Voltage Estimations for Optimal Electric Vehicle Charging Coordination **33**
2.1 Introduction 33
2.2 Preliminaries 35
2.3 Data-Driven Model 36
2.4 Case Study 43
2.5 Conclusion 46

3 Load-Responsive Pricing for Congestion Management in Day-Ahead Retail Energy Markets **48**
3.1 Introduction 48
3.2 Load Responsive Pricing 51
3.3 Optimal-α LRP 53
3.4 Inverse-Rank LRP 56

3.5 Case Study 58
3.6 Real-world Considerations 68
3.7 Conclusion 70

Conclusion **72**
Summary of findings 72
Policy recommendations 73
Areas for future research 74

Bibliography **76**

A Chapter 1 Retail Tariffs **88**

List of Figures

1.1 PG&E Summer Commercial TOU Hours 13
1.2 PG&E BEV Tariff TOU Hours for EVs 14
1.3 Distribution Feeder Model 19
1.4 Peak Load in July with B-10 Tariff 21
1.5 Typical Load in July with B-10 Tariff 22
1.6 Peak Load Day in May with B-10 Tariff 22
1.7 Load in July with B-19 Tariff 23
1.8 Load in July with BEV Tariff 25
1.9 Typical Load in July with TEST-EV Tariff 26

2.1 One-line diagram of the DistFlow equation variables 36
2.2 One-line diagram of IEEE-13 Node Test Feeder 38
2.3 Distribution of load hours for a single Mid-Sized House model 40
2.4 Data flows between feeder models 40

3.1 LRP price and cost curves 52
3.2 Constant α LRP 53
3.3 IR-LRP example 58
3.4 Load profile for Case Study I 62
3.5 Prices for Case Study I 63

List of Tables

1.1 Peak EV load with BEV and TEST-EV Tariffs 24
1.2 EV Customer Volumetric Costs 27
1.3 Distribution System Minimum Voltages 27
1.4 Total ACC Costs 28
1.5 Percent Savings From Switching Tariffs 29

2.1 Modifications to the IEEE 13 node load data for each node 39
2.2 Test Error and RMSE (per unit) for voltage magnitude of each load node 41
2.3 Number of non-zero coefficients per phase of voltage estimator 42
2.4 Distribution system voltage results 46
2.5 Cost results 46
2.6 Computation time 47

3.1 β_t values for Case Study I 59
3.2 IR-LRP values for Case Study I 60
3.3 Optimal-α values for Case Study I 61
3.4 IR-LRP τ_t and η values for Case Study II 66
3.5 Distribution system voltage results for Case Study II 67
3.6 Customer cost results for Case Study II 68
3.7 Percent difference between tariff costs in Case Study II 68

Acknowledgments

First and foremost, I would like to express my profound gratitude to Duncan Callaway, whose guidance, patience, and knowledge have been invaluable throughout this journey. Your unwavering commitment to academic rigor and relentless dedication to bettering my work have been instrumental in my development as a researcher. I also owe a great debt of thanks to Dan Kammen and Sascha von Meier. Dan, your constant reminders about the importance of equity in our discussions have become a foundational pillar of my research. Sascha, your insightful questions have always pushed me to delve deeper and consider problems from new angles. Working with each of you has been transformative, and I am a better researcher because of it.

In addition, I am grateful for many of the other faculty at UC Berkeley. Severin Borenstein, your course, advising, and guidance during my qualifying exam were indispensable. Steve Weissman, your course gave me insights into energy regulation that shaped my thinking on public policy. The ERG Core Faculty was also critical to my success. Each of you influenced my thinking; learning from you was a joy. I would also like to recognize the late Gene Rochlin. It is a surprise to no one who knew Gene, but he was right: Staring at a wall was a perfectly adequate research method (and sometimes the only one that would work).

My deepest gratitude extends to the Energy and Resources Group community, whose dedication to providing an enriching, supportive environment has been an integral part of my successful journey. I am grateful to staff members, past and present, who keep ERG working every day. Without you, no one in the department would be able to function. I cannot express my gratitude to my fellow students, especially the ERG 2016 cohort. Your camaraderie, resilience, and shared sense of purpose have been a source of constant motivation. To my dear friends Jose, Adam, Anna, Micah, Jessie, Valeri, Nancy, Rachel, Taryn, and Anna, your unwavering support and shared moments of laughter and frustration have made this journey enjoyable and manageable. Thank you for being there. My sincere appreciation also goes out to the EMAC research group. Your thought-provoking questions and constructive feedback have significantly contributed to my work and personal growth.

I would also like to thank Kevin Schneider, Mingxi Liu, and Antoine Lesage-Landry, whose expertise and advice were instrumental.

Last but certainly not least, I would like to express my utmost gratitude to my amazing partner, Tzipora, and my family. Your love, patience, and unwavering belief in me have been my bedrock during the highs and lows of this graduate school experience.

Finally, to anyone who has ever taken the time to commiserate with me over the trials and tribulations of grad school life or stare at an overhead power line with me, I am immensely thankful.

Introduction

Background and motivation

For most of the 141-year history of the U.S. electrical grid, customers purchased energy that was generated by large power plants and transmitted from vast distances to their homes and businesses [1]. However, a rise in new technologies has changed this paradigm in the past several decades. With energy storage systems, solar photovoltaics (PV), electric vehicles, and a host of "smart" devices, customers who were once *passive consumers* are becoming *active participants*, shifting their consumption patterns based on prices and sometimes selling electricity back into the grid. The technologies behind this change, known collectively as distributed energy resources (DERs), have the potential to provide substantial economic and environmental benefits, but they also can cause major disruptions to electricity service if mismanaged [2]. Importantly, this fundamental change in customer behavior impacts the distribution system—the last leg of the electric grid that supplies energy to the customer—more than any other section of the network.

The research presented here focuses on how regulators and distribution system operators should adapt in this evolving paradigm. The balance between costs and reliability prevents us from rebuilding the electric grid from the ground up for DERs, and instead, we must find ways to integrate them into our existing system. To make a high DER adoption future work, we must change how we operate the grid.

Distributed Energy Resources

The Federal Energy Regulatory Commission (FERC), in Order 2222, defines distributed energy resources as

> "'. . . any resource located on the distribution system, any subsystem thereof or behind a customer meter.' These resources may include, but are not limited to, resources that are in front of and behind the customer meter, electric storage resources, intermittent generation, distributed generation, demand response, energy efficiency, thermal storage, and electric vehicles and their supply equipment – as long as such a resource is 'located on the distribution system, any subsystem thereof or behind a customer meter.'" [3]

For an individual customer, installing DERs can bring benefits such as cost reductions in their utility bills, increased resilience during outages, and potential sources of income by selling energy back into the electric grid [4]. While at a societal level, aggregated DERs can participate in energy markets to reduce social costs and increase system resilience [5]. In addition, DERs can substantially contribute to decarbonization by electrifying carbon-intensive heating and transportation while also providing carbon-free energy to the electric grid from solar PV and small-scale wind [6]–[8]. U.S. lawmakers have prioritized electrification by investing billions of dollars into DER and electrification programs. Recent examples include $7.5 billion invested in electric vehicle charging stations in the Bipartisan Infrastructure Law of 2021 [9], and tax credits for electric vehicles and home energy storage systems in the Inflation Reduction Act of 2022 [10].

However, parts of the electric grid, specifically the distribution system, were not designed for the levels of DER adoption necessary for decarbonization. Large deployments of DERs can lead to grid congestion, requiring new approaches to power systems operations and regulation [11], [12]. While it is possible to overbuild the electrical distribution system to meet the peak demand of newly electrified loads and prevent negative consequences of DERs, controlling their real-time operation may be a lower-cost path to mitigate their negative impacts [13], [14]. An important area of research in this space is known as congestion management.

Congestion Management in the Distribution System

Distribution system congestion can occur when coincidental power consumption from multiple customers exceeds the system's peak capacity, and electricity service is affected. System congestion can lead to overcurrent conditions on distribution equipment, voltage excursions at the customer service connection, or excessive power losses for the utility. All three have been modeled or observed in the distribution system as a result of DER operations [15]–[19]. However, one area researchers have underexplored is the relationship between tariff designs and congestion. As more DERs come onto the grid and customers become more flexible with their consumption, they will have new optimization opportunities to minimize the costs associated with their electricity tariffs. Can customers cause congestion in the distribution system when minimizing their costs? We explore this question in Chapter 1 and show that current tariff designs (including tariffs with a price on peak consumption) are inadequate for preventing system congestion and undervoltage conditions.

Researchers are actively exploring several ways to address distribution system congestion from DERs. While distribution system operators (DSOs) can use devices such as capacitor banks and voltage regulators to adjust system conditions or sometimes reconfigure distribution feeders through switching schemes, the primary way to address congestion is to reduce load during times of peak coincidental consumption [20], [21]. DSOs can reduce load through direct load control measures or indirect approaches through monetary incentives and prices. Direct load control allows DSOs to determine how loads should operate and sends control signals to those loads. In contrast, indirect approaches send price signals to customers to

incentivize them to shift load. These indirect methods are popular in the U.S. because it leaves control decisions up to the customer and can incentivize market innovations. We examine the literature on direct load control in Chapter 2 and develop a method to reduce the data required for direct control of electric vehicles (EVs) in the EV charging coordination problem. While in Chapter 3, we review indirect load control and propose a pricing structure to address the same EV charging coordination problem.

Purpose of this Research

This dissertation examines the relationship between DER operations and the electrical distribution system. We first explore how "business as usual" approaches to DERs could negatively impact the grid. Specifically, we study how current electricity tariffs provide an incentive structure for customers to optimize their DERs and how their optimized consumption could lead to congestion issues on the distribution system. Then, we explore data-driven tools for addressing congestion in the distribution system. We collect data from simulated smart meters and develop a voltage estimator to manage congestion through a centralized optimized DER dispatch approach. Finally, we propose an electricity tariff design that provides the benefits of centralized congestion management, but instead through price signals sent to customers.

The overarching questions for this dissertation are:

1. How does the relationship between tariff designs and future DER operations impact customers, utilities, and the electrical distribution system?

2. How can we reduce congestion in the distribution system to increase the benefits from DERs?

To answer these questions, we integrate ideas and concepts from three separate areas of research: Power System Economics, Data Science and Statistical Methods for Power Systems, and Electrical Distribution System Engineering.

Significance of this Research

At its core, our work examines the intersection of policy and power system design to find the engineering and economic impacts when new technologies are adopted. This line of research is significant from both a practical and academic perspective. We examine how current DER operations and tariff designs can cause congestion issues for the electric grid and several ways to address these issues. From a practical perspective, we develop policy and engineering solutions for regulators and operators to implement without needing distribution system upgrades. We limit our algorithms to using only data available from existing sensors

and examine pricing structures that could be implemented with heuristics if more advanced forecasts are not possible.

From an academic perspective, this work contributes to several research areas. We show that the relationship between tariff design and DERs can have larger impacts on customers, the utility, and the electrical distribution system than previously studied. We also contribute to the literature on data science in power systems by showing how data collected only at metered locations can be used to estimate system conditions for DER optimization. Finally, we develop new ideas at the intersection of power system economics and control to incorporate distributed congestion management into dynamic prices.

Scope and Limitations

The scope of this research is the deployment and operations of DERs in the electrical distribution system in the United States. As such, the feeder models, load models, and tariff designs come from the U.S. and may not apply to power grids in other countries. Even in the U.S., utility companies custom-build distribution feeders for the locations they serve. Significant design differences exist from networked dense urban distribution systems to long radial systems used in rural communities. Thus, the specific congestion issues or remedies we show on one distribution feeder cannot apply to all. However, the analysis and algorithms we develop in this work can be used for most distribution feeders and adapted to support many more.

As for limitations, we approach the work presented in this dissertation through a modeled-based framework using models created by the research community. While experts in their respective fields meticulously built these models, each comes with its assumptions and simplifications compared to the real world. Importantly, we acknowledge that the results from the case studies in this dissertation are from modeled data and would differ from any results from studies reproducing this work in the real world.

In addition, the vast number of combinations of DERs, customer types, feeder models, and congestion issues necessitated that we limit our investigations to specific problem designs. We focused on the EV charging coordination problem for commercial customers and limited grid congestion to undervoltage conditions to allow for an in-depth analysis of DER operations and grid congestion. While several other negative conditions can arise from grid congestion, we found a gap in the literature around DER-related undervoltage. We hope to build on our results to address overcurrent and overvoltage conditions from DER-related congestion in the future.

Finally, a limitation that we do not address in this work is the issue of communication delays. We assume that data collected from all meters are synchronized. While this assumption is not realistic, it allowed us to explore the value of data-driven approaches and applications of smart meter data. Other researchers have explored methods to deal with communication delays in control algorithms in the distribution system [22]. Future work would be to integrate their approaches into the work presented here.

Overview of Chapters

Overview of Chapter 1

In Chapter 1, we explore the relationship between current electricity tariffs and future DER operations. Across the country today, commercial customers can often choose between different electricity tariffs based on their needs and preferences. With the mass adoption of DERs in the future, such as electric vehicles, commercial customers may also have better control over their consumption patterns. If customers can control their DERs to minimize costs, what current tariff designs would benefit them most? How would customer switching tariffs affect utility revenue, and would any of these tariff designs lead customers to cause congestion-related undervoltage in the distribution system?

To answer these questions, we modeled commercial customers optimizing their EV charging under different PG&E tariffs, including a new tariff designed specifically for commercial electric vehicle customers, the BEV tariff. This tariff uses a novel subscription-based power charge in its tariff design instead of the traditional demand charge used in other commercial tariffs [23]. To our knowledge, subscription power charges have never been used before for electricity tariffs.

We model customers optimizing their load across different seasons to capture the prices in each tariff and compare the total costs for a customer with a large fleet of electric vehicles and a smaller fleet. Once we calculate the optimal charging strategy for each customer, we model them in an open-source grid simulation software using a feeder model based on a PG&E distribution feeder, measuring voltage and wholesale energy costs.

This work addresses two gaps in the literature. First, it compares the economic value of a subscription-based tariff to standard commercial customer tariffs with demand charges for customers with flexible loads. Second, it compares the potential undervoltage effects on the distribution system and wholesale costs that arise from EVs following different retail tariffs as price signals. To our knowledge, neither of these issues has been examined in the literature before.

We find that undervoltage would occur in our distribution feeder under all four tariffs we examine. This result indicates that current tariff designs are insufficient for congestion management, and additional measures are required. We also find that customers could see nearly a 15% reduction in costs by switching from one tariff to another. This cost savings for the customer is also reflected in a potentially problematic revenue gap for the utility when customers switch tariffs. Finally, we show that subscription-based tariffs are less efficient than traditional demand charge-based tariffs, but the lower prices in the BEV tariff mask its inefficiency.

Overview of Chapter 2

In Chapter 2, we explore ways to add a voltage constraint to the same EV charging coordination problem as Chapter 1. While the retail tariffs used in Chapter 1 have demand

charges or a power subscription that limits peak consumption, in this chapter, we examine how customers would respond to an hourly energy price without a price on power. There is a growing interest in this type of pricing since it can better reflect wholesale energy costs [24], [25]. We use these costs to determine the optimal EV charging strategy for each customer taking into account system voltage.

In optimal powerflow analysis, voltage is a non-convex constraint and requires approximations or relaxations for efficient optimization. However, these techniques typically require complete knowledge of the distribution system connectivity or periodic test injections to measure the system conditions. This chapter presents a novel three-phase data-driven linear voltage magnitude estimator based on past smart meter and substation data. This estimator is trained offline solely on data readily available for the distribution system operator and reduces the size of the voltage constraint by only estimating voltage at customer service connections.

We train our estimator on data from a previous month without EVs and use it to predict voltage for a constraint in our EV charging coordination problem over a simulated month with potential undervoltage congestion. We then compare the performance results of our estimator to a standard linearized voltage approximation. We show that our voltage estimator and linear voltage approximations can prevent undervoltage in the EV charging coordination problem. However, when used in this optimization, our estimator is faster and more accurate than the linearized voltage approximation, requiring less computational memory and no knowledge of the distribution system network connectivity.

Overview of Chapter 3

In Chapter 2, we prevented undervoltage situations in the EV charging coordination problem with a centralized optimization. While effective, centralized optimizations require direct control methods for controlling DERs, and some customers do not want to give up control over their devices. In addition, direct control can interfere with the proper operation of energy markets if the system operator does not consider market prices. As an alternative, researchers have explored indirect methods to create price signals for DER control.

The most common approach researchers have used for creating indirect control price signals is to send a time-varying scalar \$/kWh energy price for customers each time period, often by calculating distribution level locational marginal prices (DLMP) or determined by transactive energy markets [24]–[26]. When optimizing load over a day, these scalar energy prices create linear cost curves for customers to optimize their costs. However, past research has shown that quadratic energy costs provide better results than linear energy costs since quadratic cost curves create one solution when optimized compared to multiple solutions with linear optimization [27]. A challenge with implementing this type of pricing is that in past research, quadratic costs were calculated based on system conditions either from a modified DLMP formulation or as part of a dynamic power tariff [27], [28]. These requirements prevented quadratic pricing from being implemented with other pricing schemes, such as real-time or day-ahead time-varying energy prices.

In Chapter 3, we describe a novel method for calculating quadratic costs and introduce a new pricing scheme for day-ahead congestion management of DERs, referred to as Load Responsive Prices (LRPs). This approach calculates the minimum required quadratic price for customers to optimize their load to match a desired load shape. Using the LRP method, we can determine the optimal load profile of customers from offline analyses and then use day-ahead prices (potentially taken from the wholesale market) to calculate LRPs. We also develop an effective heuristic for system operators to implement LRP without calculating optimal load profiles.

We find that customers optimizing using LRPs consume the same way as customers following direct load control methods but without knowing the load levels the system operator requires. We show this holds for both uni-directional and bi-directional DERs. In addition, we show that customer cost increases from using LRPs can be less than 5% compared to direct load control methods in our EV charging coordination problem. Finally, we end the chapter with a discussion of various implementation considerations. We discuss ways to reduce customer cost increases, methods for addressing incorrect forecasts, and other important issues for practitioners.

Chapter 1

The impacts of retail tariff design on electric vehicle charging for commercial customers

Power engineers have examined the potential impacts on the electric grid of high electric vehicle (EV) adoption, while energy economists have shown issues with modern electricity retail tariff design. However, little work has shown how customer decisions regarding their tariff and optimizing EV charging costs could affect the utility and the customer. If commercial customers can optimize their charging profile, how do different tariff structures affect local distribution system voltage, utility cost recovery, and customer bills? To answer this question, we model commercial customers optimizing their EV charging to minimize costs using real-world tariffs. Then, we model the voltage impacts of customers charging EVs on a realistic distribution feeder. Finally, we calculate the costs of EV charging for customers and the distribution utility. We find that current tariff designs do not support large-scale deployments of EVs without system upgrades or additional control measures. We also find that customers can reduce costs nearly 15% by switching retail tariffs, leading to a potential revenue gap for the utility. Finally, we show that new power subscription-based tariffs are less efficient than traditional demand charge-based tariffs, and instead, designing tariffs for load optimization can reduce costs for both the customer and the utility.

1.1 Introduction

There is a growing interest in the workplace charging of electric vehicles (EVs) [29]. For businesses with fleets of vehicles, this may become necessary with policy initiatives to reduce their carbon footprint [30]. For companies with employees commuting to work in light-duty vehicles, electric vehicle charging may become a service provided to employees [31]. For

ISO/RTOs curtailing excess renewables during working hours, daytime charging of electric vehicles is a possible approach to reduce curtailment [32]. Regardless of why commercial electricity customers choose to install electric vehicle charging stations, customers need to consider their electricity rates when building these charging stations.

Many retail tariffs for commercial customers charge a time-of-use (TOU) energy charge for electricity [33]. For larger customers, that tariff can also include a demand charge that captures the cost of peak power consumption [34]. With the addition of EV charging stations or electric vehicle supply equipment (EVSE) to a customer's site, a customer with many EVs may find their electricity bill is significantly higher or lower if they choose a different tariff than their current one [35]. In addition to standard commercial tariffs, some electricity retailers are now introducing EV-specific tariffs. One such tariff uses a subscription-based design instead of a demand charge[23].

In 2019, the California Public Utilities Commission CPUC approved Pacific Gas and Electric (PG&E) to enact a new electric vehicle charging rate [36]. This rate was specifically designed to support the goals of California Senate Bill 350, which "codifies PG&E's obligation to help California attain widespread transportation electrification" by creating a fuel-switching incentive for customers to switch from gasoline to electricity. The proposed rate design that PG&E put forward, the BEV tariff, was one with a single TOU hour schedule for all seasons of the year and a subscription plan for power consumption.

In the past, electrical utility companies have not used power subscription-based tariffs in retail electricity pricing. As such, there is little research on their effects in the electricity sector. However, there is growing interest in using subscription electricity tariffs due to the decrease in marginal costs from renewable resources [37], [38]. Based on the literature on subscription pricing in other industries, we know that these tariffs, sometimes referred to as three-part tariffs, generate more revenue for sellers than two-part tariffs for the same goods [39]–[42]. In the energy economics literature, there has been significant work on dynamic pricing and demand charges in electricity tariffs [43]–[48]. However, until recently, this work has not been connected to the power systems engineering work that examines the impacts on the electric grid of electric vehicle adoption [49]–[51]. With the advent of smart energy management systems and the load size that electric vehicles present, price-signal controlled charging of electric vehicles can cause concerns not seen with other types of load.

The most significant work on this issue comes from Powell et al. [52]. They analyzed the control strategies for EV charging at a commercial building under different retail tariffs and the effects those EVs have on the local transformer and customer bills. They found that when customers have a tariff that includes a price on power, such as a demand charge, the best strategy for transformer health is for customers to optimize their charging to minimize their own costs. In addition, Powell et al. is the only paper we know that modeled a power subscription-based tariff. In their paper, they compare a draft version of the same power subscription tariff that we examine in this chapter. They found that optimizing towards the subscription tariff produced a similar charging profile and transformer health outcomes to following a demand charge but with less of a response to the price on power since the subscription price was less than the demand charge.

While Powell et al. focused on local transformer loading and customer costs, we are unaware of any research on the impact of different EV electricity tariffs on distribution system voltage and utility company cost recovery. Since the synchronized responses of electric vehicles to time-varying prices may cause congestion, affect system-wide voltage and customer power quality [20], different price patterns can drive different voltage impacts. Additionally, because EV charging patterns are highly flexible and can be optimized against varying price signals, different time-varying tariffs could significantly impact utility revenue.

Furthermore, since Powell et al. published their work, TOU hours have been updated for the power subscription tariff and the demand charge-based tariff they used for comparison [36]. The new TOU hours align peak pricing hours to better reflect peak prices in the wholesale market in the region. The off-peak hours now coincide with high solar output in the middle of the day. These new TOU hours have a significant effect on the price-signal controlled workplace charging of electric vehicles because these vehicles will be able to charge during off-peak hours in the morning and early afternoon. While other researchers have examined these new TOU hours in the context of energy storage [53], [54], to our knowledge, no other research has investigated the impact of these new TOU hours on electric vehicle charging.

Researchers have also explored other tariff designs for smart EV charging [55]. However, this work focuses on transformer impacts from EV charging. Other recent work has examined the hosting capacity of distribution feeders for EVs and note voltage as a concern [56], [57]. However, this work does not examine the impacts of tariffs on EV charging behavior.

With the increase in EV adoption and smart charging, researchers need to better understand the relationship between electricity tariffs and impacts of optimized EV charging. We explore how current electricity tariffs provide an incentive structure for customers to optimize their DERs and how their optimized consumption could lead to congestion issues on the distribution system. In our work, we model multiple commercial customers that optimize their charging costs under different tariffs to determine the effects on customer costs, distribution system voltage, and utility company revenue. For our simulations, we use existing tariffs from Pacific Gas and Electric (PG&E) that a commercial customer could choose between today. We optimize each customer's EV load to minimize their costs and use these load profiles with modeled customer data for a realistic distribution feeder to measure the impact on system voltage and the costs to the utility to supply the EVs with energy. We show that the relationship between tariff design and DERs can have larger impacts on customers, the utility, and the electrical distribution system than previously studied.

The three main contributions of this work are

1. We find that none of the commercial retail tariff designs we investigate prevent undervoltage or support large-scale deployments of price signal-controlled electric vehicles without upgrading the distribution system or additional control measures.

2. We also find that customers can see a nearly 15% reduction in costs by switching from

one existing tariff to another, leading to a potential revenue gap for the utility.

3. Finally, we show that new power subscription-based tariffs are less efficient than traditional demand charge-based tariffs, and instead, designing tariffs for load optimization can reduce costs for both the customer and the utility.

The issues we study in this paper are relevant across many utilities. However because tariff designs and distribution systems are strongly heterogeneous, we take a case study approach, and generalize where appropriate. At the highest level, this paper provides generalizable knowledge by (1) developing a framework for examining engineering and economic impacts of different tariff designs in a system with significant EV loading and (2) highlighting potential opportunities and challenges that should be considered in EV tariff design in any context.

The organization of the rest of this chapter is as follows: The Methods section outlines our analytical approach and describes the simulation models used for EVs, tariffs, buildings, and the distribution feeder. Then in the results section we report our numerical results, we first report the voltage effects of EV charging on the distribution system, followed by the revenue to the utility company and the costs to individual commercial customers for optimizing their charging for each tariff option. In the discussion section we analyze the implications of our results and their potential policy impacts. Finally, we conclude with a section summarizing our results and the policy implications of this work for rate-making and electric vehicle charging policy.

1.2 Methodology

We used a three-step analysis approach to determine the effects of different retail tariffs on the customer, the utility company, and the electrical distribution system. First, we solved a cost-minimizing electric vehicle charging optimization problem for each retail tariff over a billing month, assuming EV charging control and full knowledge of daily loading. We solved this problem for three different months in the year, one in each of the retail pricing seasons. Next, we extracted the EV charging profiles from the output of the optimization problem and added them as loads in a distribution system feeder model for a time-series powerflow analysis. In that analysis, we measured local voltages at each building location and total feeder loading for every hour of the month. Finally, we used the total feeder loading from the powerflow analysis to calculate the utility's costs for the EV load. Each step of this analysis is explained further in the following subsections.

Retail Tariffs

In this study, we modeled the following PG&E commercial tariffs: B-10 [58], B-19 [59], and BEV [23]. Commercial customers in PG&E's territory with up to 499 kW peak usage can select the B-10 or B-19 tariff as their electricity tariff regardless of whether they have

electric vehicles. In addition, commercial customers with electric vehicles can instead choose the BEV tariff for EV charging at their location. However, they must separately meter their EVs to use the BEV tariff and still use the B-10 or B-19 tariff for their other loads. Therefore, we modeled BEV customers with a B-10 tariff for their building loads and the BEV tariff for their EVs. In addition to the above tariffs, we created a fourth tariff model, the TEST-EV tariff. This tariff uses the prices and TOU hours of the BEV tariff but the power pricing structure of the B-10 tariff. The rest of this subsection describes the structure of each tariff we modeled in more detail. See the Appendix for the dollar amounts used for each price in the tariffs.

The retail tariffs in this work use volumetric energy and volumetric power costs in their total monthly cost calculations. However, each retail tariff uses different prices or pricing structures for the energy and power components. The literature on electric utility tariffs interchangeably uses "parts" or "components" to describe these costs [60], [61]. However, we strictly use the term "component" to differentiate between energy and power costs in a tariff. In contrast, we use "parts" to describe the pricing structure for each component (e.g., the energy component of a tariff can have a fixed cost "part" and a volumetric cost "part"). We use this language to align our terminology with the broader economics literature on pricing structures for analysis of the subscription pricing model of the BEV tariff [39]. Since the fixed costs are the same for the tariffs we examined, we describe but exclude the fixed costs from our models to simplify calculations. Additionally, we only model the standard secondary connection prices for each tariff. We do not model other PG&E specific programs such as Peak Day Pricing, standby charges, or power factor correction. In the following, we first describe the energy component in detail and then address the power component of each tariff.

For the energy component, each tariff uses a two-part tariff design. In a two-part tariff design, the first part is a fixed cost and the second part is a volumetric cost based on the units of consumption. For the energy component, these volumetric costs are priced in $/kWh. In addition, these tariffs use time-of-use (TOU) hours for the volumetric energy prices. These hours are specific time intervals in which energy is cheaper or more expensive on a given day. Each electricity retailer sets its TOU hours, which typically reflect average wholesale energy costs at different times of the day.

The B-10 and B-19 tariffs use the same three-season TOU hour schedule, while the BEV tariff uses a single schedule year-round. Each schedule has up to three different pricing periods for a given day. For the Summer TOU hours, there are "Peak," "Partial Peak," and "Off-Peak" hours (Figure 1.1). For the Spring TOU hours, there are "Peak," "Off-Peak," and "Super Off-Peak" hours (Figure 1.2). The BEV tariff uses the same hours as the Spring TOU schedule, but the BEV tariff hours apply all year. In addition, the Winter TOU hours are the same as the Spring TOU schedule but without a "Super Off-Peak" period. Each of these periods has different volumetric energy consumption charges, with "Peak" being the most expensive and "Super Off-Peak" being the least.

For the power component of the retail tariffs, the B-10 and B-19 tariffs again use two-part tariff designs, where the volumetric costs are known as demand charges with pricing

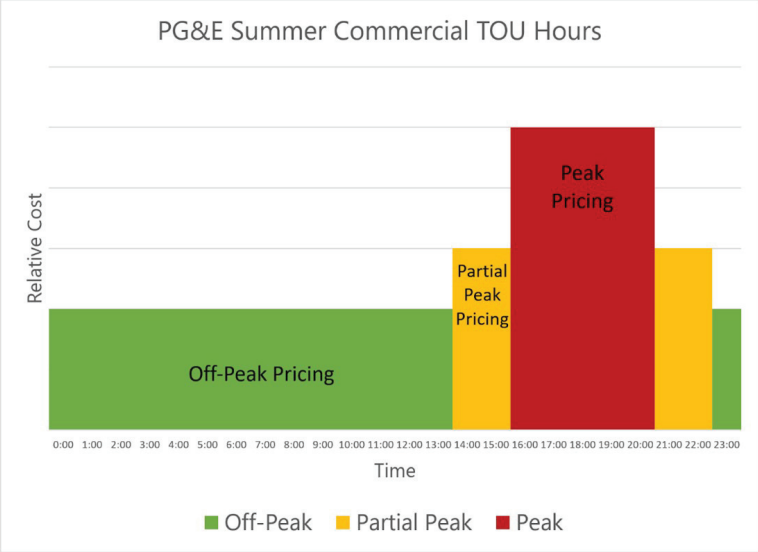

Figure 1.1: The relative costs of energy in different TOU periods for PG&E's Summer Commercial Customer Hours. Note: The relative pricing levels shown here are only relative to other TOU periods in this figure; they are not relative to the prices in Figure 2.

in \$/kW. The B-10 tariff uses a fixed-level demand charge, in which a customer is charged for their peak power consumption in a billing cycle. In contrast, the B-19 tariff has time-differentiated demand charges instead of a fixed-level demand charge. These are a set of multiple demand charges calculated for the maximum power consumption during different intervals related to the TOU periods. In the B-19 tariff, a customer sees a separate demand charge for their maximum power consumption in the "Peak" TOU period, their maximum power consumption during "Partial Peak", and a demand charge for the overall maximum power consumption at any time in the billing period. This last demand charge may be for the same period as the "Peak" or "Partial Peak" demand charge if the overall maximum power consumption occurs during one of these TOU periods. For billing periods in months where there is no "Partial Peak" TOU period, only the "Peak" and overall maximum power consumption are billed. In practice, PG&E calculates the power used in demand charges by averaging measured power over 15-minute periods. However, due to the hourly load profiles of our data, we modeled all demand charges on an hourly time scale in our analysis.

Representative equations for the B-10 tariff and the B-19 tariff are provided below. In Equation (1.1) the fixed costs are the non-volumetric components of each tariff. Equation (1.2) represents the tariff volumetric energy costs, with x_t representing power consumed at time t in each of the different TOU time periods $p_,p_2, p_3$ and TOU is the energy price for the respective periods. While the structure is the same for both tariffs, the specific prices differ, with the B-10 tariff having higher energy prices than the B-19 tariff. Equation (1.3) represents the different demand charge formulations for B-10 and B-19. DC is the demand

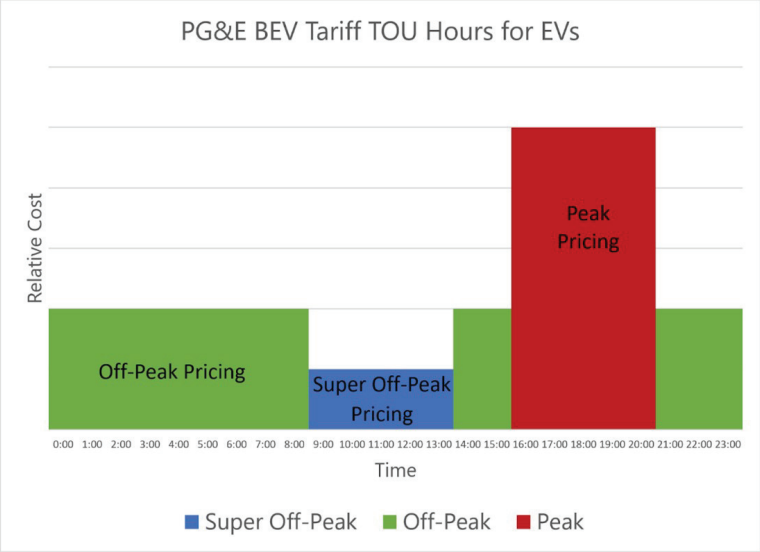

Figure 1.2: The relative costs of energy in different TOU periods for PG&E's Spring Commercial Customer Hours and BEV Tariff Hours. The Winter Commercial Customer TOU schedule is the same but without the Super Off-Peak period. Note: The relative pricing levels shown here are only relative to other TOU periods in this figure; they are not relative to the prices in Figure 1.

charge price for either the time period (B-19) or overall (B-10). X_{t_1} represent the set of power consumed at each hour in the first TOU period used in the tariff for a given season. $[X_{t_1}, X_{t_2}, X_{t_3}]$ represent the combined set of power consumed at each hour in all of the TOU periods used in the tariff for a given season. The sum of Equations (1.2)-1.3 creates the total monthly cost for a commercial customer, Equation (1.4).

$$C_1 = \text{Fixed Costs} \tag{1.1}$$

$$C_2 = \sum_{t_1 \in p_1} TOU_{p_1} \cdot x_{t_1} + \sum_{t_2 \in p_2} TOU_{p_2} \cdot x_{t_2} + \sum_{t_3 \in p_3} TOU_{p_3} \cdot x_{t_3} \tag{1.2}$$

$$C_3 = \begin{cases} DC \cdot \max x_t \in [X_{t_1}, X_{t_2}, X_{t_3}], & \text{if tariff} = \text{B10} \\ DC_1 \cdot \max x_{t_1} \in X_{t_1} & \\ \quad + DC_2 \cdot \max x_{t_2} \in X_{t_2} & \text{if tariff} = \text{B19.} \\ \quad + DC_3 \cdot \max x_{t_3} \in [X_{t_1}, X_{t_2}, X_{t_3}], & \end{cases} \tag{1.3}$$

$$\text{Total Monthly Cost}_{\text{B10 or B19}} = C_1 + C_2 + C_3 \tag{1.4}$$

In the BEV tariff, the power cost is designed as a subscription plan for EV charging. The customer chooses a subscription level for the peak power their EV charging will consume in

a given month, similar to the monthly allowances in American cell phone minute plans of the 1990s and early 2000s. In the BEV subscription, customers buy their expected power in 10kW blocks for a smaller EV charging load (BEV-1) or 50kW blocks for a larger EV charging load (BEV-2). Customers pay the price of the blocks purchased regardless of the amount of power EVs consumed in that billing period. At the end of the billing period, the maximum EV power used is compared to the subscription level chosen by the customer. If the customer's maximum EV power is higher than the total power they bought in the subscription blocks, they are charged a volumetric overage fee. This overage fee can be seen functionally as a very high fixed-level demand charge for EV power that exceeded their subscription level. If the customer's maximum EV power consumption is less than or equal to the subscription blocks they purchased, then they do not pay any additional fees. The BEV tariff's subscription mechanism is an example of a three-part tariff design. Lambrecht et al. state that a "three-part tariff is defined by an access price, an allowance, and a marginal price for any usage in excess of the allowance" [39]. The allowance level separates a three-part tariff from a two-part tariff that has an access fee (fixed costs) and a marginal price (volumetric cost) [62].

Comparing the BEV tariff to the B-10 or B-19 tariff, the BEV tariff has a significantly lower equivalent demand charge, even if the consumer faces an overage fee. However, while the B-10 and B-19 tariffs calculate costs based on measured consumption, the customer is expected to estimate their load to select a subscription level when using the BEV tariff. To separate the effects of this lower equivalent demand charge and the new pricing mechanism of subscriptions, we created the artificial TEST-EV tariff. The TEST-EV tariff is identical to the BEV tariff except for how the power costs are calculated. Instead of a subscription, the TEST-EV rate uses a \$/kW equivalent demand charge derived from the subscription prices in the BEV tariff. See the Appendix for the dollar values of the BEV and TEST-EV tariff.

Representative equations for the BEV and TEST-EV tariff are below in (1.5)-(1.9). $\hat{x}_t$ represents power consumed by EVs at time t in the set of power consumption values over the different EV TOU periods $\hat{p}_1, \hat{p}_2, \hat{p}_3$. TOU is the Time-of-Use energy price, Φ is the subscription rate cost, β is the size of the block for the subscription, and γ is the number of blocks a customer purchased for their subscription. If a customer's power exceeds their selected subscription level, then they are charged for the excess energy at the overage rate cost, Θ. Equation (1.7) represents the different power components formulations for the BEV and TEST-EV tariff. In addition to the EV tariff costs, the total monthly cost for a customer would include their building loads. Equation (1.9) represents this for a customer using the BEV or TEST-EV tariff and model this as the B-10 tariff for the building loads.

$$C_1 = \text{Fixed Costs for EVs} \tag{1.5}$$

$$C_2 = \sum_{t_1 \in \hat{p}_1} TOU_{\hat{p}_1} \cdot \hat{x}_{t_1} + \sum_{t_2 \in \hat{p}_2} TOU_{\hat{p}_2} \cdot \hat{x}_{t_2} + \sum_{t_3 \in \hat{p}_3} TOU_{\hat{p}_3} \cdot \hat{x}_{t_3} \tag{1.6}$$

$$C_3 = \begin{cases} \Theta \cdot \max\left(\max \hat{x}_t \in [\hat{X}_{t_1}, \hat{X}_{t_2}, \hat{X}_{t_3}] - \gamma\beta, 0\right) & \\ \quad + \Phi\gamma\beta, & \text{if tariff = BEV} \\ DC_{\text{EV}} \cdot \max \hat{x}_t \in [\hat{X}_{t_1}, \hat{X}_{t_2}, \hat{X}_{t_3}], & \text{if tariff = TEST-EV.} \end{cases} \tag{1.7}$$

$$C_4 = \text{Fixed Costs for non-EVs loads} \tag{1.8}$$

$$\text{Total Monthly Cost}_{\text{BEV or TEST-EV}} = C_1 + C_2 + C_3 + C_4 \tag{1.9}$$

Building Models

To model the building loads at each EV charging location, we used commercial and industrial building models from the Department of Energy's Commercial Reference Building models [63]. We selected two prototypical commercial buildings as EV site hosts: the medium-sized office building model and the warehouse model. We assumed nearly full electrification of transportation at each site, motivated by the announced phaseout of gas powered vehicles in California [64]. Each building model provided hourly electric load profiles that responded to changes in modeled temperature and occupancy [65].

The warehouse building model represents a 52,045 sq. ft, single-floor industrial building with charging hours from 8 am to 5 pm, and a max non-EV load of 82 kW. We modeled each warehouse with a fleet of 10 EVs to model a small fleet of delivery vehicles. Although delivery vehicles are typically active during the day, advocates in the postal industry are exploring night-time deliveries [66]. In addition, the BEV tariff incentivizes customers to charge during the day-time Super Off-Peak Period. We modeled the BEV tariff at the warehouse buildings as BEV-1, with 10kW block size increments in the subscription.

The medium-sized office building model represents a 53,628 sq. ft, three-story office building with charging hours from 7 am to 8 pm, and a max non-EV load of 238 kW. While this charging window is large, we selected it maximize load flexibility while reflecting the occupancy of the DOE Commercial Reference Buildings. We modeled each medium-sized office building with 250 EVs to model a full parking lot of employee vehicles. We modeled the BEV tariff at the medium-sized office buildings as BEV-2S, a building with a secondary distribution connection and 50kW block size increments in the subscription.

EV Models

We modeled each EV as a stationary load during charging hours with a maximum charging rate of 7.2 kW. We also modeled each EV to require 20 kWh of daily energy. This energy is equivalent to 1/3 of a full charge of a 60kWh battery on a light-duty vehicle or 1/9 of a full charge for a medium-duty electric vehicle [67], [68]. We assumed this amount of energy as an extreme case in which vehicles only charge at each workplace and EV owners do not charge their vehicle at home or other locations. We modeled all EVs to be connected to EVSEs and assumed they could charge at any point the optimization dispatched them.

Electric vehicle charging optimization problem

To measure the potential impacts of controlled electric vehicle charging, we developed a linear programming model to minimize the cost of charging a fleet or collection of electric vehicles at customer locations (1.10). $f\left(\hat{x}(t), x(t)\right)$ is a time-varying cost function over time $t = 1{:}24\,\text{hours}$, where equations (1.5)-(1.9) were used to model each of the different tariffs. $\hat{x}(t)$ are the EV loads and $x(t)$ are the non-controllable building loads.

The mathematical program minimizes the total cost to the customer for their building loads and the charging of all the electric vehicles at the customer's site. In our analysis, we only optimized the EV charging; the building loads were treated as exogenous to the optimization and only included because several retail tariffs use a customer's combined maximum power consumption to calculate the demand charge component of the tariff.

$$
\begin{aligned}
\min_{\hat{x}} \text{Cost} = & \sum_{t=1}^{24 \text{ hours}} f(\hat{x}(t), x(t)) \qquad (1.10)\\
s.t. \quad & (\hat{x}(t) + x(t)) \leq \text{Local loading limit} \\
& \hat{x}(t) \leq \text{EV operating constraints} \\
& \sum_{t=1}^{24\text{hrs}} \hat{x}(t) = \text{charging energy required for} \\
& \qquad\qquad\qquad \text{EVs at the building}
\end{aligned}
$$

We ran the optimization daily for each retail tariff, keeping the constraints the same but using the objective function in each case to reflect the cost components of the tariffs. For tariffs with a demand charge, we communicated peak load values across subsequent days in the month for the optimization to consider the potential increase in monthly demand charge. For the BEV tariff, ran the optimization twice over the month to calculate optimal subscription levels. Since the subscription levels are discrete blocks, we first determined the optimal subscriptions by formulating the problem as a mixed-integer linear program. Then we re-ran the optimization as a linear program with the maximum subscription level calculated from the mix-integer linear program.

We modeled each customer site to schedule EV charging at the building with perfect daily foresight of total EV energy required but we assume no knowledge of demand on future days. While perfect daily foresight is a strong assumption, we used it to keep the problem a tractable linear program and provide a lower bound on the costs following each price signal.

We performed this analysis over the simulated months of May, July, and December. We selected these months to capture the costs from following the TOU hours of the three different seasonal periods PG&E uses. Each month is the same number of days in length and does not include daylight-savings time shifts.

Electrical distribution system powerflow analysis

Once we solved the dispatch problem for the retail rates as price signals, we extracted the hourly charging profiles for each EV and used them as additional loads in an electrical distribution time series powerflow analysis. We performed two different analyses from this. First, we determined the effects of the optimized charging profiles on the local electrical distribution system voltage. ANSI C84.1 requires customers on the distribution system to receive a normalized voltage of 1.05 to 0.95 of the expected system voltage [69]. We measured voltage at all customer locations to determine if and when voltage was outside of the ANSI limits. For this analysis, we only examined the distribution system impacts in July because it had the highest demand from other loads and put the feeder most at risk for undervoltage. For the second analysis, we measure the losses in the distribution system to capture the full amount of energy required to charge the EVs bulk power grid. We applied this analysis for all three months we simulated.

Grid Model

For the powerflow analysis, we modeled a single electrical distribution system feeder in Gridlab-D [70]. We modified a three-phase, unbalanced feeder model created by PG&E to model an existing 12.47 kV urban distribution feeder in the inland area Northern California [71]. The feeder is 17 miles long, with overhead and underground power lines supplying 2,894 residential customers, 270 commercial customers, and 91 industrial customers (Fig. 1.3). To provide load diversity, we modified the feeder model to incorporate 10 different building models from the Department of Energy's Commercial Reference Building models and Building America House Simulation Protocols for the residential building models [63], [72]. We modeled all 91 industrial customers on the feeder as warehouse buildings and five of the commercial customers as medium-sized office buildings. The feeder originally was modeled with a single large solar resource that we disaggregated into distributed solar at customer locations to more accurately represent the solar resources on the grid. For ambient temperature and solar insolation, we modeled building and solar PV models using TMY3 climate data for the Sacramento Area [73]. We modeled a total of 2,160 EVs on the distribution feeder, 10 EV at each of the 91 warehouses and 250 EVs at each of the 5 office buildings, for a combined load of 43.2 MWh per day or 1.34 GWh per month. We assumed the EV load was balanced across all three phases at each building. In addition, we increased the size of the capacitor banks to correct for the new load models and replaced the originally incorrectly modeled underground line models with 15kV concentric neutral underground line models from the IEEE 13-node feeder [74]. Before running our powerflow analysis, we also verified that the feeder could support charging the total number of EVs we modeled without voltage constraint violations.

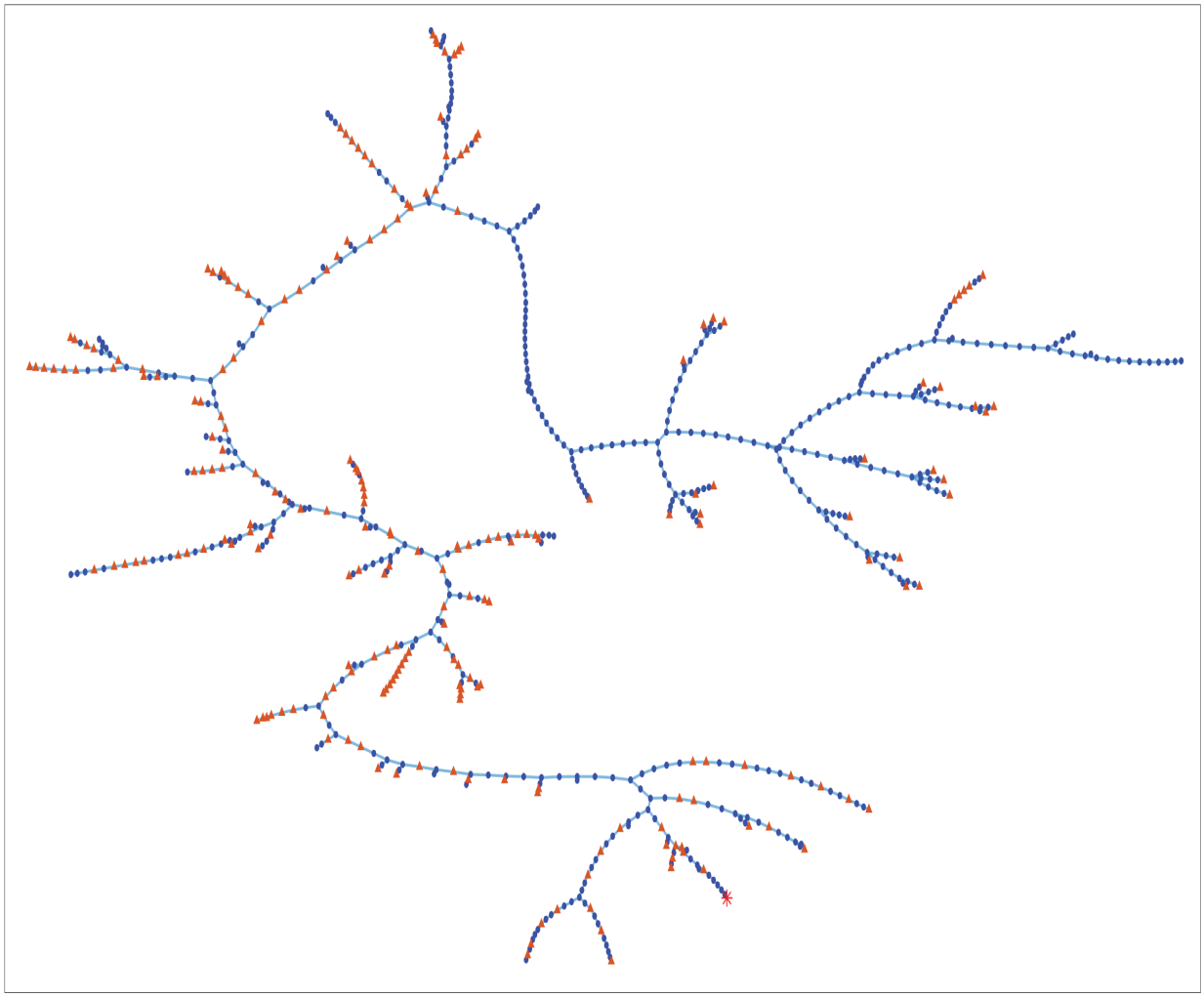

Figure 1.3: Graph representation of the distribution feeder model with 678 nodes in a force-directed layout (identified as Feeder D0001 in [71]). The red star indicates the distribution substation and orange triangles are the 221 load locations identified in the original feeder model.

Wholesale cost calculations

Once we completed the powerflow analysis with the additional EV loading, we used the measured loading at the feeder substation to calculate the wholesale cost of providing energy to the entire distribution feeder. We measured this cost for the feeder with and without the modeled buildings and EVs to determine losses from charging the vehicles and measure the additional power needed from the transmission system to supply the EVs under different charging strategies. We assumed any changes in loading on the distribution system feeder were too small to affect the wholesale price.

For wholesale prices, we use hourly electricity prices from the Avoided Cost Calculator [75]. This calculator, developed by the energy consulting firm E3, is used by the California Public Utilities Commission to determine the benefit of distributed energy resources [76]. The ACC calculates the avoided cost of energy for every hour of the year by modeling the combined costs of wholesale energy, system capacity, and environmental damages from greenhouse gases. The ACC is updated yearly and projects costs for 30 years into the future.

Specifically, we use the 2022 ACC electricity prices for the PG&E climate area 12 in the year 2023. We selected this climate area after discussions with PG&E modelers about ideal locations to model their electric distribution feeder model. See the Grid Model subsection for more details on this distribution feeder model. In addition, we selected 2023 for pricing data to match the days of the week and the calendar of our building model data.

Computation

All calculations and simulations were performed on an AMD Ryzen 7 3700X desktop PC with 64GB of RAM, running Windows 10. Linear programs were solved in MATLAB R2020a [77] using YALMIP [78] with Gurobi [79] as the solver. Distribution system powerflow simulations were modeled in Gridlab-D [70].

1.3 Results

EV optimization load results

We first examined the EV load profiles from the optimizations. We found that Warehouse and Medium Office customers both optimize their EV charging in a similar manner to minimize costs for the month. When optimizing under a tariff with a demand charge, such as the B-10, the demand charges are much larger than TOU energy charges. As a result, the optimal load profile for customers is to maximize EV charging at all hours up to the peak load level of the month. This creates a flat load profile for the customer on the peak energy-consuming day of the month (Fig. 1.4). However, to simulate the uncertainty of building loads, we assumed the customer would not know what this peak level was or when it would occur. As such, the customer would optimize each day, determining their demand charge as the maximum of the peak loading and the peak loading of all previous days that month. This

resulted in the customer resetting their peak load level throughout the month. In days after the peak load day, customers will consume each hour up to the load level set by the demand charge and avoid peak TOU hours if possible (Fig. 1.5). Customer load shapes showed the same behavior over July and December. However, the temperature increased throughout May, with peak loading occurring on May 30th (Fig. 1.6). Since our customers did not have a prediction of their peak load, they would optimize throughout the month with only the peak they had already experienced. This results in customers flattening their load to peak load levels below the peak they are paying for by the end of the month. Customers in this situation pay more in TOU energy charges in the first 29 days of the month compared to a customer that would know their peak.

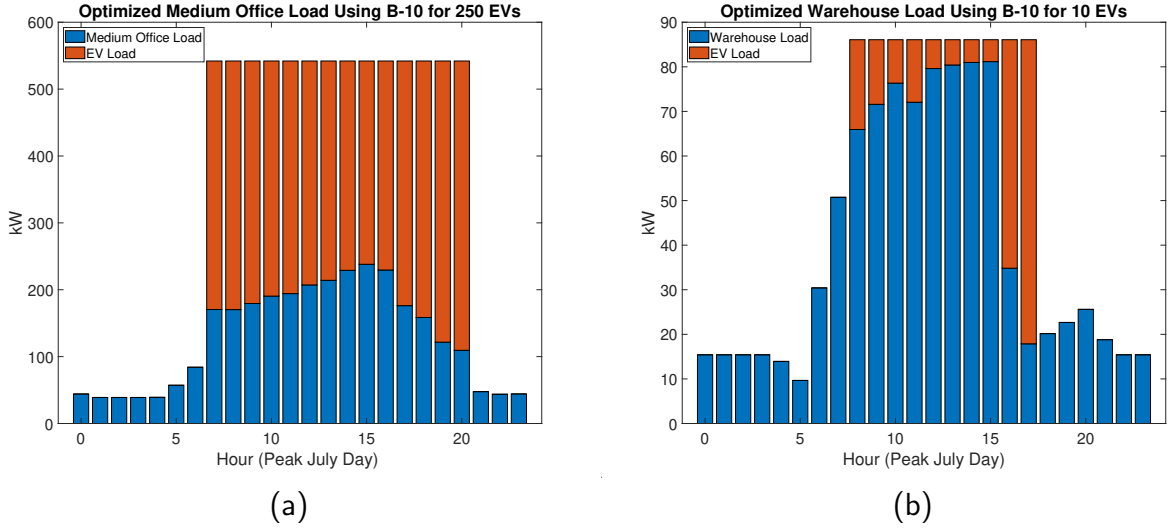

Figure 1.4: The optimized hourly load profile of customers when optimizing under the B-10 tariff on the maximum load day of the month. (a) Medium Office Customer in July (b) Warehouse Customer in July

Unlike the B-10 tariff, the B-19 tariff has time-differentiated demand charges. When a customer optimizes load under this tariff, the customer follows similar demand charge behavior as B-10 but will have two separate flat load levels in the Summer, one for Summer Peak periods and one for Summer Off-Peak/Partial Peak periods (Fig. 1.7). The customer will not optimize for the the Summer Partial Peak demand charge because it is significantly smaller than the Summer Max demand charge. Similarly, in Winter or Spring months, customers optimizing their load under the B-19 tariff will ignore the Winter Peak demand charge because the Winter Max demand charge is greater than ten times the cost. Customers also ignored the TOU costs for the Winter Super Off-Peak Period to create a flat load profile across all TOU hours within the EV charging window.

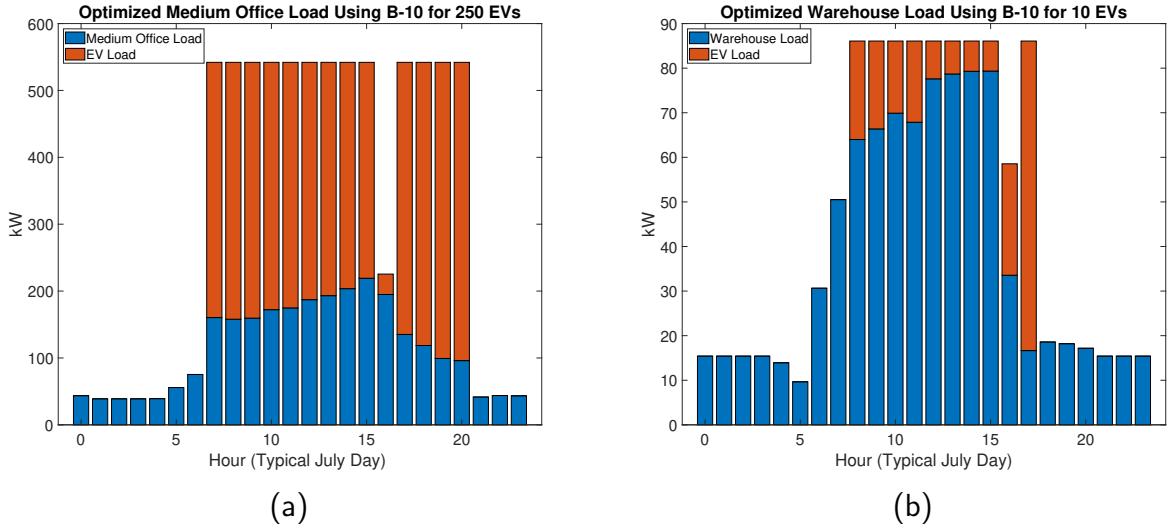

Figure 1.5: The optimized hourly load profile of customers when optimizing under the B-10 tariff on a typical load day of the month. (a) Medium Office Customer in July (b) Warehouse Customer in July

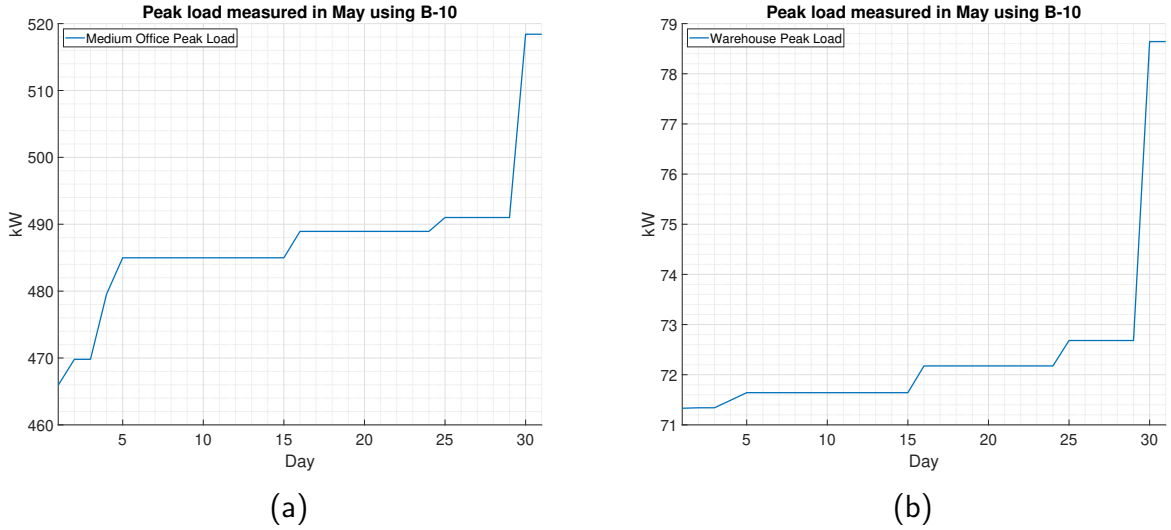

Figure 1.6: The Peak load measured at each (a) Medium Office Customer and (b) Warehouse Customer throughout May used for determining demand charge costs. The maximum load hour would not occur until May 30th.

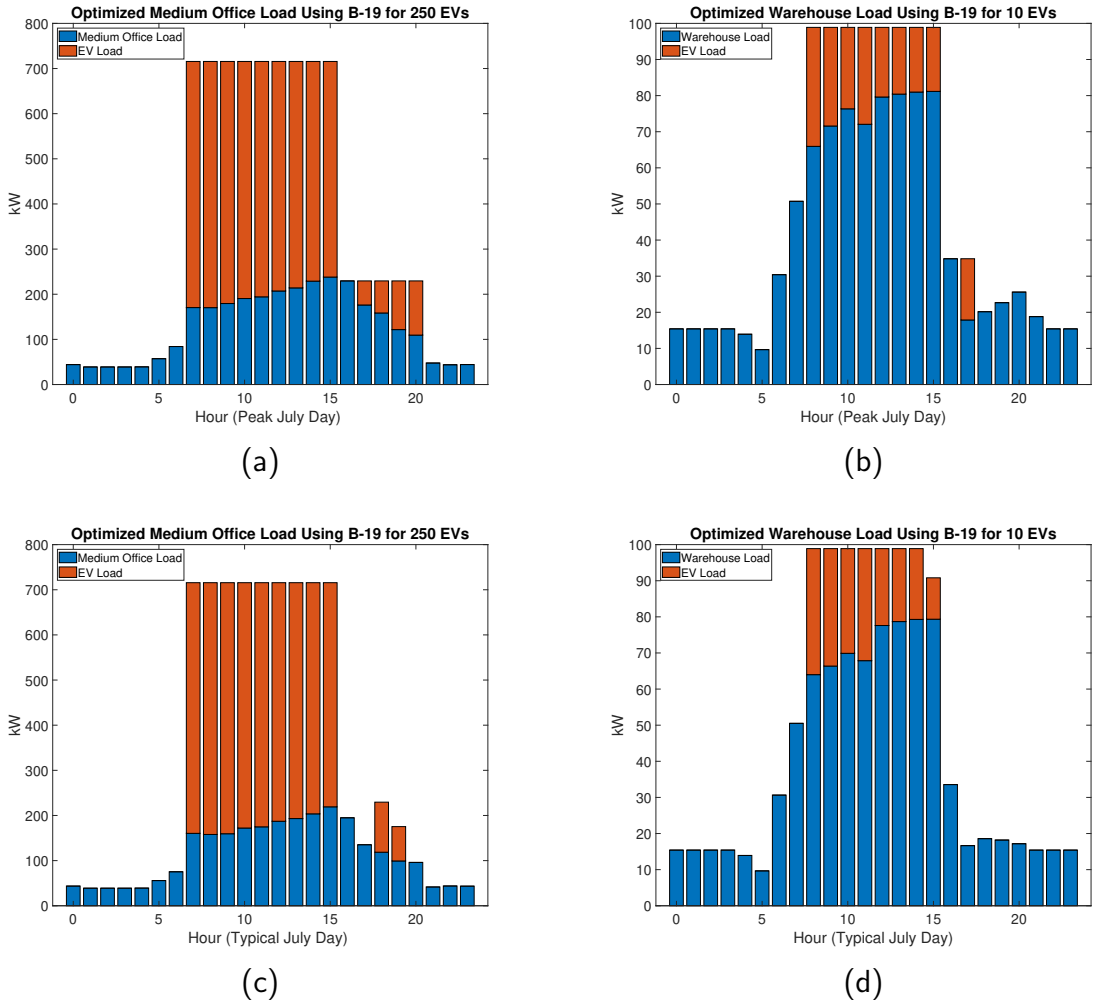

Figure 1.7: The optimized hourly load profile of the (a) Medium Office Customer and (b) Warehouse Customer on the peak load day in July under the B-19 tariff. The load profiles for the same (c) Medium Office Customer and (d) Warehouse Customer on a typical load day in July under the B-19 tariff. Unlike the B-10 tariff, the time-differentiated demand charges in the B-19 tariff limited EV load in Off-Peak and Partial Peak hours separately.

Customers optimizing for the BEV tariff also primarily optimized for the power costs based on their subscription level (Fig. 1.8). However, the BEV tariff is only for the electric vehicles at each customer location. As such, the BEV tariff has an identical load profile for each day of the month and a similar load profile for all three months in this test. The May and December load profiles for the Medium Office customer are slightly different than the July load profile due to both being valid optimal solutions to the problems. As seen in the next section, the costs were the same for customers for all three months.

Customers optimizing for the TEST-EV tariff showed a similar load behavior to the BEV tariff (Fig. 1.9). However, level under the TEST-EV tariff was determined by the power consumed by the customer instead of a block subscription program, the customer was able to save money by increasing their power consumption to reduce consumption during the Peak TOU hours (Table 1.1). EV load profile results were identical across all three months we tested.

Table 1.1: The optimized peak load for each building type under the BEV and TEST-EV Tariffs

Tariff	Peak Medium Office EV Loading	Peak Warehouse EV Loading
BEV	550 kW	20 kW
TEST-EV	555.6 kW	25 kW

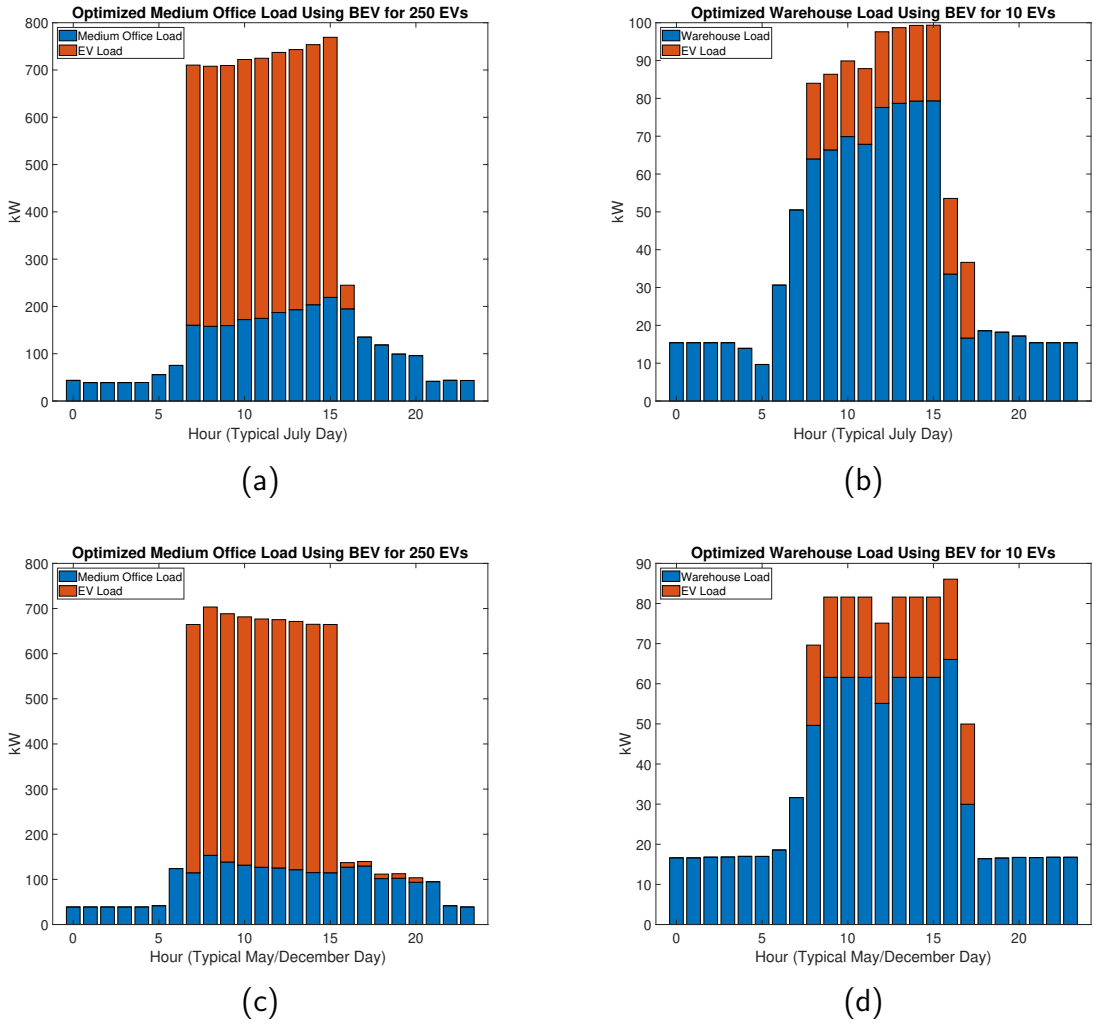

Figure 1.8: The optimized hourly load profile of the (a) Medium Office Customer and (b) Warehouse Customer on a typical day in July under the BEV tariff. The load profiles for the same (c) Medium Office Customer and (d) Warehouse Customer on a typical load day in May or December under the BEV tariff. Unlike the B-10 or B-19 tariff, the BEV tariff only applies to EV loads.

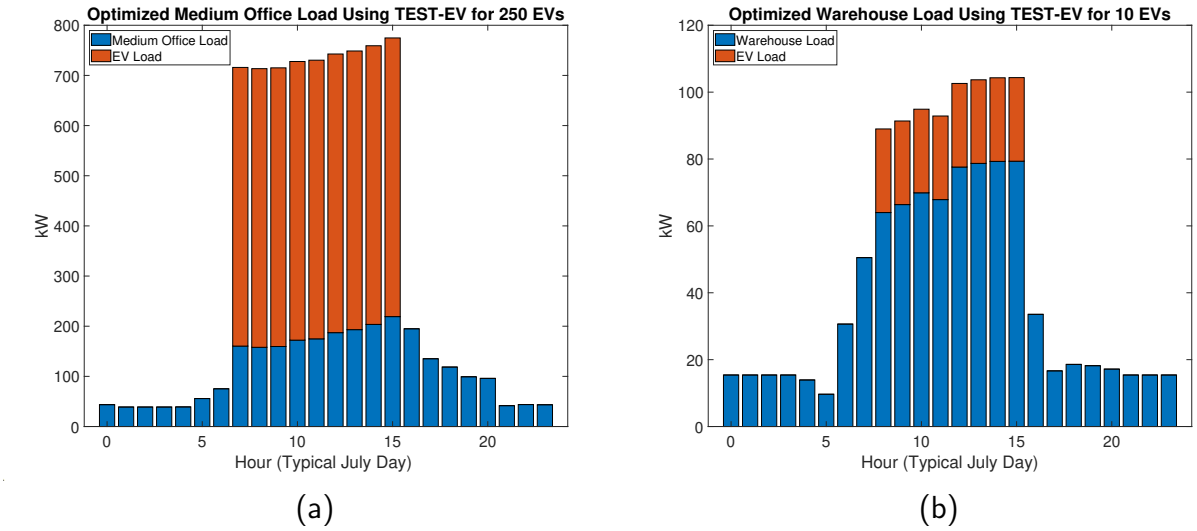

Figure 1.9: The optimized hourly load profile of customers when optimizing under the TEST-EV tariff on a typical load day of the month. (a) Medium Office Customer in July (b) Warehouse Customer in July

Cost to the customer

We extracted the volumetric EV costs for each tariff and reported them for buildings we modeled in Table 1.2. We also calculated a "seasonal weighted sum" to reflect the three spring months, four summer months, and five winter months in a billing year. Note that these seasonally weighted sums approximate a billing year but do not exactly match the total costs because we are using 31-day months for our analysis.

We found that the hypothetical TEST-EV tariff was the cheapest for customers to follow. For existing tariffs, the B-19 was the cheapest tariff to optimize against for the smaller warehouse customer, while the BEV tariff was cheaper for the larger medium-sized office customers. In both cases, the B-10 tariff was the most expensive tariff for customers to use as a price signal.

Voltage effects on the distribution feeder

We distributed the load profiles generated in the optimization above across our feeder model to examine system voltage in July. The peak loading on the feeder prior to adding the EVs was 17.76MW at 3pm on July 10th. This is due primarily to July 10th having the highest temperature of the year in our TMY3 data. With the EVs on the feeder, peak loading increased to between 20.86 MW and 23.26 MW, depending on the tariff used as a price signal for the EVs. Table 1.3 summarizes these results along with the voltage impacts for

Table 1.2: EV volumetric costs for Medium-Sized Office and Warehouse building models by month, and seasonally weighted sum.

Building Type	Tariff	May	July	December	Seasonally Weighted Sum
Medium-Sized Office	B-10	$ 28,094.24	$ 35,937.60	$ 29,863.91	$ 377,352.67
	B-19	$ 23,518.29	$ 30,560.85	$ 25,636.52	$ 320,980.87
	BEV	$ 19,153.69	$ 19,153.69	$ 19,153.69	$ 229,844.28
	TEST-EV	$ 18,804.97	$ 18,804.97	$ 18,804.97	$ 225,659.64
Warehouse	B-10	$ 973.95	$ 1,296.88	$ 1,159.07	$ 13,904.72
	B-19	$ 769.69	$ 1,1693.18	$ 980.53	$ 11,888.44
	BEV	$ 1,000.53	$ 1,000.53	$ 1,000.53	$ 12,006.36
	TEST-EV	$ 747.98	$ 747.98	$ 747.98	$ 8,975.76

each retail tariff.

We measured the minimum voltage at load locations on the feeder and counted the hours where the voltage was below the 0.95 pu ANSI minimum to determine the number of undervoltage events associated with each price signal. We found that all four tariffs caused congestion across the feeder and voltage to drop below 0.95 pu during multiple hours in the month. However, we did not observe a trend in the relationship between voltage impacts and tariff design or feeder peak loading.

Table 1.3: The minimum voltage measured across all customer locations in July, and the number of hours in the month the voltage is below the ANSI C84.1 lower limit for voltage.

Tariff	Peak Feeder Loading (MW)	Minimum Voltage (Per Unit)	Number of hours voltage is below 0.95 pu
B-10	20.86	0.88	4
B-19	23.04	0.92	4
BEV	22.74	0.93	6
TEST-EV	23.26	0.90	11

Costs to the utility

In Table 1.4, we calculated the seasonally weighted costs in ACC 2023 dollars and revenue for the utility. We calculated the total volumetric revenue a utility would receive as the summation of the costs the customers would pay for charging all the electric vehicles on the distribution feeder. We also calculated the difference between this revenue and the ACC 2023 costs as the net revenue for the utility.

We found that the B-10 tariff generated the the highest costs and largest net revenue for the utility. The TEST-EV tariff had the lowest cost and lowest revenue. For the tariffs currently available to customers, the B-19 tariff had the lowest cost for the utility, but it generated more revenue and more net revenue for the utility than the BEV tariff.

Table 1.4: Total seasonally weighted sum of costs, revenue, and net revenue for an electricity distribution utility to supply commercial EVs across the distribution feeder.

Tariff	ACC 2023 costs	Volumetric revenue	Net revenue
B-10	$ 769,832.51	$ 3,152,096.08	$ 2,382,263.57
B-19	$ 542,842.67	$ 2,686,752.79	$ 2,143,910.12
BEV	$ 552,734.36	$ 2,241,796.08	$ 1,689,061.72
TEST-EV	$ 428,255.42	$ 1,945,089.72	$ 1,516,834.30

1.4 Discussion

Undervoltage from Price-Signal Control

We found that if a large number EVs on a distribution feeder followed any of the retail tariffs we modeled as a price signal and background loading was already high, the distribution feeder could experience congestion leading to undervoltage situations. These voltage excursions highlight that customers with flexible loads following current retail tariffs can negatively impact the local distribution system and affect neighboring customers. While these tariffs were not designed explicitly to "protect the grid," the volumetric power cost components were designed to capture the cost of demand on the grid and incentivize the reduction of peak load. We found that the different load shifting incentives and prices on power of these tariffs are not effective in mitigating network impacts. In addition, we examined highly flexible daytime charging scenarios in both buildings, less flexible scenarios would increase power consumption during charging hours and exacerbate the voltage magnitude effects we observed.

In future scenarios with many EVs, either other mechanisms will need to be employed to ensure EV charging load does not exceed system constraints, or upgrades to the distribution system will be required. Since the number of hours in the month where voltage is violated

is relatively low, finding a strategy that does not require upgrades to the feeder could be more cost-effective than installing new equipment. These strategies could be adding engineering constraints to the optimizations, adjusting pricing values of the current volumetric power costs, designing other pricing mechanisms, or employing price signals that include information about the status of the distribution system like a D-LMP [80].

Costs to the Customer vs. the Utility

We found the most expensive tariff for both customers and the utility was the B-10 tariff. In Table 1.5, we show that customers with the ability to optimize their EV load would save money if they switched away from the B-10 tariff to the B-19 or BEV tariff. We found that both customer types we modeled would save nearly 15% by switching from the B-10 tariff to B-19. We also found significant savings for customers to switch from the B-10 to the BEV tariff; however, we find the other issues in the BEV tariff design that we address in the "Subscription Pricing" subsection below.

We also examined the cost savings for the utility for customers switching tariffs. In Table 1.5, we show that the utility would save over 28% in ACC 2023 cost if customers selected the BEV or B-19 tariff, with more savings if customers selected the B-19 tariff. However, the cost savings of the utility does not offset the loss of revenue from customers, and the resulting loss of net revenue ranges from 10 to 29 percent. Customer switching today could lead to a revenue shortfall; however, in the future, these differences should be examined by regulators. The loss in revenue incentivizes the utility to keep customers on the higher-cost tariff even though the lower-cost tariff is better for the customer and reduces ACC costs. If incentives were properly aligned, a reduction in ACC costs would not result in a net loss of revenue for the utility.

Table 1.5: Percentage savings from switching tariff designs.

	From B-10 to B-19	From B-10 to BEV
Savings for a Medium-Sized Office Customer	14.94%	39.09%
Savings for a Warehouse Customer	14.50%	13.65%
Cost Savings for the Utility	29.49%	28.20%
Change in Net Revenue for the Utility	-10.01%	-29.10%

In both the subscription pricing tariff and demand charge-based tariffs, the customer experiences a higher per unit cost of power compared to energy (see appendix for specific charges). This higher per unit cost makes power costs the dominant component of the bill when it comes to optimizing load. Instead of shifting load to follow lower cost TOU energy hours, the optimal action for customers with large power costs is to reduce their consumption as much as possible across all hours in a time period. With a fixed-level demand charge or flat subscription level, customers are incentivized to have a completely flat load profile at all hours of the day. In contrast, customers with time-differentiated demand charges are incentivized to limit their power consumption in different period to create different flat periods of load. However, customers are also sensitive to the relative cost of demand charges. If the Max demand charge is significantly larger than a TOU period demand charge, the optimal behavior may be to ignore the TOU period demand charge and flatten load to minimize the impact of the Max demand charge. Unfortunately, this "load flattening" strategy does not help the utility. The utility would see a cost reduction if customers followed their TOU hours because the TOU hours for these tariffs generally capture the peak prices on the wholesale market [81]. While we only modeled EV charging in this analysis, we expect that this would also hold true for any other flexible loads that a customer could optimize to minimize their costs. The optimal scenario would be one where customers with flexible loads followed prices that reflected the lowest cost energy available on the wholesale market while also keeping load at a level to not cause network impacts in the local distribution system.

A way to increase load shifting would be to lower power costs and increase the time granularity of prices. Customers would make decisions based more on the cost of energy instead of power and could consume energy when it is cheaper for the utility to purchase. More granular prices on power and energy would result in reduced costs for both the utility and the customer. Other groups have proposals for real-time pricing (RTP) tariffs that include dynamic pricing for distribution system capacity [43], and the California Public Utilities Commission ordered PG&E to look into RTP for future EV tariffs [36]. However, with the extreme price shocks related to the 2021 Texas Power Crisis, direct exposure of real-time prices to customers is less politically feasible [82].

Subscription Pricing

We designed the TEST-EV tariff to examine the subscription mechanism of the BEV tariff and to explore the efficiency of power subscription plans. We found that EVs following the TEST-EV tariff led to lower costs for both the customer and the utility company as compared to the BEV tariff. The subscription plan in the BEV tariff was more expensive for customers because customer demand did not perfectly align with the subscription block sizes. As a result, optimal customer behavior oversubscribes for the capacity they did not need or use.

When we assume that customers can buy their power in continuous kW increments (as in TEST-EV), the optimal charging strategy has slightly more load during off-peak hours than

if customers buy power in 10 or 50kW blocks (as in BEV). Using TEST-EV's equivalent demand charge results in a slightly higher power cost than BEV, but a lower volumetric energy cost that more than offsets the higher power component of the bill. Switching from the BEV tariff to the TEST-EV tariff would result in a 2% decrease in total monthly volumetric costs for an office building owner and a 25% decrease in cost for a warehouse building owner. We also note that ACC2023 costs for the utility are 22% lower for TEST-EV than for BEV.

The difference between TEST-EV and the BEV tariff is likely to be even larger than we modeled, due to our assumptions about customer capacity to forecast demand. Our optimization model assumes knowledge of the EV load for the month to chose the best subscription level. Even with perfect knowledge and cost optimization, we found BEV customers will likely over-subscribe or under-subscribe and face an overage fee. We expect that, due to forecast errors, BEV customers would tend to make sub-optimal decisions when choosing their subscription level, or a subscription level would become sub-optimal due to changes in their charging requirements throughout a billing cycle.

Researchers in other fields have identified that subscription pricing schemes like the one in the BEV tariff are problematic for customers to make optimal decisions [40] and have found that "three-part tariffs can increase customer usage and firm revenues" [41]. In addition, customers who experience overage fees from under-subscribing in one billing cycle are more likely to overpay for excess subscription allowances in the future to avoid overage fees, even when this strategy costs more [39]. Even with an optimized charging management system, a BEV customer would need to determine their subscription block size ex-ante. While some more sophisticated customers may be able to design predictive algorithms to optimize their consumption, it would be more efficient for customers to use an ex-post calculation of costs based on actual consumption data.

1.5 Conclusion

Our analysis examined how retail tariffs impact optimal commercial customer electric vehicle charging profiles and the resulting impact on customer bills, utility revenue, and distribution system voltage. We compared three time-differentiated retail tariff designs in use today as well as a hypothetical tariff that mirrors a demand-subscription tariff, but without the requirement to pre-purchase demand in fixed increments.

We found that none of the retail tariff designs we examined prevented congestion related undervoltage events on a modeled distribution feeder. The pricing incentives for power were insufficient for keeping voltage in range; demand charges alone will be insufficient to prevent distribution system upgrades. Our results highlight the importance of modeling electricity tariffs when simulating distribution system powerflow. As customers become more price responsive, tariff designs can have an effect on system voltage and impact safe grid operations.

We also found significant cost savings for customers to switch away from a fixed-level demand charge to a time-differentiated demand change. Following a time-differentiated

demand charge also reduced utility costs. However, the cost savings the utility would experience did not make up for the loss in revenue, causing an overall loss in net revenue when customers switched tariffs. We recommend regulators examine tariff options for customers to ensure the price incentives for all parties are aligned with the ACC costs.

Finally, we found that the real-world subscription plan design examined in this study was less efficient than the existing demand charge-based tariffs. Other researchers have already shown demand charges are not efficient pricing mechanisms [83]. Our findings indicate that the three-part subscription-based power charges in the BEV tariff are even less efficient. Based on these results, we recommend that utilities do not use power subscription-based tariff designs.

There are several areas of future research that can build from the work we describe here. First, while we modeled our loads on the three-phase unbalanced distribution feeder, we balanced the EV loading across the phases at each customer location. One area of future work would be to examine the impacts of unbalanced EV charging. While we focused on three-phase charging for commercial customers, residential customers and smaller commercial customers may have single or two-phase connections to the distribution system and their aggregate EV charging could lead to phase imbalance. Another area of related research would be the congestion impacts of bi-directional charging of EVs. We focused solely on unidirectional charging of EVs but other researchers have explored vehicle-to-grid approaches for demand charge management and as virtual power plants [84], [85]. A current gap in the literature is the distribution system impacts of widespread vehicle-to-grid adoption.

Chapter 2

Data-Driven Linear Three-Phase Voltage Estimations for Optimal Electric Vehicle Charging Coordination

Market analysts project that the number of electric vehicle chargers in the US will increase eight times compared to 2022. In aggregate, electric vehicle charging can create congestion management issues for distribution system operators (DSOs). In this chapter, we present a data-driven linear voltage magnitude predictor to estimate voltage based on past smart meter and substation data. We compare our voltage predictions to linearized voltage approximations and the measurements from a nonlinear power-flow solver. We then use the voltage magnitude predictor as a linear constraint for EV charging coordination in a large, three-phase unbalanced distribution feeder case study. The predictor provides a better estimate of customer voltage than linearized voltage approximations at a reduced computational requirement.

2.1 Introduction

By the year 2030, market analysts project that there will be an estimated 28 million electric vehicles (EVs) in the United States and more than eight times the number of EV chargers compared to 2022 [86]. These electric vehicles will add a significant load to the power grid that will require system upgrades, especially on the distribution system [19], [56], [57], [87], [88]. Some of these upgrades can be deferred if utilities and distribution system operators (DSOs) implement EV charging coordination strategies. However, employing charging coordination that takes into account local distribution system conditions requires either significant deployment of sensors or computationally burdensome algorithms that may not scale

with the number of distribution feeders utilities own. In this chapter, we propose a data-driven voltage estimator for EV charging coordination that significantly reduces sensor and computation requirements for DSOs compared to the state-of-the-art.

There has been extensive work in DER optimization and EV charging coordination. Many of the approaches assume that the network configuration is known and that voltage can be measured across the distribution feeder for Optimal Power Flow (OPF) formulations to set prices or directly dispatch DERs [89]–[93]. Some approaches assume less network knowledge and measurements are available, and instead use state/model estimation approaches [94]–[97].

As an alternative, several research groups have examined data-driven or measurement-based approximations [98]–[103]. In [98], the authors use an Extremum Seeking control approach with injected sinusoidal perturbations for distributed energy resources control and extend their work to a three-phase unbalanced system in [99]. The authors of [100] develop a data-driven linearization method for powerflow models. While in [101], the authors leverage the LinDistFlow equations to estimate the full impedance matrices of a balanced radial distribution system. In [102], the authors implement an iterative online estimation approach using PMU data and a recursive weighted partial least squares algorithm and extend their work to a distributed algorithm in [103]. In each of these approaches, additional sensors (such as PMUs) must be installed, or probing signals need to be injected into the system.

In this chapter, we propose a linear three-phase voltage magnitude estimator trained on recently captured smart meter and substation data. The estimator is trained offline and does not assume any knowledge of the system configuration. We use this estimator as a voltage constraint for a large-scale EV charging coordination problem and compare the results to standard linear powerflow approximations and measure voltage performance in a nonlinear powerflow simulation.

What separates our approach from the state-of-the-art is (1) our approach does not require additional sensors or injections into the distribution system, and (2) we do not attempt to estimate all voltage measurements in the distribution system; we only estimate voltage at the customer's service connection. This reduces the size of the problem and the computational requirements.

The main contribution of this work is a three-phase linear voltage magnitude estimator for unbalanced radial distribution systems. The estimator is trained solely on power and voltage measurements from smart meters and the distribution substation. To examine the accuracy of this estimator, we compare voltage estimations to time-series voltage measurements of the IEEE-13 Node Test Feeder from an industry-standard nonlinear powerflow solver. We then use the voltage estimator as a linear voltage constraint in a large EV charging coordination problem. We compare the computational efficiency of the voltage estimator to other linearized voltage constraints for the optimization and verify the constraint's effectiveness by modeling the optimization output in the same nonlinear powerflow solver. In our tests, we find our voltage estimates prevent undervoltage while also reducing costs and computational requirements compared to the linearized voltage constraints.

The rest of this chapter is organized as follows: Section 2.2 introduces the voltage re-

quirements for utilities and reviews the DistFlow equations for calculating voltage in radial distribution systems. Section 2.3 details the data-driven model we train to estimate voltage and examines the accuracy of the estimations. In Section 2.4, we apply the voltage estimator in an EV charging coordination case study to explore the estimator's performance as a voltage constraint. We then provide concluding remarks and discuss potential directions for future work in Section 2.5.

2.2 Preliminaries

ANSI C84.1

The national voltage standard in the U.S. is defined by ANSI C84.1 [69]. Originally published in 1954, the standard was based on work by both the Edison Electric Institute and the National Electrical Manufacturers Association to develop a list of standard voltage ranges for the electric grid. The standard provides acceptable minimum and maximum voltage values for both the service connection to the electric grid and at the utilization point for devices. For low voltage service, 120V-600V, the standard service range is $\pm 5\%$. While the standard provides other ranges for higher voltage systems, according to Short in [20]: "...most utilities do not follow these as limits for their primary distribution systems (utilities use the ANSI service voltage guidelines and set their primary voltage limits to meet the service voltage guidelines based on their practices)". It is important to note here that the focus of ANSI C84.1 is voltage at the service connection and downstream to the customer devices. From that perspective, the voltages at other points in the system are not important to the standard if customer service connection voltage is in range.

DistFlow Equations

In 1989, Baran and Wu proposed the now well-known DisFlow equations for calculating powerflow in radial distribution systems [104]. Equations (2.1)-(2.3) were solved recursively to calculate real power, reactive power, and voltage respectively. In the same paper, Baran and Wu show that in (2.3) if the squared impedance and current values are neglected, the squared voltage magnitude exhibits a linear relationship with real and reactive power. This relationship, originally described as the "simplified DistFlow model" in the paper, is more commonly referred to as the LinDistFlow equation (2.4) today and has been extended into three-phase versions in [105] and [106]. Detailed discussions of each of these formulations are described in [107].

$$P_{i+1} = P_i - \frac{R_{i+1}(P_i^2 + Q_i^2)}{V_i^2} - \check{P}_{i+1} \tag{2.1}$$

$$Q_{i+1} = Q_i - \frac{X_{i+1}(P_i^2 + Q_i^2)}{V_i^2} - \check{Q}_{i+1} \tag{2.2}$$

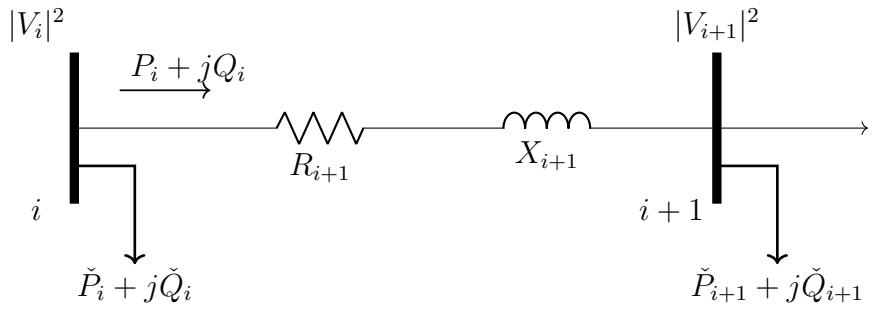

Figure 2.1: One-line diagram of the DistFlow equation variables.

$$|V_{i+1}|^2 = |V_i|^2 - 2(R_{i+1}P_i + X_{i+1}Q_i) + \frac{(R_{i+1}^2 + X_{i+1}^2)(P_i^2 + Q_i^2)}{V_i^2} \tag{2.3}$$

$$|V_{i+1}|^2 \approx |V_i|^2 - 2(R_{i+1}P_i + X_{i+1}Q_i) \tag{2.4}$$

In (2.1)-(2.4) node $i \in \{1, 2, \ldots, n\}$, where n is the number of nodes on the feeder. P_i and Q_i are the real and reactive powers flowing into the branch from node i and $\check{P}_i$, $\check{Q}_i$ are the loads being consumed in parallel at node i. The line resistance and reactance are R_i, X_i respectively, and $|V_i|$ is the node voltage magnitude. Fig. 2.1 shows a one-line diagram of the DistFlow equation variables.

2.3 Data-Driven Model

From 2.2, we use the following two facts as the basis for our data-driven model design decisions: (1) most utilities only use ANSI C84.1 for voltage at customer service connections and (2) the voltage squared across a radial feeder can be modeled linearly with respect to power. As such, we trained a voltage estimator to approximate voltage measurements only at customer service locations for a radial distribution feeder. This reduces the need to compute voltage at all nodes in the system and creates a linear voltage constraint for DSOs to perform load optimization.

Model Design

Our approach to creating the voltage magnitude estimator was to leverage the LinDistFlow voltage equation. Let $\mathcal{V}$ be the vector of voltage magnitude estimates $|\hat{V}_{\text{metered}}|^2$ at each phase of the metered nodes in a radial distribution feeder (2.5). The vector $\mathcal{V}$ has size $\gamma \times 1$,

where γ is three times the number of metered nodes n_{metered} (2.6). For nodes with only single or two connected phases, the corresponding elements in $\mathcal{V}$ for unconnected phases are zero.

$$\mathcal{V} = |\hat{V}_{\text{metered}}|^2 \tag{2.5}$$

$$\gamma = 3 \cdot n_{\text{metered}} \tag{2.6}$$

Since the LinDistFlow equation is linear in real and reactive power for squared voltage magnitude, we trained a linear model on real and reactive power to estimate $\mathcal{V}$ (2.7).

$$\mathcal{V} = \boldsymbol{\alpha_1}[\mathcal{P}; \mathcal{Q}] + \alpha_0 \tag{2.7}$$

Let $\mathcal{P}$ and $\mathcal{Q}$ be vectors of size $\gamma \times 1$. As with $\mathcal{V}$ for single or two phase nodes, the corresponding elements in $\mathcal{P}$ and $\mathcal{Q}$ for unconnected phases are zero. We vertically concatenate $\mathcal{P}$ and $\mathcal{Q}$ as denoted as $[\mathcal{P}; \mathcal{Q}]$, such that the new vector has size $2\,\gamma \times 1$. A $\gamma \times 2\,\gamma$ matrix of coefficients ($\boldsymbol{\alpha_1}$) and a $\gamma \times 1$ vector of intercepts (α_0) are trained from a linear regressor to map the $\mathcal{P}$ and $\mathcal{Q}$ measurements to the $\mathcal{V}$ estimates. To extend (2.7) for time-series estimates, $\mathcal{V}$ can be estimated as a $\gamma \times t$ matrix for times t if $\mathcal{P}$ and $\mathcal{Q}$ are measured at $\gamma \times t$.

For our linear regressor, we use the least absolute shrinkage and selection operator (LASSO) linear model (2.8). The LASSO algorithm was designed by Tibshirani to increase the prediction accuracy of ordinary least squares and provide feature selection by allowing some of the feature coefficients to be reduced to zero [108]. In the context of the three-phase voltage estimation problem, power consumed on different phases of distant nodes have near zero impact on local voltage compared to nearby power consumption. Since we assumed no knowledge of the distribution system design, we used past data and the LASSO algorithm's feature selection capacity to determine which power measurements are the most important for estimating voltage at a location. The general form of the LASSO model is:

$$\min_{\beta} \frac{1}{2}\|y - \mathcal{X}\beta\|_2^2 + \lambda\|\beta\|_1, \tag{2.8}$$

where y is the response, $\mathcal{X}$ is the vector of predictor variables, β is the vector of predictor coefficients, and λ is a tuning parameter. In our simulations, we tune λ using cross-fold validation.

Model Accuracy

To examine the accuracy of our LASSO data-driven voltage estimator, we used Gridlab-D [70] to simulate power and voltage measurements of a modified IEEE-13 Node Test Feeder and compared our estimation accuracy against the out of sample voltage measurements of the nonlinear powerflow solution. The LASSO estimator was trained in Python using SciKit-Learn. All calculations and simulations were performed on an AMD Ryzen 7 3700X desktop PC with 64GB of RAM, running Windows 11.

We calculated the root mean squared error (RMSE) and max error of the voltage estimations compared to Gridlab-D measurements at the load nodes of the IEEE-13 Node Test Feeder [74]. We did not modify the feeder parameters, however, since the original test feeder has static loads, we replaced those loads with hourly time-series loads as described in the next subsection. Fig. 2.2 is the one-line diagram of the test feeder as presented in [74]. The test feeder is a 4.16kV, three-phase unbalanced distribution feeder with single phase and two phase laterals.

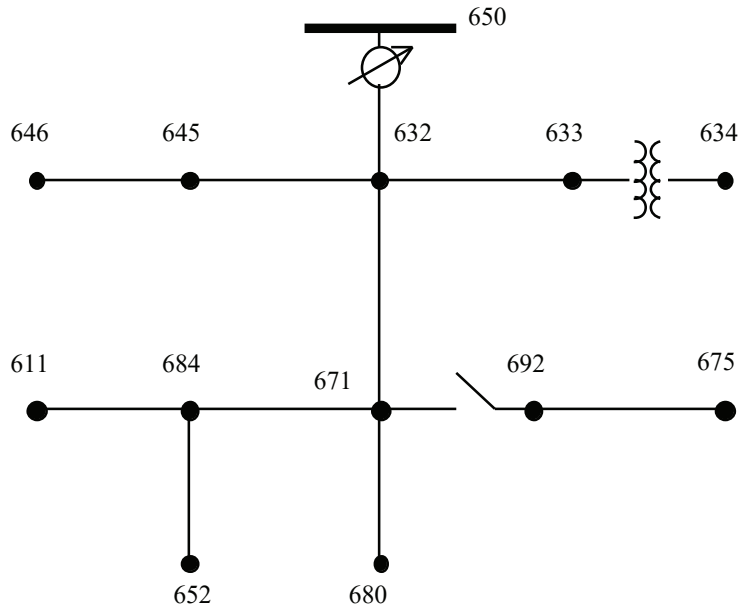

Figure 2.2: One-line diagram of IEEE-13 Node Test Feeder [74]

Design

To generate the data for this analysis, we replaced the standard spot loads on the IEEE-13 Node Test Feeder with an equivalent number of building loads using the Building America House Simulation Protocols for the residential building models [72]. Each building model has an hourly load profile for a generic year in different climate zones. Specifically, we placed Mid-Sized House models from the Sacramento Climate Zone on each phase of the load nodes such that the peak load of the houses was equivalent to the load originally on the IEEE-13 Node Test Feeder. Table 2.1 lists the number of houses at each node and peak power measurements compared to the original real power loads on the test feeder. We modeled each building with a power factor of 0.9. For this analysis, we also excluded the distributed loads on the original feeder from our model. In addition, to ensure conformity, the IEEE-13 node

feeder does not model the secondary network of the distribution system for the majority of the nodes, with the exception of Node 634.

Table 2.1: Modifications to the IEEE 13 node load data for each node

Node Name	Number of Houses	Peak Real Load (kW)	Original Real Load (kW)
load611 phase A	0	0.0	0.0
load611 phase B	0	0.0	0.0
load611 phase C	41	168.6	170.0
load634 phase A	39	160.4	160.0
load634 phase B	29	119.3	120.0
load634 phase C	29	119.3	120.0
load645 phase A	0	0.0	0.0
load645 phase B	41	168.6	170.0
load645 phase C	0	0.0	0.0
load646 phase A	0	0.0	0.0
load646 phase B	56	230.3	230.0
load646 phase C	0	0.0	0.0
load652 phase A	31	127.5	128.0
load652 phase B	0	0.0	0.0
load652 phase C	0	0.0	0.0
load671 phase A	94	386.6	385.0
load671 phase B	94	386.6	385.0
load671 phase C	94	386.6	385.0
load675 phase A	118	485.3	485.0
load675 phase B	17	69.9	68.0
load675 phase C	71	292.0	290
load692 phase A	0	0.0	0.0
load692 phase B	0	0.0	0.0
load692 phase C	41	168.6	170.0

We simulated two months of load on our distribution feeder in Gridlab-D, measuring power and voltage at each load node and the feeder head. These measurements simulate the data that could be gathered from smart meters and substation telemetry. Fig. 2.3 show the distributions of load hours for June (2.3a) and July (2.3b) respectively. While similar, June has more hours at a lower power and July has a higher peak. To create our voltage estimation model, we trained a LASSO model on only the June hourly power and voltage measurements, with 3-fold cross validation. We then extract the α_1 matrix and α_0 vector from the trained model to use as our estimator. Finally, We use the measured power data for July to estimate the voltages for the month and compared these estimations to what was measured using the powerflow solutions from Gridlab-D. Fig. 2.4 shows the data flows

between the models.

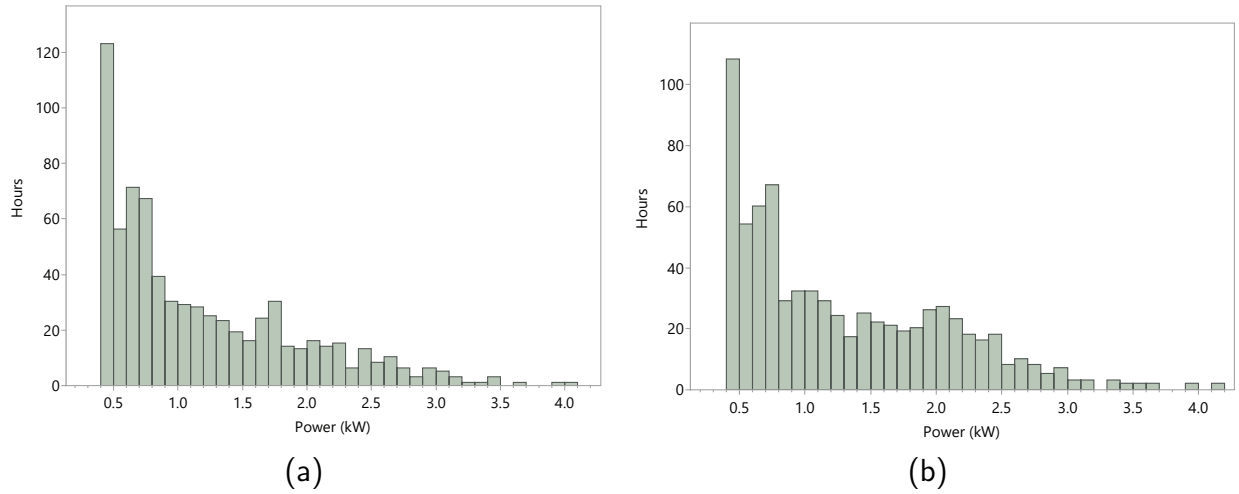

Figure 2.3: Distribution of load hours for a single Mid-Sized House model in (a) June (b) July.

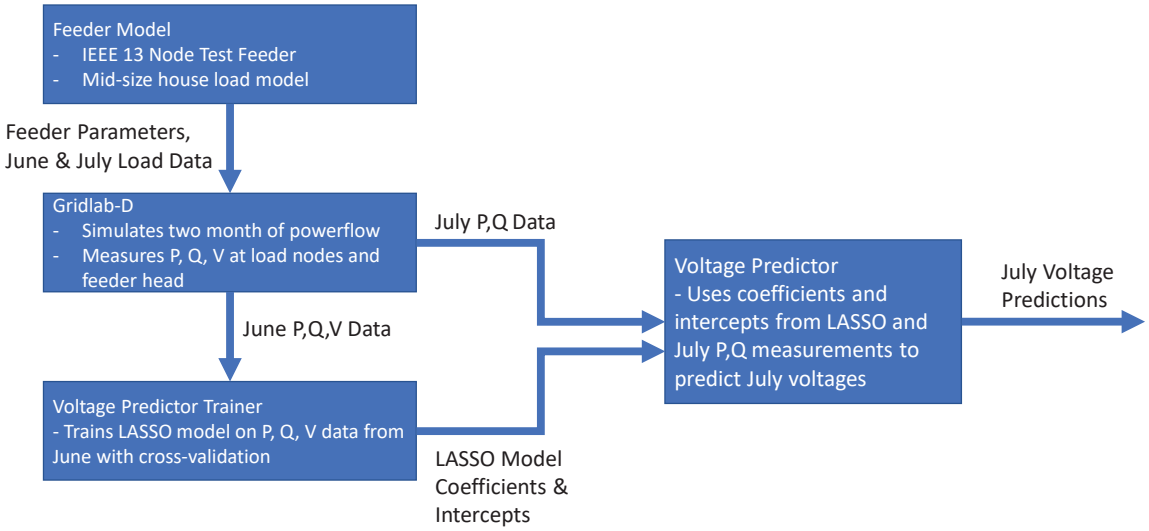

Figure 2.4: Data flows between feeder models

Results

Table 2.2 lists the voltage magnitude RMSE and max error for each phase and node over the 744 hours in the month of July. The max error for the month was less than 0.005pu with a max RMSE of less than 0.002pu. The node with the highest error were Phase C of Node 645. The estimate was least accurate here because the load affecting the voltage on Phase C of Node 645 is the delta connected load from phase B to C on Node 646. However, the LASSO estimator selected the real and reactive measured at phase C of Node 646 as the only non-zero α_1 coefficients for this estimate. The resulting average difference in the estimated vs. measured voltage at the node over the month was 1.05×10^{-4}pu with a mean absolute difference of 0.0015pu. These simulation results show that the linear voltage estimator was able to closely estimate the voltage measurements from the Gridlab-D simulation.

Table 2.2: Test Error and RMSE (per unit) for voltage magnitude of each load node

Node Name	**Max Error (per unit)**	**RMSE (per unit)**
load611 phase A	—	—
load611 phase B	—	—
load611 phase C	1.78×10^{-3}	5.41×10^{-4}
load634 phase A	1.08×10^{-3}	4.22×10^{-4}
load634 phase B	2.93×10^{-3}	1.18×10^{-3}
load634 phase C	4.25×10^{-3}	1.64×10^{-3}
load645 phase A	—	—
load645 phase B	2.43×10^{-3}	9.81×10^{-4}
load645 phase C	4.58×10^{-3}	1.87×10^{-3}
load646 phase A	—	—
load646 phase B	3.09×10^{-3}	1.24×10^{-3}
load646 phase C	4.58×10^{-3}	1.87×10^{-3}
load652 phase A	1.26×10^{-3}	5.16×10^{-4}
load652 phase B	—	—
load652 phase C	—	—
load671 phase A	4.02×10^{-4}	1.18×10^{-4}
load671 phase B	3.89×10^{-4}	1.54×10^{-4}
load671 phase C	9.82×10^{-4}	1.71×10^{-4}
load675 phase A	1.61×10^{-3}	6.65×10^{-4}
load675 phase B	4.84×10^{-4}	1.92×10^{-4}
load675 phase C	1.03×10^{-3}	3.10×10^{-4}
load692 phase A	4.04×10^{-4}	1.18×10^{-4}
load692 phase B	3.89×10^{-4}	1.54×10^{-4}
load692 phase C	9.82×10^{-4}	1.71×10^{-4}

In addition to the high estimation accuracy, it should be noted that the matrix of model parameters the LASSO model generates for the voltage estimator are sparse and much smaller

than the original admittance matrix of the feeder. Since the LASSO voltage estimator is the linear approximation of the DistFlow voltage equation (2.7) with feature selection, the voltage estimator uses a sparse vector of coefficients and an intercept to estimate the voltage at each phase of the load nodes. Table 2.3 lists the number of non-zero coefficients used by the voltage estimator for each phase and node. In total, the model required 59 non-zero coefficient values and 24 intercept values to estimate voltage at each load node. For comparison, the combined 39×39 impedance matrix for the IEEE-13 node has 216 complex non-zero values. This smaller voltage model reduces memory requirement for systems and can result in faster computation, especially when used as constraints in larger models.

Table 2.3: Number of non-zero coefficients per phase of voltage estimator

Node Name	**Non-Zero Coefficients**
load611 phase A	—
load611 phase B	—
load611 phase C	4
load634 phase A	3
load634 phase B	2
load634 phase C	3
load645 phase A	—
load645 phase B	2
load645 phase C	2
load646 phase A	—
load646 phase B	2
load646 phase C	2
load652 phase A	3
load652 phase B	—
load652 phase C	—
load671 phase A	5
load671 phase B	4
load671 phase C	4
load675 phase A	3
load675 phase B	4
load675 phase C	4
load692 phase A	4
load692 phase B	4
load692 phase C	4

2.4 Case Study

In this section we examine the accuracy of our LASSO data-driven voltage estimator model as a voltage constraint in the same electric vehicle (EV) charging coordination problem from Chapter 1. However, in this case study we are using day-ahead retail prices. We summarize the distribution system, building, and EV model design here but refer the reader to Section 1.2 for more details on the models.

The LASSO voltage model was trained in Python using SciKit-Learn and voltages were compared to powerflow simulations performed in Gridlab-D [70]. All calculations and simulations were performed on an AMD Ryzen 7 3700X desktop PC with 32GB of RAM, running Windows 11.

Design

We optimized the EV charging of two types of three-phase customers, medium office building customers and warehouse customers, each with fleets of electric vehicles operating as flexible, price-optimizing loads. These customers are connected to a 17-mile, three-phase, unbalanced distribution feeder with overhead and underground power lines supplying 2,894 residential customers, 270 commercial customers, and 91 industrial customers. To provide load diversity, we modified the feeder model to incorporate 10 different building models from the Department of Energy's Commercial Reference Building models and Building America House Simulation Protocols for the residential building models [63], [72]. We modeled all 91 industrial customers on the feeder as warehouse buildings and five of the commercial customers as medium-sized office buildings. We modeled a total of 2,160 EVs on the distribution feeder, 10 EV at each of the 91 warehouses and 250 EVs at each of the 5 office buildings, for a combined load of 43.2 MWh per day or 1.34 GWh per month. Before running our optimization, we also verified that the feeder could support charging the total number of EVs we modeled without voltage constraint violations.

For prices, we used hourly prices from the Avoided Cost Calculator developed by the energy consulting firm E3 for the California Public Utilities Commission to determine the benefit of distributed energy resources [75]. Although most commercial customers are not able to adopt an hourly pricing tariff, there is growing interest in real-time or day-head hourly pricing for retail customers [24], [25]. The ACC calculates the avoided cost of energy for every hour of the year by modeling the combined costs of wholesale energy, system capacity, and environmental damages from greenhouse gases. Specifically, we use the 2022 edition of ACC electricity prices for the PG&E climate area 12 in the year 2023 [76].

To simulate the charging coordination problem, we developed a linear programming model to minimize the daily cost of charging a fleet or collection of electric vehicles at customer locations (2.9). In this model, π_t is the ACC price at time t, $\tilde{x}_{i,b,t}$ is the sum of all EV loads and $x_{i,b,t}$ is the sum of all non-controllable building loads at building b in set of B_i buildings at node i in the set of nodes I at time t. The local loading limit prevents coincidental load from exceeding the circuit breaker limit of each customer. Real power

from a single EV, l, in the set of all EVs, L_b, at a building is represented by $w_{l,i,b,t}$ and is constrained by the EV operating constraints, which are the maximum charging rates of each EV (7.2kW) with only unidirectional flow from the grid to charge the EV. We modeled each EV requiring 20kWh per day to model an extreme case for EV charging. We also required each EV to be fully charged at the end of each day.

The linear program minimizes the total cost to the customer for their building loads and the charging of all the electric vehicles at the customer's site. In our analysis, we only optimized EV charging; the building loads were treated as exogenous to the optimization and only included for their impact on the voltage constraint and costs. We repeated this daily optimization for every day in the month of July.

$$\begin{aligned} \min_{\tilde{x}} \text{Cost} = & \sum_{t=1}^{\text{24 hours}} \sum_{i=1}^{I} \sum_{b=1}^{B_i} \pi_t \cdot (\tilde{x}_{i,b,t} + x_{i,b,t}) \\ s.t. \quad & (\tilde{x}_{i,b,t} + x_{i,b,t}) \leq \text{Local loading limit} \\ & \tilde{x}_{i,b,t} = \sum_{l=1}^{L_b} w_{l,i,b,t} \\ & w_{l,i,b,t} \leq \text{EV operating constraints} \\ & \sum_{t=1}^{\text{24hrs}} \tilde{x}_{i,b,t} = \text{charging energy required for} \\ & \qquad\qquad\qquad\qquad \text{EVs at the building} \end{aligned} \tag{2.9}$$

To keep voltage within ANSI limits, we used the LASSO voltage estimator as a constraint in the linear program (2.10).

$$\boldsymbol{\alpha_1}[(\mathcal{P}_t + \tilde{\mathcal{P}}_t); (\mathcal{Q}_t + \tilde{\mathcal{Q}}_t)] + \alpha_0 \geq |V_{min}|^2 \qquad \forall t \in 24 \text{ hours}, \tag{2.10}$$

where V_{min} is the Range A ANSI C84.1 voltage minimum value for delivered energy (0.95pu), $\boldsymbol{\alpha_1}$ is the matrix of coefficients for each power measurement and α_0 is the intercept. $\mathcal{P}$ and $\mathcal{Q}$ are the vectors of uncontrollable building load real and reactive power at each phase ϕ of the load nodes respectively, while $\tilde{\mathcal{P}}$ and $\tilde{\mathcal{Q}}$ are the vectors of controllable EV load real and reactive power. Building loads were assumed to have a power factor of 0.9 and EVs were assumed to have unity power factor. All loads were modeled as constant power loads and all loads at three-phase connected buildings were modeled as balanced three-phase loads across each phase ϕ (3.18).

$$\begin{aligned} \mathcal{P}_{\phi_i,t} &= \frac{1}{3} \sum_{b=1}^{B} (x_{i,b,t}), \quad \mathcal{Q}_{\phi_i,t} = \mathcal{P}_{\phi_i,t} \times \tan(\cos^{-1}(0.9)) \\ \tilde{\mathcal{P}}_{\phi_i,t} &= \frac{1}{3} \sum_{b=1}^{B} (\tilde{x}_{i,b,t}), \quad \tilde{\mathcal{Q}}_{\phi_i,t} = 0 \end{aligned} \tag{2.11}$$

We ran the powerflow simulation for two months, first in the month of June to create training data and then month of July with the EV load to test the results of our optimization model. For the LASSO estimator, we assume we have no historical data of how the EV load impacts voltage. As such, we trained the LASSO voltage estimator on only the building loads measured in June. While it is not realistic to assume over 2,000 electric vehicles would appear on a distribution feeder at the beginning of a single month, this provides an extreme scenario for the estimator to predict out of sample voltages from load significantly higher than the training data. Once we trained the estimator we extracted the coefficients and intercepts to use in the constraint.

To compare the results of the LASSO voltage estimator, we also solved the optimization model constrained by the LinDistFlow voltage magnitude equation for unbalanced three-phase networks (2.12), (2.13) derived in [105], [106]. The model is:

$$|V_{\phi_k,t}|^2 \approx |V_{\phi_i,t}|^2 - 2(\boldsymbol{R}_{\boldsymbol{\phi_k}}(\mathcal{P}_t + \tilde{\mathcal{P}}_t) + \boldsymbol{X}_{\boldsymbol{\phi_k}}(\mathcal{Q}_t + \tilde{\mathcal{Q}}_t)) \qquad \forall i, k \in I \tag{2.12}$$

$$|V_{\phi_k,t}|^2 \geq |V_{min}|^2 \quad \forall k \in I, \forall t \in 24 \text{ hours}, \tag{2.13}$$

where $|V_{\phi_i,t}|$, $|V_{\phi_k,t}|$ are voltages at each phase ϕ at node i and k respectively at time t, and i, k denote nodes in set I of all nodes for the feeder. The matrices of line resistance and reactance for each phase ϕ from i to k are $\boldsymbol{R}_{\boldsymbol{\phi_k}}$, $\boldsymbol{X}_{\boldsymbol{\phi_k}}$ respectively.

However, the LinDistFlow constraint requires significantly more memory than the voltage estimator constraint and caused the computer running the simulation to run out of memory when running the optimization for a full 24-hour day. To produce comparable results, we limited the LinDistFlow constraint to only apply during the 12 expected operating hours of the EVs. To further reduce the size of the problem, we only modeled the minimum voltage constraint for both the voltage estimator and the LinDistFlow constraint. We justified this relaxation due to modeling EVs only as loads, no vehicle to grid discharging was allowed. In addition to the voltage constrained models, we also model the optimization without a voltage constraint for comparison purposes. For each of the three optimization models, we perform a daily optimization for each day in the month of July. We then model the optimized EV charging profiles and building loads on the distribution feeder in Gridlab-D to determine the number of voltage violations.

Results

Table 2.4 lists the number of voltage violations over the month and maximum violation for each of the optimization scenarios. As expected, the limited LinDistFlow constraint and the data-driven constraint kept voltage above 0.95pu while the optimization without a voltage constraint created multiple violations. However, the LASSO constraint allowed the minimum voltage measured on the feeder to drop further in the acceptable range than the LinDistFlow constraint. This indicates that more of the acceptable range was used during the dispatch and should allow for a lower cost. We verified that total cost was lower by

examining the total cost of charging all of the EVs on the feeder in Table 2.5. The LASSO constraint reduced the total costs compared to the LinDistFlow constraint. We believe the the LASSO constraint performed better because the linear approximation captured some of the non-linear effects that the LinDistFlow equation ignores.

Table 2.4: The minimum voltage measured across all customer locations in July, and the number of hours in the month the voltage is below the ANSI C84.1 lower limit for voltage.

Optimization Constraint	Minimum Voltage (Per Unit)	Number of hours voltage is below 0.95 pu
No Constraint	0.9265	13
LinDistFlow (24 hour)	—	—
LinDistFlow (12 hour)	0.9575	0
LASSO	0.9536	0

Table 2.5: Total cost to charge all EVs on the distribution feeder for the month of July

Optimization Constraint	Total Cost (in ACC Dollars)
No Constraint	$52,190.90
LinDistFlow (24 hour)	—
LinDistFlow (12 hour)	$53,340.43
LASSO	$52,681.10

In addition to reducing total cost, the LASSO constraint required significantly less computing time and memory compared to the LinDistFLow constraints. Table 2.6 shows the number of non-zero elements in each optimization and the solver time. While both voltage constraints created significantly larger optimization problems that took longer to solve, the LinDistFlow constrained optimization took over 5x longer to solve than the voltage estimator constraint and more than double the number of elements in the optimization.

2.5 Conclusion

In this chapter we describe a data-driven voltage approximation based on the LASSO algorithm that can be used for distribution system operations. The approximation can be trained offline and can be deployed as a linear constraint in load optimization problems. We show though an EV charging coordination case study that a LASSO based voltage approximation can perform better than linear three-phase voltage approximation as a voltage constraint, leading to faster computation time and lower costs.

Table 2.6: Solver time and non-zero elements for the EV charging dispatch optimization with and without a minimum voltage constraint. Note, no time was measured for the 24 hour LinDistFlow due to running out of system memory.

Optimization Constraint	Average Solver Time (per simulated day)	Number of non-zero elements
No Constraint	0.5946s	354,520
LinDistFlow (24 hour)	—	294,373,288
LinDistFlow (12 hour)	83.56s	172,046,158
LASSO	15.09s	69,040,504

Although the LASSO constraint reduced the cost of charging EVs on the feeder compared to using the LinDistFlow constraint, individual customers are not guaranteed cost reductions. Centralized charging coordination strategies that take into account distribution system constraints shift customer load depending on system conditions. If customers have time-varying electricity rates, some customers may see increased costs compared to other customers in the area because of dispatch from the centralized coordination. These cost differences between customers may lead to equity concerns and should be examined by policymakers when utilizing any tariff that uses price-signal controls on the distribution system. One solution could be to add a cost-equalizing measure to the optimization for customers in the same customer class. A future area of research would be to explore equity-aware algorithms for price-signal control. In addition, we plan to extend this work to current estimations for specific lines in the distribution feeder.

Chapter 3

Load-Responsive Pricing for Congestion Management in Day-Ahead Retail Energy Markets

Regulators and utilities have been exploring real-time retail electricity pricing, with many existing "real-time pricing" programs providing day-ahead hourly pricing schedules. At the same time, customers are deploying distributed energy resources and smart energy management systems that can optimally follow price signals. In aggregate, these optimally controlled loads can create congestion management issues for distribution system operators (DSOs). In this chapter, we describe a new linear pricing mechanism for day-ahead retail electricity pricing that provides a signal for customers to follow to mitigate over-consumption while still consuming energy at hours that are preferential for system performance. We show that by creating a small linear pricing mechanism designed for price-signal control of cost-optimizing loads, we can shape customer load profiles with minor increases in customer bills that can later be returned for revenue neutrality or used in a subscription mechanism.

3.1 Introduction

As more flexible loads and distributed energy resources (DERs) are being adopted by customers, there is a growing interest in retail tariffs that provide real-time pricing [24], [25]. In practice, most of these tariffs are day-ahead hourly pricing schemes [26]. This type of pricing mechanism incentivizes customers to shift load to better follow prices on the wholesale market, reduce peak load on the system, and reduce costs. However, these pricing systems often do not take into account the effects on the distribution system.

As more customers install smart energy management systems and price-responsive loads, system operators may start to see new potential issues for the power grid, especially at

the local distribution level. Sufficient distribution system capacity is already a concern for electric vehicle adoption and other distributed energy resources (DERs) today [56]. Under day-ahead prices, customers are given a schedule of time-varying volumetric energy prices for the following day. These volumetric prices are usually set at the hourly level, however some markets may change sub-hourly. The price schedule allows customers to optimize their load profile to minimize costs. If enough loads optimize towards the same day-ahead prices, in aggregate they may create new system peaks causing system congestion, undervoltage, or overloading of system equipment.

Essentially, regulators and utilities are exploring day-ahead energy pricing so that customers can respond to prices. However, when enough customers shifting load to optimize for their prices causes grid congestion, prices will need to respond to load. At the wholesale level, this is done by using real-time markets in addition to the day-ahead market. Some researchers have proposed similar markets for the distribution system [109]. However, real-time market prices can be more challenging to optimize against because there is less time for customers to solve their optimization problems, and there is more uncertainty about prices in future hours. In addition, market operators need real-time visibility into grid conditions and fast algorithms to compute prices are spatially differentiated to address distribution system congestion. A 2021 ERPI analysis of the 55 available real-time and day-ahead retail pricing programs in the US found that only four of the programs use spatially differentiated real-time or day-ahead prices [26].

While most utility companies in the U.S. do not use day-head or real-time pricing, they do use other pricing mechanisms to reduce customer peak load that could be integrated with day-head or real-time pricing. Some utility tariffs use demand charges (monthly costs based on the peak power consumption of a customer) to recover capacity costs from customers [34]. These charges can cause customers to reduce their peak load [52]. However, demand charges were not designed for congestion management and are criticized for their economic impact, since individual customer peaks may not correlate with times of system peaks [83]. In addition, at high adoption levels of price-optimizing loads, customers are incentivized by demand charges to flatten their daily load profile instead of responding to time-varying energy prices [110].

Another way utilities can reduce peak load is through Critical Peak Pricing (CPP) programs. These programs alert customers to conserve energy during certain hours on specific days, called CPP days. However, CPP programs are typically designed to address transmission level congestion and are limited in the number of CPP days they can call per year [111].

Researchers have examined several ways to perform congestion management outside of demand charges and CPP, both through direct load control and market based approaches. In the context of day-ahead energy pricing, direct load control may interfere with customer decisions and those of third party aggregators. However, market methods for DER congestion management focus on changing customer behavior and decision making based on costs and price signals.

A rich area of research has been transactive energy markets [112]-[115]. First popularized

in [112], transactive energy markets provide prices to customers and producers to trade energy as needed to maximize net benefits. The authors of [113] use transactive control to provide demand response with commercial building loads. While in [114], the authors extend a transactive framework to provide distributed control of distribution networks. A thorough review of transactive energy markets for residential customers is provided in [115]. State of the art transactive markets work includes [116], where the authors develop a decentralized energy market for coordinating between transmission system operators, distribution system operators (DSOs), and the individual distributed energy resource (DER) owner.

An equally mature research area has been the development of Distribution Locational Marginal Pricing (DLMP) approaches to congestion management [117]-[120]. While nodal pricing in the distribution system has been discussed for many years, the authors in [117] developed one of the first formulations. DLMP has since been examined for EV charging management [89], co-optimization of power and reserves [118], and management of markets under uncertainty [120].

Other market-based mechanism that are actively being researched include incentive mechanisms such as dynamic subsidies paid by the DSO to customers [121]. Similar incentives are proposed as a Stackelberg game for bi-level optimization of the DSO and customers in [122] and as a Nash-Stackelberg-Nash game for EV coordination in [123].

Although researchers have explored many different price-signal calculation mechanisms, each of the price signals in the papers referenced above lead to a total customer cost that is linear in quantity, and this problem can be solved by each customer via a linear program. However, in [27], Huang et. al. identify quadratic programming as a superior approach to linear programming due to the multiple solutions a customer or aggregator may arrive at. They extend this work to provide a dynamic power tariff (DPT) in [28]. In both papers, the DSO is required to calculate the volumetric price of energy based on system conditions, either as a DLMP [27] or as part of the DPT [28]. However, calculating a spatially granular volumetric energy price can be time consuming for a DSO or might not be possible if the DSO does not have measurements of system conditions.

To address this problem, we separate the calculation of quadratic costs into a volumetric energy price, similar to conventional day-head prices, and a pricing component that is linearly dependent on quantity. This composite price, referred to in this chapter as Load Responsive Pricing (LRP), is then communicated to customers as the slope and intercept of a linear pricing curve for each pricing period in the day-ahead schedule. This creates a quadratic cost curve for the customer to optimize against in the day-ahead market, building in a cost for congestion management similar to the quadratic pricing used in [27]. What separates our LRP approach from earlier work is that our quadratic costs are supplemental to traditional volumetric energy prices, and we do not need to take into account real-time system conditions to construct these prices. This approach allows DSOs to determine day-ahead energy prices and optimal load profiles of price-responsive loads independently. Then, once both have been determined, the DSO can use LRP as a price-signal to drive customers to the desired load shape as a target load profile under any volumetric energy price. In addition, for situations in which DSOs have insufficient information to construct distribution-system-optimal load

profiles, we provide a heuristic method to utilize LRP for congestion management without communication between the customer and the DSO beyond transmitting meter data. It should be noted that LRP, as with all price-signal control approaches, increase costs for the customer compared to direct control. As such, we describe several ways to minimize these cost increases and to reimburse the customer for this control scheme if necessary.

The three main contributions of this work are:

1. We propose a quadratic cost mechanism, Load-Responsive Pricing (LRP), for price-signal control of flexible loads and we demonstrate its performance for distributed congestion management in a large, three-phase unbalanced distribution feeder.

2. We derive an optimal pricing strategy for LRP and show how it can shape customer load profiles to match target load profiles under any day-ahead pricing schedule.

3. We also develop a heuristic pricing algorithm for congestion management using LRP without the need for optimal powerflow analysis.

The organization of the rest of this chapter is as follows: First, Section 3.2 describes the linear pricing mechanism we propose. Next, in Section 3.3, we derive a formula for LRP price-setting based on load profiles generated by the DSO. Then we present a heuristic pricing algorithm in Section 3.4. Next, we examine the effectiveness of the LRP mechanism through case studies in in Section 3.5. We then discuss considerations a DSO or regulator would need to consider to use an LRP tariff in the real world in Section 3.6 and conclude the chapter in Section 3.7.

3.2 Load Responsive Pricing

Concept

We assume a DSO provides hourly or sub-hourly volumetric prices for energy in a 24-hour day-ahead schedule, shown in (3.1). In this equation, x_t is the load in kWh, β_t is the volumetric price in \$/kWh, and C_t is the volumetric cost of energy in dollars at time t, and where t is the interval used for the day-ahead price. The most common time interval duration is hourly. Less common time intervals include 5-min and 15-min. We make no assumptions on the source of the β_t prices; these prices can be calculated through DLMPs, scaled wholesale prices, or any other means. Customers may also be exposed to other fixed charges in this tariff. Since fix charges would not impact the response of price-signal controlled loads, we exclude these costs from the analysis in this chapter to focus on volumetric costs.

$$C_t = x_t \cdot \beta_t \tag{3.1}$$

We propose adding a linear pricing component to the dynamic tariff, where the linear component depends on the energy consumed in the given period t. This new combined price becomes a linear pricing curve π_t with a slope component α_t that controls the rate of price increases based on consumption, and an intercept β_t that is the time-varying price of energy (3.2). The purpose of this α_t component is to place a price on congestion in a given period. Equation (3.3) is the total volumetric LRP cost of energy consumption at time t. Fig. 3.1 shows π_t pricing curve and C_t cost curve for a single time t.

$$\pi_t = \alpha_t \cdot x_t + \beta_t \tag{3.2}$$

$$C_t = x_t \cdot \pi_t = x_t \left(\alpha_t \cdot x_t + \beta_t\right) = \alpha_t x_t^2 + \beta_t x_t \tag{3.3}$$

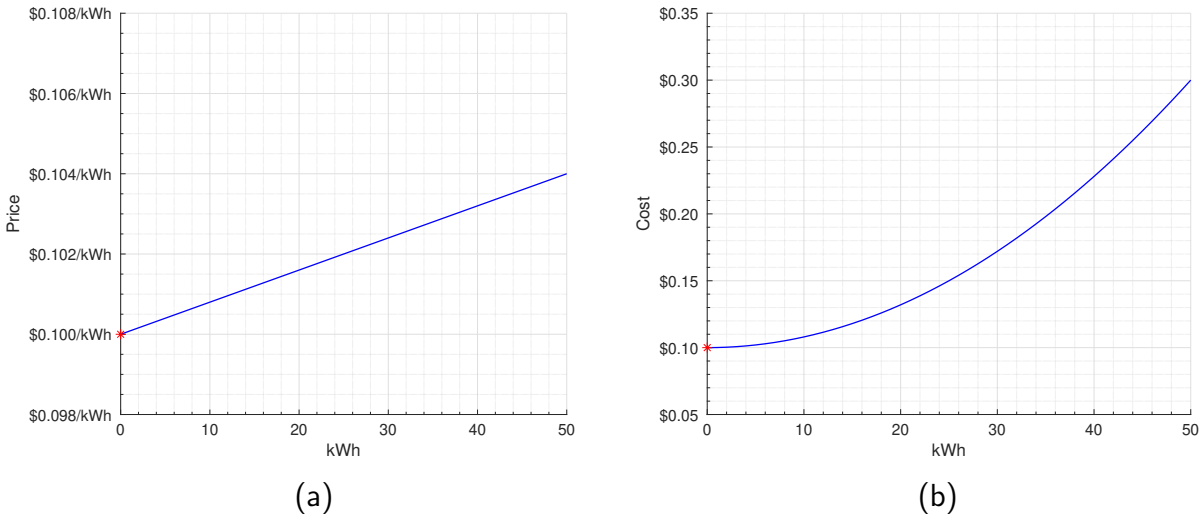

Figure 3.1: A LRP curve for energy at time t with β_t intercept and α_t slope. The value for α_t is exaggerated here for visual clarity. (a) The π_t pricing curve. (b) The total volumetric cost C_t for the time period.

Setting α in LRP

In this chapter we assume that customers will adjust the timing of their controllable load to minimize their total cost C_t and that β_t prices are greater than zero. Under these assumptions, by choosing α_t, a DSO can manage how much a customer will consume at time t. In a system without grid congestion, $\alpha_t = 0$ and the customer would just experience the volumetric energy price β_t. However, if congestion is a concern, the DSO can limit the consumption at time t of a customer by setting $\alpha_t > 0$. The simplest way to set α_t for

LRP is to set a constant α_t for all hours of the day (Fig. 3.2). However, using dynamic α_t values for different pricing periods allows the DSO to designate times when congestion is a concern and minimize cost increases at other times. In the following sections we propose two approaches to calculating α_t values based on β_t prices and system conditions. The first is an optimal-α approach that can be used if a DSO can determine optimal load profiles for its customers. However, if this is not feasible for the DSO, we also present a heuristic based system pricing in Section 3.4.

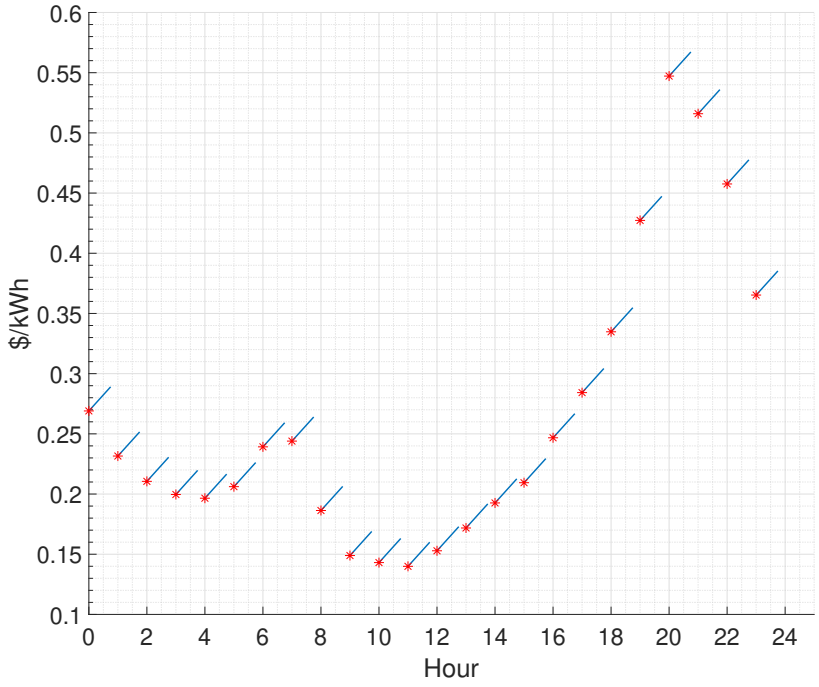

Figure 3.2: A Constant-α, hourly LRP. The intercept at each hour is the β_t (red asterisk) while the price is calculated with a slope of α for all times t

3.3 Optimal-α LRP

Concept

If the DSO can accurately forecast each customer's total energy demand over an optimization horizon, they can use the their results to calculate α coefficients in the LRP. For example, the DSO use an optimal powerflow analysis to determine the optimal load profile for controllable loads on a distribution feeder. This "optimal-α LRP" method uses the these load profiles as

a target profile for LRP customers and sets α_t values for each customer that will cause the customer to optimize to the target load levels given any set of β_t prices.

The optimal-α LRP shares some similarities to the Dynamic Power Tariff (DPT) proposed in Huang et al. [28], though the prices are constructed in different ways. Huang et al. build on their quadratic DLMP pricing work [27] by proposing a quadratic power tariff with prices determined through an iterative process between the distribution system operator (DSO) and customers (in their paper these customers are DER aggregators), where customers propose load profiles and the DSO updates the DPT prices with marginal network costs calculated from an OPF using dc powerflow. In this approach, the day-ahead prices are calculated concurrently in the same process as the load profiles are negotiated.

In the optimal-α LRP, we separate the calculation of α_t prices to occur after target load profiles and β_t energy prices are calculated. This decoupled approach allows the DSO to use any OPF strategy they wish to identify the desired load profile. At the same time, β_t prices can be determined via DLMP, directly using wholesale prices, or some other novel method. Optimal-α LRP is agnostic to the approach to calculating load profiles and β_t prices.

Formula

The optimal-α LRP calculates α_t values for each pricing period t given a set of target load profiles for customers ($\hat{x}_t$). For clarity, in the following we assume all of the customer load is controllable and separately metered from non-controllable loads. We address issues for customers with both controllable and non-controllable loads on a single meter at the end of this subsection.

The β_t values can represent wholesale market costs, and they could also include additional time-varying costs DSOs wish to pass on to customers, with the considerations described in Section 3.6. Using the β_t prices, each customer is assumed to solve their own cost minimizing quadratic optimization and the $\hat{x}_t$ values calculated by the DSO are assumed to be feasible solutions given each customer's local constraints. Equation (3.4) represents the quadratic problem customers must solve to minimize their costs, where $x_{1...n}$ is their load at times $t = 1...n$ such that their total load is equal to X.

$$\begin{aligned} \min_{x} \ & \alpha_1 x_1^2 + \beta_1 x_1 + \alpha_2 x_2^2 + \beta_2 x_2 + ... + \alpha_n x_n^2 + \beta_n x_n \\ s.t. \ & x_1 + x_2 + ... + x_n = X \end{aligned} \tag{3.4}$$

Since the customer's optimization is quadratic, there is a set of α_t values that produces a unique solution for the customer's optimal load profile given the β_t prices, as proven in the similarly formulated quadratic DLMP in [27]. By using Lagrange Multipliers, we can calculate these optimal α_t values (3.5)-(3.9).

$$\begin{aligned} \mathcal{L} = & \alpha_1 x_1^2 + \beta_1 x_1 + \alpha_2 x_2^2 + \beta_2 x_2 + ... + \alpha_n x_n^2 + \beta_n x_n \\ & + \lambda(X - x_1 - x_2 - ... - x_n) \end{aligned} \tag{3.5}$$

$$\frac{\partial \mathcal{L}}{\partial x_1} = 2\alpha_1 x_1 + \beta_1 - \lambda = 0 \tag{3.6}$$

$$\frac{\partial \mathcal{L}}{\partial x_2} = 2\alpha_2 x_2 + \beta_2 - \lambda = 0 \tag{3.7}$$

$$\vdots$$

$$\frac{\partial \mathcal{L}}{\partial x_n} = 2\alpha_n x_n + \beta_n - \lambda = 0$$

$$\frac{\partial \mathcal{L}}{\partial \lambda} = X - x_1 - x_2 - ... - x_n = 0 \tag{3.8}$$

We can solve for any α_t in terms of its β_t and the α, β, and x values from any other interval. For example,

$$\alpha_1 = \frac{2\alpha_2 x_2 + \beta_2 - \beta_1}{2x_1} \tag{3.9}$$

Equation (3.10) generalizes (3.9) to calculate optimal $\hat{\alpha}_t$ values – that is, values that cause customers to reproduce the pre-computed optimal $\hat{x}_t$ values – using a selected seed load value $\hat{x}_{t_{\text{seed}}}$, associated $\beta_{t_{\text{seed}}}$ price, and $\alpha_{t_{\text{seed}}}$ value. We can select t_{seed} and $\alpha_{t_{\text{seed}}}$ to minimize the cost to the customer. To do this, we select the time period t with the highest β_t and non-zero load (3.11). For α_{seed}, since the other $\hat{\alpha}_t$ values are calculated from α_{seed}, we select a value that is as small as practical. In our analysis, we used $\alpha_{\text{seed}} = 0$. However, there may be issues with using $\alpha_{\text{seed}} = 0$ if the DSO incorrectly forecasts customer load. We discuss forecasting issues in Section 3.6.

$$\hat{\alpha}_t = \frac{2\alpha_{t_{\text{seed}}}\hat{x}_{t_{\text{seed}}} + \beta_{t_{\text{seed}}} - \beta_t}{2\hat{x}_t} \tag{3.10}$$

$$t_{\text{seed}} = \text{argmax}_t(\beta_{\hat{x}_t > 0}) \tag{3.11}$$

Due to the structure of (3.10) and the non-negativity requirement of the quadratic optimization, we place two constraints on $\hat{\alpha}_t$ to ensure feasibility. In times t when there is no load ($\hat{x}_t = 0$), then $\hat{\alpha}_t$ would calculate to ∞. If the $\hat{\alpha}_t < 0$, then the optimization would become non-convex. In these situations, we replace $\hat{\alpha}_t$ with a finite, non-negative θ value set based on type of controllable load the customer owns using Eq. (3.12).

$$\alpha_t = \begin{cases} \theta, & \text{if } \hat{\alpha}_t = \pm\infty, \\ \theta, & \text{if } \hat{\alpha}_t < 0, \\ \hat{\alpha}_t & \text{else.} \end{cases} \tag{3.12}$$

If the controllable load the customer is optimizing is separately metered, then θ must be larger than the finite $\hat{\alpha}_t$ values calculated in (3.10) to ensure the customer follows the

target load profile $\hat{x}_t$. In this case we set θ to an arbitrarily high value of 10 to ensure finite, non-negative $\hat{\alpha}_t$ values. (We examined performance for other high values of θ and did not observe meaningful differences in the solution.)

$$\hat{x}_t = x_t + \tilde{x}_t \tag{3.13}$$

However, a high value for θ can cause a control issue for the DSO when customers have non-controllable loads (x_t) on the same meter as controllable loads ($\tilde{x}_t$) (3.13), and those controllable loads are bi-directional. If the DSO requires customers to inject energy ($\hat{x}_t < 0$) at times when $\beta_t \neq \max(\beta_t)$, then the DSO needs to ensure that injections ($\hat{x}_t < 0$) also occur at $t = \text{argmax}_t(\beta_t)$. Otherwise, in those times $\alpha_t = \theta$ and customers will optimize to $\hat{x}_t = 0$.

In contrast, a special case occurs if the controllable load is unidirectional ($\tilde{x}_t > 0$) and on the same meter as non-controllable load (3.13). In that situation, the DSO can reduces costs by ignoring $x_{t_{\text{seed}}}$ in $\hat{x}_{t_{\text{seed}}}$ when calculating $\hat{\alpha}_t$ in Eq. (3.11). Then setting $\theta = 0$ reduces $\hat{\alpha}_t$ for times t where the optimal solution would not place controllable load ($\tilde{x}_t = 0$) due to the β_t price. This reduces the price for energy in times where only non-controllable load is consuming ($x_t > 0$) to β_t. This does not work with bi-directional loads ($\tilde{x}_t < 0$), since they would not inject energy at the times prescribed in the target load profile ($\hat{x}_t < 0$).

By calculating $\hat{\alpha}_t$ from Eq. (3.10) – (3.13), we produce the minimum feasible vector of α_t prices that can produce the vector of load profiles x_t given the β_t prices and the $\alpha_{t_{\text{seed}}}$.

3.4 Inverse-Rank LRP

Concept

While the Optimal-α LRP is the minimum cost formulation of Load Responsive Pricing, it requires a target load profile for customers to optimize towards. DSOs can still utilize LRP for congestion management with other formulations as well. The "inverse-rank LRP" (IR-LRP) is a variation of the LRP tariff that manages congestion via a heuristic method to set α_t. It works by increasing α_t inversely to the β_t energy price.

Method

The method for calculating α_t values for IR-LRP assumes that price-optimizing controllable loads are most likely to cause congestion management issues at times when energy prices are the lowest in the day.

First, the DSO defines an n-length $\boldsymbol{\tau}$ as vector of evenly spaced values on an interval $[\tau_{\min}, \tau_{\max}]$. They then re-index the $\boldsymbol{\tau}$ vector such that the index of the smallest entry of $\boldsymbol{\tau}$ equals the index of the largest $\boldsymbol{\beta}$ entry, the index of the second smallest entry of $\boldsymbol{\tau}$ equals the index of the second largest entry of $\boldsymbol{\beta}$, and so on.

For our case studies and in preliminary load control testing, we found an effective linear range for $\boldsymbol{\tau}$ is $[0.1, \tau_{\max}]$ with $\tau_{\max} \in [1, 3]$ depending on how much load shifting is required by the DSO. The larger the value of $\tau_{\max}$, the more load will be shifted away from the minimum β_t period.

Then the α_t values are set by:

$$\alpha_t = \tau_t \cdot \eta, \tag{3.14}$$

where η is a customer scaling factor corresponding with the size of their combined controllable and non-controllable load on the same meter. Each customer or customer class can have an η set for their controllable load size at the time of adoption of the IR-LRP tariff. Without η or with a single η value, larger customers would see higher prices than smaller customers because they consume more non-controllable load. For example, a DSO can have an $\eta = 0.001$ for a customer class up to 100 kW and $\eta = 0.0001$ for a separate customer class up to 1000 kW. By using different η values for different customer sizes, the DSO can control how much each customer is shifting their load and also ensuring costs rise at a rate commensurate with the customer's relative shift in load.

Once a DSO has assigned an η, τ_t can be calculated each time period and multiplied by η to produce the set of α_t prices (3.14). Fig 3.3 shows a hypothetical set of IR-LRP prices with a constant controllable load.

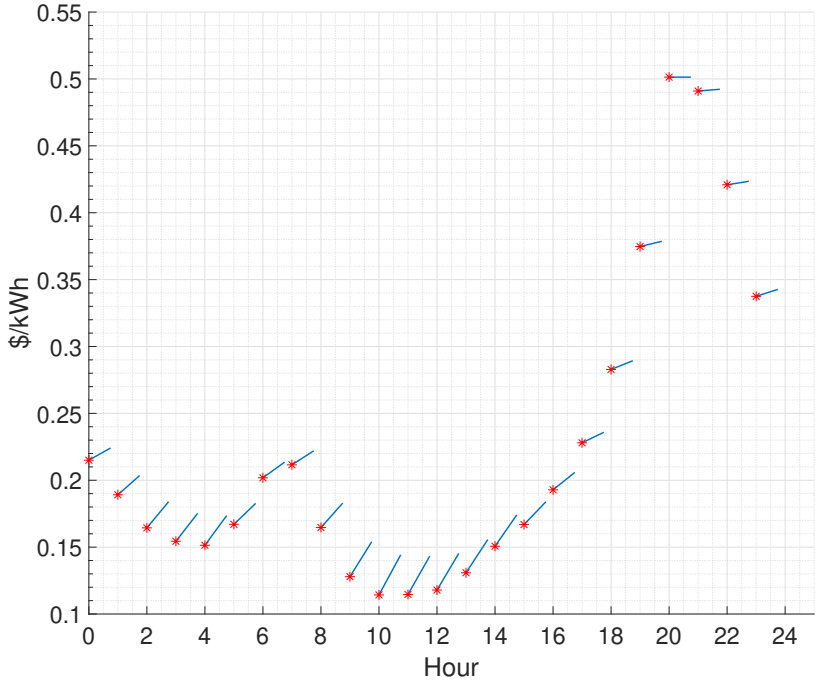

Figure 3.3: Hypothetical hourly IR-LRP example with constant load. The intercept at each hour is the β (red asterisk) while the α is the slope of the blue line. In this example, 10am is the lowest β price and has the highest α, $\alpha = 3\eta$. While 8pm has the highest β price and lowest α, $\alpha = 0$.

3.5 Case Study

To compare the LRP approaches, we modeled two case studies. The first case study is a single building to examine the effectiveness of LRP to shape a customer's load profile. The second case study measures the effects of LRP for congestion management on a test system with high potential of network congestion. To show the diversity of applications for LRP, we use different β_t price sources, load type (bi-directional vs. unidirectional), and connection (separately metered vs single meter) in each case study.

Case Study I

This first case study shows how LRP can be used for price-signal control of a single customer. We model a customer's optimal load profile under a day-ahead energy pricing tariff, the IR-LRP, and the Optimal-α LRP. We performed the optimizations in MATLAB R2020a [77] using YALMIP [78] with Gurobi [79] as the solver. All calculations and simulations were

performed on an AMD Ryzen 7 3700X desktop PC with 32GB of RAM, running Windows 10.

In this model, we assume the customer has their controllable loads separately metered from their other building loads. Specifically, we assume the customer requires 60 kWh of energy at a maximum of 20 kW. The customer also has an energy storage system they want to use to sell 10 kWh of energy to the DSO at a maximum power of 10 kW. However, for this case study we assume the DSO wants to limit peak power for this customer to 15 kW. We also assume the DSO does not have any means of communication or control of the customer except the ability to send a set of α_t and β_t prices.

Table 3.1 lists the β_t prices for this customer. We used a set of hourly volumetric energy prices designed by Lawrence Berkeley National Laboratory (LBNL) to provide full cost recovery to the utility [124]. These prices are the hourly prices from the LBNL study for March 1st, 2019 in the San Diego Gas and Electric (SDG&E) territory. We use these β_t prices both for LRP tariffs and in the day-ahead energy pricing tariff to compare the customer's load profile in a hourly pricing program without LRP.

Table 3.1: β_t values for Case Study I

Hour	β_t(\$/kWh)	Hour	β_t(\$/kWh)
0	0.2198	12	0.1455
1	0.2074	13	0.1630
2	0.2044	14	0.1711
3	0.1945	15	0.1839
4	0.2081	16	0.2739
5	0.2632	17	0.4124
6	0.3349	18	0.5185
7	0.3226	19	0.4680
8	0.2318	20	0.4213
9	0.1773	21	0.3841
10	0.1479	22	0.3393
11	0.1397	23	0.2833

We model the customer behavior and energy billing at the 15-min timescale to match the measuring frequency of an SDG&E business smart meter. However, since the prices in the case study are hourly, we report our results in hourly intervals.

IR-LRP Parameters

For this case, we assume the DSO has set $\eta = 0.001$ for the the IRP-LRP for this customer's customer class. Using these parameters for this customer and the β_t prices, the IR-LRP first creates a set of τ_t values which then generate a set of α_t prices with the largest α_t at 11:00 and the smallest α_t at 18:00 (Table 3.2).

Table 3.2: IR-LRP τ_t values in $[0.1, 1.5]$ and α_t (10^{-4}\$/kWh^2) values for Case Study I

Hour	τ_t	α_t	Hour	τ_t	α_t
0	0.83	8.30	12	1.44	14.39
1	0.95	9.52	13	1.32	13.17
2	1.01	10.13	14	1.26	12.57
3	1.07	10.74	15	1.13	11.35
4	0.89	8.91	16	0.65	6.48
5	0.71	7.09	17	0.28	2.83
6	0.47	4.65	18	0.10	1.00
7	0.53	5.26	19	0.16	1.61
8	0.77	7.70	20	0.22	2.22
9	1.20	11.96	21	0.34	3.43
10	1.38	13.78	22	0.40	4.04
11	1.50	15.00	23	0.59	5.87

Optimal-α LRP Design

In contrast to the IR-LRP where the DSO creates prices to curtail load at its peak, the Optimal-α LRP allows a DSO to incentivize a customer to follow a specific load profile. In this case, we assume the DSO knows the customer's energy needs and wants the customer to consume and discharge energy at the levels in Table 3.3. We make no assumptions on the approach the DSO took to calculate these values and the DSO does not communicate this target load profile to the customer. Instead, the DSO uses this target load profile to calculate α_t values for the customer to use in their optimization to recreate this load profile as their optimal solution.

Using the Optimal-α formula, we calculate the optimal α_t prices for the customer (Table 3.3). Note that $\alpha_t = 10$ for hours when there is no load in the target load profile. As such, the customer's cost in those hours is \$0 when they optimize their load.

Results

Using the day-ahead pricing, IR-LRP, and Optimal-α LRP, we model the customer minimizing their costs in a 24-hour optimization. Figure 3.4 shows the resulting load profiles for this customer following these three tariffs. Under day-ahead pricing, the customer maximizes their consumption up to their local load limit (20 kW) for the three lowest β_t hours of the day. In contrast, under the IR-LRP tariff, the customer's load was spread across more hours. Finally, under the Optimal-α LRP tariff, the customer followed the target load profile of the DSO to within 0.06 kWh accuracy. This accuracy can be improved to 0.002 kWh when the optimization is performed in watt-hours instead of kilowatt-hours. These results show that LRP can effectively shift customer load.

Table 3.3: Optimal-α LRP target load profile (kWh) and α_t (10^{-4}\$/kWh^2) values for Case Study I

Hour	kWh	α_t	Hour	kWh	α_t
0	0.	10	12	13	0.0033
1	0.	10	13	3.	0.0115
2	0.	10	14	5.	0.0061
3	0.	10	15	0.	10
4	0.	10	16	0.	10
5	0.	10	17	0.	10
6	0.	10	18	-10.	0.0143
7	0.	10	19	0.	10
8	10.	1×10^{-13}	20	0.	10
9	2.	0.0136	21	0.	10
10	12.	0.0035	22	0.	10
11	15.	0.0031	23	0.	10

Figure 3.5 shows the total marginal \$/kWh price at each hour for the three different tariffs. We calculate the IR-LRP and Optimal-α LRP \$/kWh at the resulting load levels from Figure 3.4. The IR-LRP had a maximum hourly price increase of \$0.0227/kWh over the day-ahead pricing tariff, and the Optimal-α LRP had a maximum price increase of \$0.0461/kWh. However, the price the customer would receive for the energy they sold back to the grid fell by \$0.1425/kWh. Over the course of a billing period, these changes would result in increased bills for the customer. We explore monthly billing effects of LRP in Case Study II and discuss several strategies a DSO could employ to mitigate these cost increases in Section 3.6.

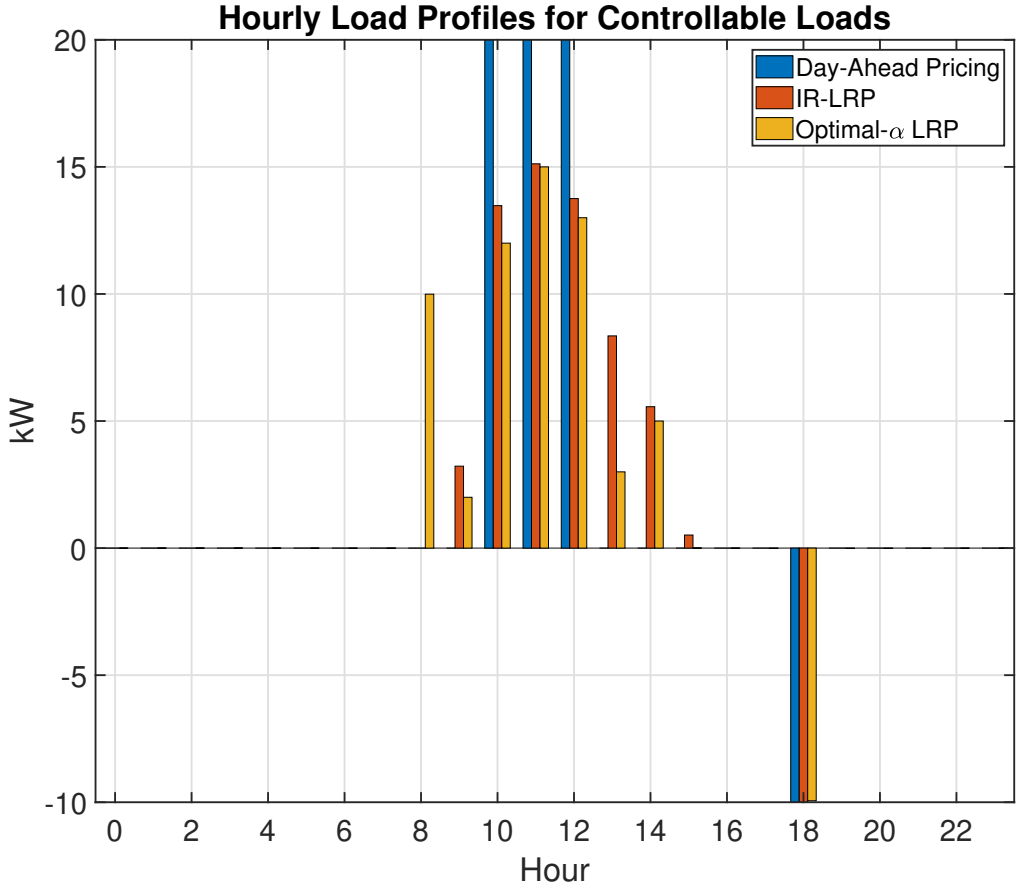

Figure 3.4: Case Study I - Load profile for a customer following the day-ahead pricing tariff, IR-LRP, and Optimal-α LRP

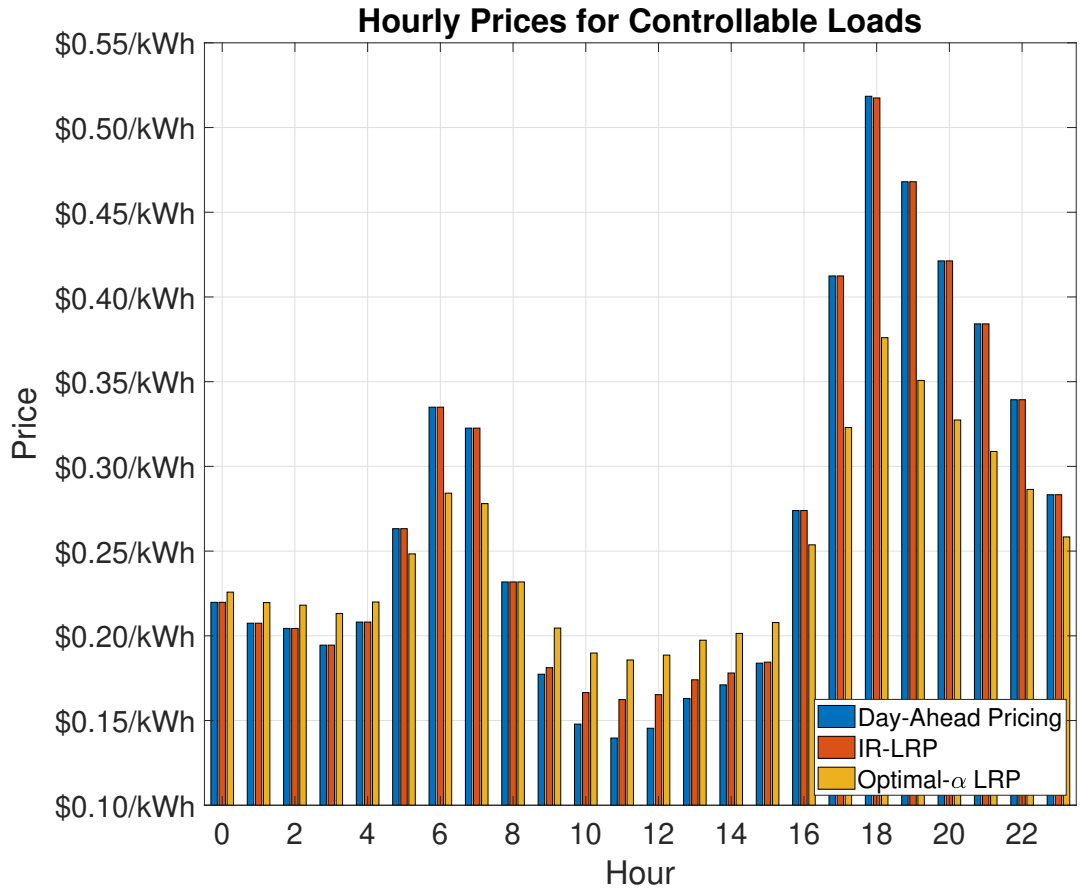

Figure 3.5: Case Study I - Prices for a customer following the day-ahead pricing tariff, IR-LRP, and Optimal-α LRP

Case Study II

To examine the congestion management capabilities of LRP, we use the same test system we described in Chapter 1. We summarize the distribution system, building, and EV model design here but refer the reader to Section 1.2 for more details on the models. In this model, we compared commercial customers optimizing their EV charging in a centralized optimization to a decentralized LRP approach where customers optimized only for their costs. We modeled the centralized optimization as a cost minimizing linear program under day-ahead hourly prices.

We performed the optimizations in MATLAB R2020a [77] using YALMIP [78] with Gurobi [79] as the solver and the distribution system powerflow simulations were modeled in Gridlab-D [70]. All calculations and simulations were performed on an AMD Ryzen 7 3700X desktop PC with 32GB of RAM, running Windows 10.

Model Design

For our distribution feeder, we used a 17-mile, three-phase unbalanced distribution feeder created by PG&E to model an existing urban distribution feeder in the inland area of Northern California [71]. The feeder has overhead and underground power lines supplying 2,894 residential customers, 270 commercial customers, and 91 industrial customers. To provide load diversity, we modified the feeder model to incorporate 10 different building models from the Department of Energy's Commercial Reference Building models and Building America House Simulation Protocols for the residential building models [63], [72].

We optimized the EV charging of two types of three-phase customers, medium office building customers and warehouse customers, each with fleets of electric vehicles operating as flexible, price-optimizing loads. We modeled all 91 industrial customers on the feeder as warehouse buildings and five of the commercial customers as medium-sized office buildings. We modeled a total of 2,160 EVs on the distribution feeder, 10 EVs at each of the 91 warehouses and 250 EVs at each of the 5 office buildings, for a combined load of 43.2 MWh per day or 1.34 GWh per month. Before running our optimization, we verified that the feeder could support charging the total number of EVs we modeled without voltage constraint violations if the vehicles did not all charge in the same time period.

For prices, we used the same hourly prices from Chapter 2. These prices come from the Avoided Cost Calculator developed by the energy consulting firm E3 for the California Public Utilities Commission to determine the benefit of distributed energy resources [75]. The ACC calculates the avoided cost of energy for every hour of the year by modeling the combined costs of wholesale energy, system capacity, and environmental damages from greenhouse gases. Specifically, we use the 2022 edition of ACC electricity prices for the PG&E climate area 12 in the year 2023 [76]. We used the ACC prices as both a measure of the total social cost and as a day-ahead hourly price for the office building and warehouse customers.

Centralized Optimization

To simulate the centralized optimization, we use the same linear programming model developed in Chapter 2 to minimize the daily cost of charging a fleet or collection of electric vehicles at customer locations (3.15). Where π_t is the ACC price at time t, $\tilde{x}_{i,b,t}$ is the sum of all EV loads and $x_{i,b,t}$ is the sum of all non-controllable building loads at building b in set of B_i buildings at node i the set of nodes I at time t. The local loading limit prevent coincidental load from exceeding the circuit breaker limit of each customer. Real power from a single EV l in the set of all EVs L_b at a building is represented by $w_{l,i,b,t}$ and is constrained by the EV operating constraints, which are the maximum charging rates of each EV (7.2kW) with only unidirectional flow from the grid to charge the EV. We modeled each EV requiring 20kWh/day to model an extreme case for EV charging. We also required each EV to be fully charged at the end of each day.

$$\begin{aligned}
\min_{\tilde{x}} \text{Cost} = & \sum_{t=1}^{24 \text{ hours}} \sum_{i=1}^{I} \sum_{b=1}^{B_i} \pi_t \cdot (\tilde{x}_{i,b,t} + x_{i,b,t}) \\
s.t. \quad & (\tilde{x}_{i,b,t} + x_{i,b,t}) \leq \text{Local loading limit} \\
& \tilde{x}_{i,b,t} = \sum_{l=1}^{L_b} w_{l,i,b,t} \\
& w_{l,i,b,t} \leq \text{EV operating constraints} \\
& \sum_{t=1}^{24\text{hrs}} \tilde{x}_{i,b,t} = \text{charging energy required for EVs at the building}
\end{aligned} \tag{3.15}$$

The linear program minimizes the total cost to the customer for their building loads and the charging of all the electric vehicles at the customer's site. In our analysis, we only optimized EV charging; the building loads were treated as exogenous to the optimization and only included for their impact on the voltage constraint and costs. We repeated this daily optimization for every day in the month of July.

We performed the centralized optimization first without a voltage constraint and then with a linearized voltage magnitude constraint (3.16) and (3.17) based on the LinDistFlow equations developed by Baran and Wu [104] and extended into three-phase versions in [105] and [106]. This LinDisFlow (LDF) constraint ensured voltage magnitude at all nodes in the centralized optimization was kept at or above 0.95pu as required by ANSI C84.1 [69].

$$\begin{aligned}
|V_{\phi_k,t}|^2 \approx |V_{\phi_i,t}|^2 - 2(R_{\phi_k}(\boldsymbol{P}_t + \tilde{\boldsymbol{P}}_t) + X_{\phi_k}(\boldsymbol{Q}_t + \tilde{\boldsymbol{Q}}_t)) \\
\forall i, k \in I
\end{aligned} \tag{3.16}$$

$$|V_{\phi_k,t}|^2 \geq |V_{min}|^2 \quad \forall k \in I, \forall t \in 24 \text{ hours}, \tag{3.17}$$

where $|V_{\phi_i,t}|$, $|V_{\phi_k,t}|$ are voltages at each phase ϕ at node i and k respectively at time t, and i, k denote nodes in set I of all nodes for the feeder. The line resistance and reactance for each phase ϕ from i to k are R_{ϕ_k}, X_{ϕ_k} respectively. $\boldsymbol{P}_t$ and $\boldsymbol{Q}_t$ are the vectors of uncontrollable building load real and reactive power at each phase ϕ of the load nodes respectively, while $\tilde{\boldsymbol{P}}_t$ and $\tilde{\boldsymbol{Q}}_t$ are the vectors of controllable EV load real and reactive power at time t. Building loads were assumed to have a power factor of 0.9 and EVs were assumed to have unity power factor. All loads were modeled as constant power loads and all loads at three-phase connected buildings were modeled as balanced three-phase loads across each phase ϕ (3.18). $V_{\min}$ is the ANSI C84.1 voltage minimum value for delivered energy (0.95pu).

$$P_{\phi_i,t} = \frac{1}{3}\sum_{b=1}^{B}(x_{i,b,t}), \quad Q_{\phi_i,t} = P_{\phi_i,t} \times \tan(\cos^{-1}(0.9)) \tag{3.18}$$
$$\tilde{P}_{\phi_i,t} = \frac{1}{3}\sum_{b=1}^{B}(\tilde{x}_{i,b,t}), \quad \tilde{Q}_{\phi_i,t} = 0$$

However, customers in a central optimization with a voltage constraint would experience different costs based on their location in the distribution feeder. Customers in more congested areas might need to shift more load into higher cost hours than customers in less congested areas. While we leave equity considerations of this to policymakers, in our optimization all EV load of the same building model type are optimized to have the same load profile to allow for a simple comparison of customer bills across the distribution feeder.

LRP Designs

For the LRP tariffs, we had each customer optimize against their α_t and β_t prices. The β_t prices were the same ACC prices used in the centralized optimization. While the α_t was calculated using the IR-LRP and Optimal-α LRP formulas.

Table 3.4 lists the IR-LRP values used in this case study. Note that η scaling factors for medium office building and warehouse building models are equivalent to \$0.0001/100kWh and \$0.0001/10kWh. These η values were based on the order of magnitude of the non-controllable load at each building model.

Table 3.4: IR-LRP τ_t and η values for Case Study II

τ_t range	Office Building η	Warehouse η
[0.1, 3]	1×10^{-6}	1×10^{-5}

For the Optimal-α LRP, we used the EV load profiles from the centralized optimization with the LDF constraint as target load profiles. The maximum absolute difference between the target load profiles and those generated by the optimal-α LRP was 3.57×10^{-4} kWh. The

resulting voltage profiles when modeled in Gridlab-D had a maximum absolute difference of 8.97×10^{-6} V. Since the EV loads were modeled as unidirectional loads and on the same meter as the building loads, we used the maximum β_t hour with EV load from our target load profiles when calculating the α_{seed} using (3.11). This allowed $\alpha_t = 0$ for all hours t where $\tilde{x}_{i,b,t} = 0$.

Results

Table 3.5 lists the number of voltage violations over the month and maximum violation for each of the optimization scenarios. Table 3.6 shows the volumetric cost to an individual customer for following each of the different tariffs and social cost of all customers on the feeder optimizing against each tariff (measured in ACC costs).

As expected, the ACC optimization without a voltage constraint caused severe voltage violations multiple times throughout the month. While the 9 days of voltage violations might be mitigated with CPP programs, since most CPP programs limit CPP events to less than 20 per year, it may not be possible to control voltage over the entire year with CPP programs only. However, the costs of the ACC optimization provides a cost basis to compare the other tariff designs.

The centralized optimization with the LDF constraint and both LRP tariffs kept voltage above 0.95pu. The centralized optimization with LDF constraint tariff resulted in the lowest cost for a customer. However, from the social cost perspective, the IR-LRP cost less to charge EVs across the entire distribution feeder. We believe this was due to the linear nature of the LDF constraint limiting the acceptable voltage range. If the voltage constraint in the centralized optimization could exactly model voltage in the distribution feeder, then the centralized optimization with this voltage constraint would have a lower social cost.

Table 3.5: The minimum voltage measured across all customer locations in July, and the number of days voltage is below the ANSI C84.1 lower limit for voltage in Case Study II

Tariff	Minimum Voltage (Per Unit)	Number of days voltage < 0.95 pu
ACC	0.9265	9
ACC w/ LDF Constraint	0.9524	0
Optimal-α LRP	0.9524	0
IR-LRP	0.9563	0

Table 3.7 lists the percent difference between these costs and the costs of optimizing against the ACC tariff without constraints. While the LRP tariffs did increase costs, as expected from a price-signal control approach, the cost increase were less than 10% when compared to the centralized optimization that resulted in voltage violations. A question for rate-makers would be if the value of a decentralized congestion management would more

Table 3.6: The monthly volumetric costs when optimizing under each tariff for an office building customer, warehouse customer, and the social cost (in ACC dollars) of all medium office and warehouse customers on the distribution feeder in Case Study II

Tariff	Office Building	Warehouse	Social Cost
ACC	\$10,940.59	\$1,638.69	\$203,824.11
ACC w/ LDF Constraint	\$11,068.12	\$1,649.60	\$205,453.89
Optimal-α LRP	\$11,439.58	\$1,712.87	\$205,453.89
IR-LRP	\$11,538.82	\$1,681.13	\$204,455.22

than the precent increase in cost for customers. In the following Section we explore this issue and provide recommendations for reducing costs to the customer.

Table 3.7: The percent difference between the ACC tariff monthly volumetric costs and costs of other tariffs in Case Study II

Tariff	Office Building	Warehouse	Social Cost
ACC	—	—	—
ACC w/ LDF Constraint	1.17%	0.67%	0.80%
Optimal-α LRP	4.56%	4.53%	0.80%
IR-LRP	5.47%	2.59%	0.31%

3.6 Real-world Considerations

While we have shown the LRP approach is an effective price-signal for congestion management, there are several potential issues that a DSO would need to consider before adopting this tariff. In this section, we discuss the real-world considerations of the LRP tariff design. We start with general considerations of an LRP tariff and then discussion considerations of both variations of the LRP tariff provided in this chapter.

First, the LRP tariff is complex compared to standard two-part tariffs with constant marginal costs. The LRP tariff is designed to influence the behavior of automated devices and works best when the customer is able to employ a quadratic optimization solver. This tariff should not be used as the default tariff for customers unless they have a sophisticated level of automation and control over their loads.

Second, this tariff assumes the β_t prices are accurate price signals and that β_t prices would be sufficient signals if network congestion was not an issue. If customers are not

consuming in the preferred time period of the DSO, the DSO should first adjust β_t prices to incentivize consumption during those hours. Only after the β_t price is set for each time period should the α_t prices be set to create a soft cap incentive on consumption. The LRP tariff can compensate if β_t prices are incentivizing for times that are problematic for the DSO but this comes at the cost of high α_t prices for customers, leading to the next consideration.

Third, LRP can have important cost impacts. We propose that this tariff should not capture more revenue than a real-time tariff and a well designed LRP tariff can minimize the cost impacts on consumers. However, a poorly designed tariff can cause significant cost increases for customers since the costs grow quadratically with load. The DSO or regulator will need to carefully set $\boldsymbol{\alpha}$ and $\boldsymbol{\beta}$ for each customer or customer class to prevent excessive cost burdens. In addition, revenue balancing mechanisms may need to be deployed. Baseline load profiles like those used in the real-time pricing scheme at Georgia Power, subscription plans, or annual credits to return excess revenue to customers could all be explored as ways to keep any sales generated by the $\boldsymbol{\alpha}$ coefficient revenue neutral.

Fourth, we have shown two different ways to calculate α_t prices for an LRP tariff. There are potentially other methods as well. Prices could be set with a granularity as low as the specific customer at a single location on a distribution feeder or as broad as a customer class in a utility service territory. The one key consideration for calculating α_t values is that they should always be non-negative for unidirectional loads or positive for bi-directional loads to preserve the quadratic formulation of the customer's optimization problem.

Finally, the LRP tariff only provides a price for real power. In the future, DSOs may want to incentivize customers to provide reactive power. The LRP tariff could be used to incentivize reactive power but this would require putting a price reactive power and is beyond the scope of this work.

Optimal-α LRP Considerations

The optimal-α LRP calculates the minimum $\boldsymbol{\alpha}$ required at each time period for customers to shift load to follow a target profile determined through the DSO's optimization. However, there are several issues that can arise with the optimal-α LRP. First, as seen in Case Study II, optimal-α LRP does not guarantee the the total costs for the customer will be the minimum cost possible. If the target load profile is not optimal, the results of Optimal-α LRP will not be either.

Second, the optimal-α LRP depends on an accurate forecast to calculate α_t values. The structure of LRP ensures that customers will still optimize their load if the forecast is wrong however different issues arise if the DSO overestimates vs. underestimates their forecast.

If the DSO overestimates customer load in their forecast, customers will follow the general load shape the DSO intended with $\boldsymbol{\alpha}$ at a lower energy consumption at each time period. However, if a DSO underestimates load in their forecast, congestion issues can quickly arise. One solution to this issue is to always overestimate the expected load in the forecast. From a congestion management perspective, this is not a problem. Overestimating load will only cause congestion if the overestimated load level would be enough to cause congestion.

In cases where overestimating is not an option or if customer load exceeds the overestimated forecast, the customer a DSO underestimated will follow the load shape the DSO intended unless in any time period $\alpha_t = 0$. In those periods customers only optimize against β_t and will consume energy without a linear price on quantity. As such, the majority of overestimated load will occur when $\alpha_t = 0$. One way to mitigate this issue is to assign any $\hat{\alpha}_t = 0$ a nonzero value after the calculating the $\hat{\alpha}_t$ prices. For example, if a DSO uses $\alpha_{t_{\text{seed}}} = 0$, then after calculating the $\hat{\alpha}_t$ values, the DSO could set $\alpha_{t_{\text{seed}}} = \min(\hat{\alpha}_t)$. Then overestimated load will not cluster at $\alpha_{t_{\text{seed}}}$.

Third, the Optimal-α LRP calculates α_t prices assuming that customers can accurately follow their target load profiles provided by the DSO. If customers have binding constraints in their optimization preventing this, the DSO's optimization should be updated to endogenize these constraints and recalculate the target profiles.

Finally, since the DSO calculates prices based on the optimal load profile for each customer, the DSO could measure a customer's deviation from this ideal profile. This deviation could be the basis for performance metrics that compensate the customer for participating in the LRP tariff.

IR-LRP Considerations

The IR-LRP is an effective heuristic pricing tariff for near communication-free congestion management that does not require any additional sensing or control equipment to deploy. However, it has several drawbacks and considerations that are important to highlight. First, the algorithm is a heuristic that assumes the β_t prices will cause congestion management issues that need to be mitigated. The IR-LRP does not have knowledge of the status of the grid or customer loads. Instead, the IR-LRP assumes that the worst congestion will occur at the lowest β_t prices.

Second, the IR-LRP algorithm is effective for over-consumption at low β_t price times but is not effective at controlling bi-directional loads at high cost hours. The α_t calculation does provide incentives to curtail solar or discharging of energy storage back onto the grid during expensive β_t price hours, and this could lead to over-voltage situations. In those circumstances, changing the β_t price is the best strategy to prevent over-voltage.

Finally, with more advanced sensing and grid awareness, a DSO could deploy IR-LRP with dynamic $\boldsymbol{\tau}$ and η values to improve load control and reduce costs. However, if a DSO has this ability, other price setting algorithms may be more effective to use in the first place (such as the optimal-α LRP).

3.7 Conclusion

In this chapter we describe a new linear pricing method, Load Responsive Pricing (LRP), for congestion management of price-signal controlled loads. We detail two different methods for calculating prices with LRP and show in case studies how customers would follow these

price signals. We also show how this control method can alleviate network congestion. This work provides an alternative to previous price signal control research by leveraging other load optimization schemes beyond DLMP and provides a heuristic for deployment into the real-world without bi-directional communication or control.

While we proposed the LRP tariff for day-ahead prices, an LRP approach could be used in other applications. One application could be as a control signal for non-monetary systems, such as an internal price-signal for a microgrid where decentralized optimization would reduce the computational burden of the central energy management system. Another application could be a sub-hourly α prices with hourly β prices. This would allow a DSO to create a sub-hourly ramp to reduce hourly discontinuities in aggregate load that may occur under hourly pricing. We intend to explore both areas in future research.

As DSOs and regulators explore real-time pricing options and customer loads become more flexible with smarter optimization strategies, congestion management will become a more important issue for grid operations. Traditional volumetric energy pricing cannot alleviate congestion without real-time sensing, optimization, and communication of prices. LRP provides an additional control vector that traditional volumetric energy pricing does not have with a negligible increase communications and a potential revenue-neutral increase in customer costs.

Conclusion

DERs can unlock new economic potential and contribute significantly to decarbonization. However, without proper management, mass adoption of DERs could lead to congestion issues, such as undervoltage, on distribution feeders. Public utility commissions and regulators in states like California are already looking to prepare for high DER adoption future [125]. However, over 200,000 distribution circuits exist in the U.S., totaling over 6.5 million miles [126], [127]. As such, there are limits to how much we can do with computationally burdensome algorithms, system upgrades, and sensor installations. Scalable solutions to congestion management are imperative to unlock the full potential of DERs and ensure the safe, reliable operation of the electric grid.

This dissertation examined the DER congestion management problem and investigate the relationship between tariff design and DER operations. Chapter 1 focused on measuring the impact of this relationship in a high DER adoption future. In Chapter 2, we explored data-driven methods to address congestion management to create computationally scalable solutions for DER congestion. Then in Chapter 3, we return to tariff design to provide a pricing mechanism for DER operations that integrates congestion management into electricity tariffs. In the following section, we summarize the findings from each chapter, offer policy recommendations, and suggest future research areas.

Summary of findings

In Chapter 1, we modeled commercial customers with fleets of electric vehicles, optimizing their EV charging to minimize costs. We showed how retail tariffs impact electric vehicle charging profiles and the resulting impact on customer bills, utility revenue, and distribution system voltage. We also compared tariffs with different demand charges and a tariff with a power subscription to determine the efficiency of power subscription pricing.

We showed congestion-related undervoltage occurred on our model distribution feeder, regardless of the tariff choice. Both demand charge and power subscription plans would cause customers to flatten their load profiles but at insufficient levels to prevent system congestion. We also found that customers could significantly reduce their costs if they switched from a fixed-level demand charge to a time-differentiated demand change. However, this cost savings translated to lost revenue for the utility. While time-differentiated demand charges also reduced utility costs, the loss in revenue was greater and caused an overall loss in net revenue

when customers switched tariffs. Finally, we found that the power subscription examined in this study was less efficient than the existing demand charge-based tariffs researchers have previously criticized for inefficiency.

In Chapter 2, we explored data-driven approaches to congestion management. Specifically, we developed a data-driven voltage estimator based on the LASSO algorithm for distribution system operations. By training the estimator offline on measured smart meter and substation data, we could deploy it as a linear constraint in load optimization problems. We showed high accuracy in voltage estimation on standard test systems and measured its performance on the same EV charging coordination problem from Chapter 1. We found that the LASSO-based voltage estimator could perform better than linear three-phase voltage approximations as a voltage constraint, leading to faster computation time and lower costs.

In Chapter 3, we described a new pricing method, Load Responsive Pricing (LRP), for congestion management of price-signal controlled loads. We detailed two different methods for calculating prices with LRP and showed in case studies how customers would follow these price signals. We also showed how DSOs could use LRP to provide decentralized congestion management and incentivize customers to follow optimal load forecasts by only communicating day-ahead prices. We found this control method could alleviate network congestion and described ways to minimize the cost increase customers would experience from price-signal control.

Policy recommendations

We suggest several important policy recommendations from this work. First, policymakers need to consider that our current tariff and market designs can impact DER operations in the race to decarbonize and electrify loads. Poorly designed electricity pricing mechanisms can not only be economically inefficient but can also perversely incentivize DER operations, such as using energy storage for demand charge management [128]. We recommend that policymakers and regulators move away from demand charge-based tariffs and avoid power subscription tariffs. The price on peak power that these tariffs provide causes cost-optimizing customers to flatten their load profile instead of responding efficiently to time-varying energy prices [44], [83].

Second, policymakers should investigate the cost differences between retail tariff designs and eliminate higher-cost options. We found that customers who cost-optimize their load can save money by selecting one tariff over another. While the lower-cost tariff also reduces wholesale costs for the DSO, the higher-cost tariff generates more net revenue. This revenue difference incentivizes the DSOs to keep customers on the higher-cost tariff even though the lower-cost tariff reduces overall costs for all parties.

Third, policymakers should consider optional tariffs designed for customers with smart energy management systems and aggregators to control customer loads. However, pricing mechanisms in these tariffs need to address congestion management. If all customers on a distribution feeder receive the same schedule of day-ahead scalar energy prices, they will

optimize their consumption towards the same lowest-cost hours and potentially cause grid congestion. Providing pricing mechanisms like LRP would incentivize customers to follow the day-ahead energy prices and incentivize customers to limit their peak consumption to mitigate congestion. However, there are equity implications if DSOs give customers different prices based on their location to address congestion. Policymakers should decide how they want to address the equity and fairness impacts of distribution system congestion management.

Areas for future research

There are several important areas of future research related to this dissertation. The first area researchers could explore is to create a standard set of test cases for comparing electricity tariffs. We created our test case by combining multiple load models across the research space. A set of standard test cases would make future studies of existing and proposed tariffs easier for researchers and allow us to provide better policy recommendations.

Another future research area would be to test data-driven voltage estimators on real-world systems. While our results in distribution system modeling software are encouraging, validating the performance on a physical system should be a priority before DSOs adopt any data-driven estimator for control. To accomplish real-world testing, researchers would also need to integrate work from others on communication delays [22].

In addition to further testing, researchers could extend the physics-informed approach of our voltage estimator to other mathematical approximations. Future work could create quadratic data-driven estimators to predict overcurrent conditions in distribution feeder power lines. Other research could include exploring different congestion-related impacts on the distribution system, such as mitigating overvoltage and excess power losses.

For LRP, there are several future areas to explore. First, researchers could examine how DSOs could use LRP for multi-scale pricing. For example, the intercept price from LRP could come from hourly energy prices, while the linear slope price could vary every five or fifteen minutes to provide ramping control. In addition, researchers could explore LRP for real-time energy markets or decentralized control in microgrids or multi-building energy management systems.

An open question also remains in equity impacts of congestion management. Although we recommend that policymakers address equity, researchers should explore different approaches to ensure fairness and equity in electricity tariffs with congestion management. With direct control approaches, DSOs could add price equity metrics to a centralized optimization. While DSOs using indirect methods could ensure customers are given prices that enable equity and fairness. However, further research should be conducted to determine what are the best approaches and what the value of such mechanisms are.

Finally, we performed all of our research on radial distribution feeders. A future research area would be to test the congestion management tools we developed here in meshed distribution networks [129]. While engineers designed meshed networks to prevent under-

voltage under high loads, there are significant gaps in the literature around meshed network distribution systems and open questions on DER integration into these systems.

Bibliography

[1] M. Willrich, *Modernizing America's Electricity Infrastructure*. The MIT Press, Oct. 2017, ISBN: 978-0-262-34240-7. DOI: 10.7551/mitpress/11045.001.0001.

[2] "Unlocking the Potential of Distributed Energy Resources," IEA, Paris, 2022. [Online]. Available: https://www.iea.org/reports/unlocking-the-potential-of-distributed-energy-resources.

[3] FERC Order 2222, "Participation of Distributed Energy Resource Aggregations in Markets Operated by Regional Transmission Organizations and Independent System Operators," Federal Energy Regulatory Commission, Docket No. RM18-9-000, Sep. 17, 2020.

[4] H. Kramer, R. Brown, R. Tang, and J. Granderson, "The Value of Distributed Energy Resources to Owners: A Current Market Landscape," Presentation for Better Buildings Alliance, U.S. Department of Energy, May 2020. [Online]. Available: https://betterbuildingssolutioncenter.energy.gov/webinars/value-distributed-energy-resources-owners-a-current-market-landscape.

[5] B. Shen, F. Kahrl, and A. J. Satchwell, "Facilitating power grid decarbonization with distributed energy resources: Lessons from the united states," *Annual Review of Environment and Resources*, vol. 46, no. 1, pp. 349–375, 2021. DOI: 10.1146/annurev-environ-111320-071618.

[6] D. Steinberg, D. Bielen, J. Eichman, *et al.*, "Electrification and Decarbonization: Exploring U.S. Energy Use and Greenhouse Gas Emissions in Scenarios with Widespread Electrification and Power Sector Decarbonization," National Renewable Energy Lab.(NREL), Golden, CO (United States), 2017. DOI: 10.2172/1372620.

[7] E. Larson, C. Greig, J. Jenkins, *et al.*, "Net-Zero America: Potential Pathways, Infrastructure, and Impacts," Princeton University, interim report, Dec. 15, 2020. [Online]. Available: https://netzeroamerica.princeton.edu/img/Princeton_NZA_Interim_Report_15_Dec_2020_FINAL.pdf.

[8] "Accelerating Decarbonization of the U.S. Energy System," National Academies of Sciences, Engineering, and Medicine, Washington, DC: The National Academies Press, 2021. DOI: 10.17226/25932. [Online]. Available: https://www.nap.edu/catalog/25932/accelerating-decarbonization-of-the-us-energy-system.

[9] "A Guidebook to the Bipartisan Infrastructure Law," The White House, Washington D.C., May 2022. [Online]. Available: https://www.whitehouse.gov/build/guidebook/.

[10] "Building a Clean Energy Economy: A Guidebook to the Inflation Reduction Act's Investments in Clean Energy and Climate Action," The White House, Washington D.C., Jan. 2023. [Online]. Available: https://www.whitehouse.gov/cleanenergy/inflation-reduction-act-guidebook/.

[11] I. J. Pérez-Arriaga, J. D. Jenkins, and C. Batlle, "A regulatory framework for an evolving electricity sector: Highlights of the mit utility of the future study," *Economics of Energy & Environmental Policy*, vol. 6, no. 1, Mar. 2017, ISSN: 21605882. DOI: https://doi.org/10.5547/2160-5890.6.1.iper. [Online]. Available: http://www.proquest.com/docview/2526350122/abstract/7A6C9885F29843BCPQ/2.

[12] P. De Martini and L. Kristov, *Distribution Systems in a High Distributed Energy Resources Future*. Oct. 2015, vol. FEUR Report No. 2. [Online]. Available: https://eta-publications.lbl.gov/sites/default/files/lbnl-1003797.pdf.

[13] R. Dobbe, O. Sondermeijer, D. Fridovich-Keil, D. Arnold, D. Callaway, and C. Tomlin, "Toward distributed energy services: Decentralizing optimal power flow with machine learning," *IEEE Transactions on Smart Grid*, vol. 11, no. 2, pp. 1296–1306, Mar. 2020, ISSN: 1949-3061. DOI: 10.1109/TSG.2019.2935711.

[14] R. Hledik, J. Lazar, and L. Schwartz, *Distribution System Pricing with Distributed Energy Resources*. Aug. 2017. DOI: 10.2172/1375194.

[15] K. Clement-Nyns, E. Haesen, and J. Driesen, "The impact of charging plug-in hybrid electric vehicles on a residential distribution grid," *IEEE Transactions on Power Systems*, vol. 25, no. 1, pp. 371–380, Feb. 2010, ISSN: 1558-0679. DOI: 10.1109/TPWRS.2009.2036481.

[16] R. Passey, T. Spooner, I. MacGill, M. Watt, and K. Syngellakis, "The potential impacts of grid-connected distributed generation and how to address them: A review of technical and non-technical factors," en, *Energy Policy*, Sustainability of biofuels, vol. 39, no. 10, pp. 6280–6290, Oct. 2011, ISSN: 0301-4215. DOI: 10.1016/j.enpol.2011.07.027.

[17] J. A. P. Lopes, F. J. Soares, and P. M. R. Almeida, "Integration of electric vehicles in the electric power system," en, *Proceedings of the IEEE*, vol. 99, no. 1, pp. 168–183, Jan. 2011, ISSN: 0018-9219, 1558-2256. DOI: 10.1109/JPROC.2010.2066250.

[18] M. A. Cohen and D. S. Callaway, "Effects of distributed pv generation on california's distribution system, part 1: Engineering simulations," en, *Solar Energy*, Special issue: Progress in Solar Energy, vol. 128, pp. 126–138, Apr. 2016, ISSN: 0038-092X. DOI: 10.1016/j.solener.2016.01.002.

[19] M. Blonsky, A. Nagarajan, S. Ghosh, K. McKenna, S. Veda, and B. Kroposki, "Potential impacts of transportation and building electrification on the grid: A review of electrification projections and their effects on grid infrastructure, operation, and planning," en, *Current Sustainable/Renewable Energy Reports*, vol. 6, no. 4, pp. 169–176, Dec. 2019, ISSN: 2196-3010. DOI: 10.1007/s40518-019-00140-5.

[20] T. A. Short, *Electric Power Distribution Handbook*, Second Edition. CRC Press, 2014, ISBN: 9781466598652. DOI: 10.1201/b16747.

[21] S. Huang, Q. Wu, Z. Liu, and A. H. Nielsen, "Review of congestion management methods for distribution networks with high penetration of distributed energy resources," in *IEEE PES Innovative Smart Grid Technologies, Europe*, ISSN: 2165-4824, Oct. 2014, pp. 1–6. DOI: 10.1109/ISGTEurope.2014.7028811.

[22] G. S. Ledva, E. Vrettos, S. Mastellone, G. Andersson, and J. L. Mathieu, "Managing communication delays and model error in demand response for frequency regulation," *IEEE Transactions on Power Systems*, vol. 33, no. 2, pp. 1299–1308, Mar. 2018, ISSN: 1558-0679. DOI: 10.1109/TPWRS.2017.2725834.

[23] PG&E Electricity Tariff, "Electric Schedule BEV," PG&E Electricity Rate Schedule. [Online]. Available: https://www.pge.com/tariffs/assets/pdf/tariffbook/ELEC_SCHEDS_BEV.pdf.

[24] A. Madduri, M. Foudeh, P. Philips, and A. Gupta, "Advanced Strategies for Demand Flexibility Management and Customer DER Compensation," California Public Utilities Commission, Energy Division White Paper and Staff Proposal, Jun. 22, 2022. [Online]. Available: https://www.cpuc.ca.gov/-/media/cpuc-website/divisions/energy-division/documents/demand-response/demand-response-workshops/advanced-der---demand-flexibility-management/ed-white-paper---advanced-strategies-for-demand-flexibility-management.pdf.

[25] "2022 Assessment of Demand Response and Advanced Metering," Federal Energy Regulatory Commission, Staff Report, Dec. 2022. [Online]. Available: https://ferc.gov/media/2022-assessment-demand-response-and-advanced-metering.

[26] "Benchmarking Study of U.S. Regulated Utility Real Time Pricing Programs, Architecture and Design: Final Report," EPRI, Palo Alto, CA, 3002021204, 2021. [Online]. Available: https://www.epri.com/research/programs/072127/results/3002021204.

[27] S. Huang, Q. Wu, S. S. Oren, R. Li, and Z. Liu, "Distribution locational marginal pricing through quadratic programming for congestion management in distribution networks," *IEEE Transactions on Power Systems*, vol. 30, no. 4, pp. 2170–2178, Jul. 2015, ISSN: 1558-0679. DOI: 10.1109/TPWRS.2014.2359977.

[28] S. Huang, Q. Wu, M. Shahidehpour, and Z. liu, "Dynamic power tariff for congestion management in distribution networks," *IEEE Transactions on Smart Grid*, vol. 10, no. 2, pp. 2148–2157, Mar. 2019, ISSN: 1949-3061. DOI: 10.1109/TSG.2018.2790638.

[29] "Transportation electrification framework," Tech. Rep., Feb. 3, 2020. [Online]. Available: https://www.cpuc.ca.gov/WorkArea/DownloadAsset.aspx?id=6442463904.

[30] "Advanced Clean Fleets Regulation," California Air Resources Board. [Online]. Available: https://ww2.arb.ca.gov/our-work/programs/advanced-clean-fleets.

[31] "Workplace Charging for Plug-In Electric Vehicles," Alternative Fuels Data Center, Department of Energy. [Online]. Available: https://afdc.energy.gov/fuels/electricity_charging_workplace.html.

[32] "Managing Oversupply," California Independent System Operator (CAISO). [Online]. Available: http://www.caiso.com/informed/Pages/ManagingOversupply.aspx.

[33] J. Sherwood, A. Chitkara, D. Cross-Call, and B. Li, "A Review of Alternative Rate Designs: Industry experience with time-based and demand charge rates for mass-market customers," Rocky Mountain Institute, May 2016. [Online]. Available: https://rmi.org/wp-content/uploads/2017/04/A-Review-of-Alternative-Rate-Designs-2016.pdf.

[34] J. McLaren, N. Laws, K. Anderson, and S. Mullendore, "Identifying Potential Markets for Behind-the-Meter Battery Energy Storage: A Survey of U.S. Demand Charges," National Renewable Energy Laboratory, Report number: NREL/BR-6A20-68963, Aug. 2017. [Online]. Available: https://www.nrel.gov/docs/fy17osti/68963.pdf.

[35] "Business Electric Vehicle (EV) rate plans," Pacific Gas and Electric. [Online]. Available: https://www.pge.com/en_US/small-medium-business/energy-alternatives/clean-vehicles/ev-charge-network/electric-vehicle-rate-plans.page.

[36] "Decision approving application for pacific gas and electric company's commercial electric vehicle rates," Oct. 24, 2019.

[37] L. Huber and R. Bachmeier, "What netflix and amazon pricing tell us about rate design's future: Alexa, pull up my energy service subscription plan!" en, *Public Utilities Fortnightly*, Sep. 2018.

[38] H. Lo, S. Blumsack, P. Hines, and S. Meyn, "Electricity rates for the zero marginal cost grid," en, *The Electricity Journal*, vol. 32, no. 3, pp. 39–43, Apr. 1, 2019, ISSN: 1040-6190. DOI: 10.1016/j.tej.2019.02.010.

[39] A. Lambrecht, K. Seim, and B. Skiera, "Does uncertainty matter? consumer behavior under three-part tariffs," *Marketing Science*, vol. 26, no. 5, pp. 698–710, 2007, publisher: INFORMS, ISSN: 0732-2399.

[40] M. D. Grubb, "Selling to overconfident consumers," en, *American Economic Review*, vol. 99, no. 5, pp. 1770–1807, Dec. 2009, ISSN: 0002-8282. DOI: 10.1257/aer.99.5.1770.

[41] E. Ascarza, A. Lambrecht, and N. Vilcassim, "When talk is 'free': The effect of tariff structure on usage under two- and three-part tariffs," *Journal of Marketing Research (JMR)*, vol. 49, no. 6, pp. 882–899, Dec. 2012, publisher: American Marketing Association, ISSN: 00222437. DOI: 10.1509/jmr.10.0444.

[42] M. D. Grubb and M. Osborne, "Cellular service demand: Biased beliefs, learning, and bill shock," *The American Economic Review*, vol. 105, no. 1, pp. 234–271, 2015, publisher: American Economic Association, ISSN: 0002-8282.

[43] S. Borenstein, "The long-run efficiency of real-time electricity pricing," *The Energy Journal*, 2005. [Online]. Available: https://faculty.haas.berkeley.edu/borenste/download/EnJo05RTPsim.pdf.

[44] S. Borenstein, "Time-varying retail electricity prices: Theory and practice," *Electricity Deregulation*, 2009. [Online]. Available: https://faculty.haas.berkeley.edu/borenste/download/RTPchap05.pdf.

[45] A. Faruqui, "The ethics of dynamic pricing," en, *The Electricity Journal*, vol. 23, no. 6, pp. 13–27, Jul. 1, 2010, ISSN: 1040-6190. DOI: 10.1016/j.tej.2010.05.013.

[46] R. Hledik and A. Faruqui, "Competing perspectives on demand charges," en, *Public Utilities Fortnightly*, p. 6, Sep. 2016.

[47] R. Passey, N. Haghdadi, A. Bruce, and I. MacGill, "Designing more cost reflective electricity network tariffs with demand charges," en, *Energy Policy*, vol. 109, pp. 642–649, Oct. 1, 2017, ISSN: 0301-4215. DOI: 10.1016/j.enpol.2017.07.045.

[48] R. Hledik, "Rediscovering residential demand charges," en, *The Electricity Journal*, vol. 27, no. 7, pp. 82–96, Aug. 1, 2014, ISSN: 1040-6190. DOI: 10.1016/j.tej.2014.07.003.

[49] T. Lipman, D. Callaway, G. Fierro, *et al.*, "Open-source, open-architecture software platform for plug-in electric vehicle smart charging in california," en, California Energy Commission, CEC-500-2020-005, Mar. 2020. [Online]. Available: https://www.energy.ca.gov/publications/2020/open-source-open-architecture-software-platform-plug-electric-vehicle-smart.

[50] "Understanding the Grid Impacts of Plug-In Electric Vehicles (PEV): Phase 1 Study - Distribution Impact Case Studies," EPRI, Palo Alto, CA. 1024101., 2012.

[51] G. Montes and F. Katiraei, "Laboratory Testing and Field Measurement of Plug-in Electric Vehicle (PEV) Grid Impacts," California Energy Commission. Publication Number: CEC-500-2015-093, 2015.

[52] S. Powell, E. C. Kara, R. Sevlian, G. V. Cezar, S. Kiliccote, and R. Rajagopal, "Controlled workplace charging of electric vehicles: The impact of rate schedules on transformer aging," en, *Applied Energy*, vol. 276, p. 115 352, Oct. 15, 2020, ISSN: 0306-2619. DOI: 10.1016/j.apenergy.2020.115352.

[53] L. D. Smith and D. S. Kirschen, "Impacts of time-of-use rate changes on the electricity bills of commercial consumers," in *2021 IEEE Power & Energy Society General Meeting (PESGM)*, 2021, pp. 1–5. DOI: 10.1109/PESGM46819.2021.9638125.

[54] L. D. Smith and D. S. Kirschen, "Should storage-centric tariffs be extended to commercial flexible demand?" In *2022 IEEE Power & Energy Society General Meeting (PESGM)*, 2022, pp. 1–5. DOI: 10.1109/PESGM48719.2022.9916738.

[55] F. Daneshzand, P. J. Coker, B. Potter, and S. T. Smith, "Ev smart charging: How tariff selection influences grid stress and carbon reduction," *Applied Energy*, vol. 348, p. 121 482, 2023, ISSN: 0306-2619. DOI: https://doi.org/10.1016/j.apenergy.2023.121482.

[56] S. Elmallah, A. M. Brockway, and D. Callaway, "Can distribution grid infrastructure accommodate residential electrification and electric vehicle adoption in northern california?" en, *Environmental Research: Infrastructure and Sustainability*, vol. 2, no. 4, p. 045 005, Nov. 2022, ISSN: 2634-4505. DOI: 10.1088/2634-4505/ac949c.

[57] A. Jenn and J. Highleyman, "Distribution grid impacts of electric vehicles: A california case study," en, *iScience*, vol. 25, no. 1, p. 103 686, Jan. 2022, ISSN: 2589-0042. DOI: 10.1016/j.isci.2021.103686.

[58] PG&E Electricity Tariff, "Electric Schedule B-10," PG&E Electricity Rate Schedule. [Online]. Available: https://www.pge.com/tariffs/assets/pdf/tariffbook/ELEC_SCHEDS_B-10.pdf.

[59] PG&E Electricity Tariff, "Electric Schedule B-19," PG&E Electricity Rate Schedule. [Online]. Available: https://www.pge.com/tariffs/assets/pdf/tariffbook/ELEC_SCHEDS_B-19.pdf.

[60] J. Lazar, *Electricity Regulation In the US: A Guide*, en, Second Edition. Montpelier, VT: The Regulatory Assistance Project, 2016. [Online]. Available: http://www.raponline.org/knowledge-center/electricityregulation-%20in-the-us-a-guide-2.

[61] A. Faruqui, "Rate design 3.0: Future of rate design," eng, *Public Utilities Fortnightly*, vol. 156, no. 5, pp. 34–38, 2018, publisher-place: Arlington publisher: Public Utilities Reports, Inc, ISSN: 1078-5892.

[62] S. Borenstein and L. W. Davis, "The equity and efficiency of two-part tariffs in u.s. natural gas markets," en, Tech. Rep., Dec. 31, 2010, DOI: 10.3386/w16653. [Online]. Available: https://www.nber.org/papers/w16653.

[63] M. Deru, K. Field, D. Studer, *et al.*, "U.s. department of energy commercial reference building models of the national building stock," en, Tech. Rep., Feb. 1, 2011, DOI: 10.2172/1009264, NREL/TP–5500-46861, 1 009 264. [Online]. Available: http://www.osti.gov/servlets/purl/1009264-pitlfN/.

[64] "Governor Newsom Announces California Will Phase Out Gasoline-Powered Cars & Drastically Reduce Demand for Fossil Fuel in California's Fight Against Climate Change," State of California, Office of the Governor, Sep. 23, 2020. [Online]. Available: https://www.gov.ca.gov/2020/09/23/governor-newsom-announces-california-will-phase-out-gasoline-powered-cars-drastically-reduce-demand-for-fossil-fuel-in-californias-fight-against-climate-change/.

[65] S. Ong and N. Clark, "Commercial and Residential Hourly Load Profiles for all TMY3 Locations in the United States," National Renewable Energy Laboratory, Nov. 25, 2014. DOI: 10.25984/1788456. [Online]. Available: https://data.openei.org/submissions/153.

[66] E. Barreiro, "Night-time deliveries are the solution to urban delivery challenges," *Parcel and Postal Technology International*, Dec. 2020. [Online]. Available: https://www.parcelandpostaltechnologyinternational.com/features/night-time-deliveries-are-the-solution-to-urban-delivery-challenges.html.

[67] "2019 Chevrolet Bolt EV Specifications," Chevrolet. [Online]. Available: https://media.gm.com/media/us/en/chevrolet/vehicles/bolt-ev/2019.tab1.html.

[68] V. Vijayenthiran, "This is the electric van Rivian will build for Amazon," Motor Authority, Oct. 8, 2020. [Online]. Available: https://www.motorauthority.com/news/1129886_this-is-the-electric-van-rivian-will-build-for-amazon.

[69] ANSI C84.1, "American National Standard for Electric Power Systems and Equipment - Voltage Ratings (60 Hertz)," National Electrical Manufacturers Association, 2016.

[70] D. P. Chassin, K. Schneider, and C. Gerkensmeyer, "GridLAB-D: An open-source power systems modeling and simulation environment," ISSN: 2160-8563, Apr. 2008, pp. 1–5. DOI: 10.1109/TDC.2008.4517260.

[71] J. Mead, V. Donde, and J. Garnett (Pacific Gas and Electric Company), "Advanced Control Technologies for Distribution Grid Voltage and Stability with Electric Vehicles and Distributed Generation," California Energy Commission, Publication number: CEC-500-2015-046, 2014.

[72] R. Hendron and C. Engebrecht, "Building america house simulation protocols (revised)," en, Tech. Rep., Oct. 1, 2010, DOI: 10.2172/989422, NREL/TP–550-49246, DOE/GO-102010–3141, 989 422. [Online]. Available: http://www.osti.gov/servlets/purl/989422/.

[73] S. Wilcox and W. Marion, "Users manual for tmy3 data sets," en, Tech. Rep., May 2008. [Online]. Available: https://www.nrel.gov/docs/fy08osti/43156.pdf.

[74] W. Kersting, "Radial distribution test feeders," in *2001 IEEE Power Engineering Society Winter Meeting*, vol. 2, 2001, pp. 908–912. DOI: 10.1109/PESW.2001.916993.

[75] Resolution to adopt updates to the Avoided Cost Calculator for use in demand-side distributed energy resource cost-effectiveness analyses, California Public Utilities Commission, Resolution E-5228, Sep. 15, 2022. [Online]. Available: https://docs.cpuc.ca.gov/PublishedDocs/Published/G000/M496/K462/496462187.PDF.

[76] 2022 ACC Electric Model version 1b. [Online]. Available: https://www.cpuc.ca.gov/industries-and-topics/electrical-energy/demand-side-management/energy-efficiency/idsm.

[77] *MATLAB:R2020a*. Natick, Massachusetts: The Mathworks, Inc., 2020.

[78] J. Löfberg, "YALMIP: A Toolbox for Modeling and Optimization in MATLAB," Taipei, Taiwan, 2004.

[79] "Gurobi Optimizer," Gurobi Optimization, LLC, 2020. [Online]. Available: https://www.gurobi.com.

[80] P. Andrianesis, M. Caramanis, R. D. Masiello, R. D. Tabors, and S. Bahramirad, "Locational marginal value of distributed energy resources as non-wires alternatives," *IEEE Transactions on Smart Grid*, vol. 11, no. 1, pp. 270–280, Jan. 2020, event-title: IEEE Transactions on Smart Grid, ISSN: 1949-3061. DOI: 10.1109/TSG.2019.2921205.

[81] A. Dhar, "Optimal non-residential tou period analysis," Tech. Rep., Dec. 2, 2016.

[82] "Texas set to ban griddy-like electricity plans after blackouts," en, *Bloomberg.com*, Apr. 29, 2021. [Online]. Available: https://www.bloomberg.com/news/articles/2021-04-29/texas-set-to-ban-griddy-like-electricity-plans-after-blackouts.

[83] S. Borenstein, "The economics of fixed cost recovery by utilities," en, *The Electricity Journal*, vol. 29, no. 7, pp. 5–12, Sep. 1, 2016, ISSN: 1040-6190. DOI: 10.1016/j.tej.2016.07.013.

[84] W. B. Heredia, K. Chaudhari, A. Meintz, M. Jun, and S. Pless, "Evaluation of smart charging for electric vehicle-to-building integration: A case study," *Applied Energy*, vol. 266, p. 114 803, May 2020, ISSN: 0306-2619. DOI: 10.1016/j.apenergy.2020.114803.

[85] M. İnci, M. M. Savrun, and Ö. Çelik, "Integrating electric vehicles as virtual power plants: A comprehensive review on vehicle-to-grid (v2g) concepts, interface topologies, marketing and future prospects," en, *Journal of Energy Storage*, vol. 55, p. 105 579, Nov. 2022, ISSN: 2352-152X. DOI: 10.1016/j.est.2022.105579.

[86] "EV Chargers: How many do we need?" S&P Global Mobility, Jan. 2023. [Online]. Available: https://www.spglobal.com/mobility/en/research-analysis/ev-chargers-how-many-do-we-need.html.

[87] "Summary Report on EVs at Scale and the U.S. Electric Power System," U.S. DRIVE Grid Integration Team, Department of Energy, Nov. 2019. [Online]. Available: https://www.energy.gov/eere/vehicles/articles/summary-report-evs-scale-and-us-electric-power-system-2019.

[88] S. Sridhar, C. Holland, A. Singhal, *et al.*, "Distribution system planning for growth in residential electric vehicle adoption," in *2022 IEEE Power & Energy Society General Meeting (PESGM)*, Jul. 2022, pp. 1–5. DOI: 10.1109/PESGM48719.2022.9917240.

[89] R. Li, Q. Wu, and S. S. Oren, "Distribution locational marginal pricing for optimal electric vehicle charging management," *IEEE Transactions on Power Systems*, vol. 29, no. 1, pp. 203–211, Jan. 2014, ISSN: 1558-0679. DOI: 10.1109/TPWRS.2013.2278952.

[90] W. Wei, J. Wang, N. Li, and S. Mei, "Optimal power flow of radial networks and its variations: A sequential convex optimization approach," *IEEE Transactions on Smart Grid*, vol. 8, no. 6, pp. 2974–2987, Nov. 2017, ISSN: 1949-3061. DOI: 10.1109/TSG.2017.2684183.

[91] M. Nick, R. Cherkaoui, J.-Y. L. Boudec, and M. Paolone, "An exact convex formulation of the optimal power flow in radial distribution networks including transverse components," *IEEE Transactions on Automatic Control*, vol. 63, no. 3, pp. 682–697, Mar. 2018, ISSN: 1558-2523. DOI: 10.1109/TAC.2017.2722100.

[92] L. Bai, J. Wang, C. Wang, C. Chen, and F. Li, "Distribution locational marginal pricing (dlmp) for congestion management and voltage support," *IEEE Transactions on Power Systems*, vol. 33, no. 4, pp. 4061–4073, Jul. 2018, ISSN: 1558-0679. DOI: 10.1109/TPWRS.2017.2767632.

[93] P. Andrianesis, M. Caramanis, and N. Li, "Optimal distributed energy resource coordination: A decomposition method based on distribution locational marginal costs," *IEEE Transactions on Smart Grid*, vol. 13, no. 2, pp. 1200–1212, Mar. 2022, ISSN: 1949-3061. DOI: 10.1109/TSG.2021.3123284.

[94] A. Primadianto and C.-N. Lu, "A review on distribution system state estimation," *IEEE Transactions on Power Systems*, vol. 32, no. 5, pp. 3875–3883, Sep. 2017, ISSN: 1558-0679. DOI: 10.1109/TPWRS.2016.2632156.

[95] M. Lave, M. J. Reno, and J. Peppanen, "Distribution system parameter and topology estimation applied to resolve low-voltage circuits on three real distribution feeders," *IEEE Transactions on Sustainable Energy*, vol. 10, no. 3, pp. 1585–1592, Jul. 2019, ISSN: 1949-3037. DOI: 10.1109/TSTE.2019.2917679.

[96] W. Wang and N. Yu, "Estimate three-phase distribution line parameters with physics-informed graphical learning method," *IEEE Transactions on Power Systems*, vol. 37, no. 5, pp. 3577–3591, Sep. 2022, ISSN: 1558-0679. DOI: 10.1109/TPWRS.2021.3134952.

[97] C. Qin, B. Vyakaranam, P. Etingov, M. Venetos, and S. Backhaus, "Machine learning based network parameter estimation using ami data," in *2022 IEEE Power & Energy Society General Meeting (PESGM)*, Jul. 2022, pp. 1–5. DOI: 10.1109/PESGM48719.2022.9917034.

[98] D. B. Arnold, M. D. Sankur, M. Negrete-Pincetic, and D. S. Callaway, "Model-free optimal coordination of distributed energy resources for provisioning transmission-level services," *IEEE Transactions on Power Systems*, vol. 33, no. 1, pp. 817–828, Jan. 2018, ISSN: 1558-0679. DOI: 10.1109/TPWRS.2017.2707405.

[99] M. D. Sankur, R. Dobbe, A. von Meier, and D. B. Arnold, "Model-free optimal voltage phasor regulation in unbalanced distribution systems," *IEEE Transactions on Smart Grid*, vol. 11, no. 1, pp. 884–894, Jan. 2020, ISSN: 1949-3061. DOI: 10.1109/TSG.2019.2950875.

[100] Y. Liu, N. Zhang, Y. Wang, J. Yang, and C. Kang, "Data-driven power flow linearization: A regression approach," *IEEE Transactions on Smart Grid*, vol. 10, no. 3, pp. 2569–2580, May 2019, ISSN: 1949-3061. DOI: 10.1109/TSG.2018.2805169.

[101] H. Xu, A. D. Domínguez-García, V. V. Veeravalli, and P. W. Sauer, "Data-driven voltage regulation in radial power distribution systems," *IEEE Transactions on Power Systems*, vol. 35, no. 3, pp. 2133–2143, May 2020, ISSN: 1558-0679. DOI: 10.1109/TPWRS.2019.2948138.

[102] S. Nowak, Y. C. Chen, and L. Wang, "Measurement-based optimal DER dispatch with a recursively estimated sensitivity model," *IEEE Transactions on Power Systems*, vol. 35, no. 6, pp. 4792–4802, Nov. 2020, ISSN: 1558-0679. DOI: 10.1109/TPWRS.2020.2998097.

[103] S. Nowak, Y. C. Chen, and L. Wang, "Distributed measurement-based optimal der dispatch with estimated sensitivity models," *IEEE Transactions on Smart Grid*, vol. 13, no. 3, pp. 2197–2208, May 2022, ISSN: 1949-3061. DOI: 10.1109/TSG.2021.3139450.

[104] M. Baran and F. Wu, "Optimal sizing of capacitors placed on a radial distribution system," *IEEE Transactions on Power Delivery*, vol. 4, no. 1, pp. 735–743, Jan. 1989, ISSN: 1937-4208. DOI: 10.1109/61.19266.

[105] L. Gan and S. H. Low, "Convex relaxations and linear approximation for optimal power flow in multiphase radial networks," in *2014 Power Systems Computation Conference*, Aug. 2014, pp. 1–9. DOI: 10.1109/PSCC.2014.7038399.

[106] M. D. Sankur, R. Dobbe, E. Stewart, D. S. Callaway, and D. B. Arnold, "A linearized power flow model for optimization in unbalanced distribution systems," *arXiv:1606.04492 [math]*, Nov. 2016, arXiv: 1606.04492. [Online]. Available: http://arxiv.org/abs/1606.04492.

[107] D. K. Molzahn and I. A. Hiskens, "A survey of relaxations and approximations of the power flow equations," en, *Foundations and Trends® in Electric Energy Systems*, 2019, ISSN: 2332-6557, 2332-6565. DOI: 10.1561/3100000012. [Online]. Available: http://www.nowpublishers.com/article/Details/EES-012.

[108] R. Tibshirani, "Regression shrinkage and selection via the lasso," *Journal of the Royal Statistical Society. Series B (Methodological)*, vol. 58, no. 1, pp. 267–288, 1996, ISSN: 0035-9246.

[109] Y. Ding, S. Pineda, P. Nyeng, J. Østergaard, E. M. Larsen, and Q. Wu, "Real-time market concept architecture for ecogrid eu—a prototype for european smart grids," *IEEE Transactions on Smart Grid*, vol. 4, no. 4, pp. 2006–2016, Dec. 2013, ISSN: 1949-3061. DOI: 10.1109/TSG.2013.2258048.

[110] P. K. Phanivong and D. S. Callaway, "The impacts of retail tariff design on electric vehicle charging for commerical customers," *IEEE Transactions on Energy Markets, Policy, and Regulation*, In Review.

[111] T. Schittekatte, D. S. Mallapragada, P. L. Joskow, and R. Schmalensee, "Electricity retail rate design in a decarbonized economy: An analysis of time-of-use and critical peak pricing," National Bureau of Economic Research, Working Paper 30560, Oct. 2022. DOI: 10.3386/w30560. [Online]. Available: http://www.nber.org/papers/w30560.

[112] R. Ambrosio, "Transactive energy systems [viewpoint]," *IEEE Electrification Magazine*, vol. 4, no. 4, pp. 4–7, Dec. 2016, ISSN: 2325-5889. DOI: 10.1109/MELE.2016.2614234.

[113] H. Hao, C. D. Corbin, K. Kalsi, and R. G. Pratt, "Transactive control of commercial buildings for demand response," *IEEE Transactions on Power Systems*, vol. 32, no. 1, pp. 774–783, Jan. 2017, ISSN: 1558-0679. DOI: 10.1109/TPWRS.2016.2559485.

[114] J. Li, C. Zhang, Z. Xu, J. Wang, J. Zhao, and Y.-J. A. Zhang, "Distributed transactive energy trading framework in distribution networks," *IEEE Transactions on Power Systems*, vol. 33, no. 6, pp. 7215–7227, Nov. 2018, ISSN: 1558-0679. DOI: 10.1109/TPWRS.2018.2854649.

[115] S. Nizami, W. Tushar, M. J. Hossain, C. Yuen, T. Saha, and H. V. Poor, "Transactive energy for low voltage residential networks: A review," *Applied Energy*, vol. 323, p. 119 556, Oct. 1, 2022, ISSN: 0306-2619. DOI: 10.1016/j.apenergy.2022.119556. [Online]. Available: https://www.sciencedirect.com/science/article/pii/S0306261922008674.

[116] M. H. Ullah and J.-D. Park, "Transactive energy market operation through coordinated tso-dsos-ders interactions," *IEEE Transactions on Power Systems*, vol. 38, no. 2, pp. 1976–1988, Mar. 2023, ISSN: 1558-0679. DOI: 10.1109/TPWRS.2022.3212065.

[117] P. Sotkiewicz and J. Vignolo, "Nodal pricing for distribution networks: Efficient pricing for efficiency enhancing DG," *IEEE Transactions on Power Systems*, vol. 21, no. 2, pp. 1013–1014, May 2006, ISSN: 1558-0679. DOI: 10.1109/TPWRS.2006.873006.

[118] M. Caramanis, E. Ntakou, W. W. Hogan, A. Chakrabortty, and J. Schoene, "Co-optimization of power and reserves in dynamic t&d power markets with nondispatchable renewable generation and distributed energy resources," *Proceedings of the IEEE*, vol. 104, no. 4, pp. 807–836, Apr. 2016, ISSN: 1558-2256. DOI: 10.1109/JPROC.2016.2520758.

[119] S. Mohammadi, M. R. Hesamzadeh, and D. W. Bunn, "Distribution locational marginal pricing (DLMP) for unbalanced three-phase networks," *IEEE Transactions on Power Systems*, vol. 37, no. 5, pp. 3443–3457, Sep. 2022, ISSN: 1558-0679. DOI: 10.1109/TPWRS.2021.3138798.

[120] Z. Zhao, Y. Liu, L. Guo, L. Bai, Z. Wang, and C. Wang, "Distribution locational marginal pricing under uncertainty considering coordination of distribution and wholesale markets," *IEEE Transactions on Smart Grid*, vol. 14, no. 2, pp. 1590–1606, Mar. 2023, ISSN: 1949-3061. DOI: 10.1109/TSG.2022.3200704.

[121] S. Huang and Q. Wu, "Dynamic subsidy method for congestion management in distribution networks," *IEEE Transactions on Smart Grid*, vol. 9, no. 3, pp. 2140–2151, May 2018, ISSN: 1949-3061. DOI: 10.1109/TSG.2016.2607720.

[122] S. Fattaheian-Dehkordi, M. Tavakkoli, A. Abbaspour, M. Fotuhi-Firuzabad, and M. Lehtonen, "An incentive-based mechanism to alleviate active power congestion in a multi-agent distribution system," *IEEE Transactions on Smart Grid*, vol. 12, no. 3, pp. 1978–1988, May 2021, ISSN: 1949-3061. DOI: 10.1109/TSG.2020.3037560.

[123] S. Lv, S. Chen, and Z. Wei, "Coordinating urban power-traffic networks: A subsidy-based nash–stackelberg–nash game model," *IEEE Transactions on Industrial Informatics*, vol. 19, no. 2, pp. 1778–1790, Feb. 2023, ISSN: 1941-0050. DOI: 10.1109/TII.2022.3182124.

[124] B. F. Gerke, M. Stübs, S. Murthy, *et al.*, "Potential bill impacts of dynamic electricity pricing on California utility customers," Lawrence Berkeley National Laboratory, Dec. 2022. [Online]. Available: https://escholarship.org/uc/item/2wj199mq.

[125] R.21-06-017, "Order Instituting Rulemaking to Modernize the Electric Grid for a High Distributed Energy Resources Future," California Public Utilities Comission, Jan. 2017.

[126] Form EIA-861, "Annual Electric Power Industry Report," U.S. Energy Information Administration, 2021. [Online]. Available: https://www.eia.gov/electricity/data/eia861/.

[127] Quadrennial Energy Review, "Transforming the Nation's Electricity System: The Second Installment of the QER," U.S. Department of Energy, Jan. 2017. [Online]. Available: https://www.energy.gov/policy/articles/quadrennial-energy-review-second-installment.

[128] J. Neubauer and M. Simpson, "Deployment of behind-the-meter energy storage for demand charge reduction," NREL, NREL/TP-5400-63162, Jan. 2015. DOI: 10.2172/1168774. [Online]. Available: https://www.osti.gov/biblio/1168774.

[129] K. Schneider, P. Phanivong, and J.-S. Lacroix, "IEEE 342-node low voltage networked test system," in *2014 IEEE PES General Meeting — Conference & Exposition*, 2014, pp. 1–5. DOI: 10.1109/PESGM.2014.6939794.

Appendix A

Chapter 1 Retail Tariffs

The following are the costs for secondary connected customers from the B-10 [58], B-19 [59], and BEV [23] tariffs used in this study. Dollar amounts and charges were taken from PG&E's electric rate schedule on December 1st, 2020. The tables on the left are the power charges associated with each tariff, while the tables on the right are the energy charges. Customers below 100 kW in EV demand are assigned to the BEV-1 rate, while customers over 100 kW are assigned the BEV-2-S rate. Customers with exactly 100 kW of EV load can choose which BEV rate they want.

B-10 Demand Charge	
Season	$/kW
Summer	13.42
Winter	13.42

B-19 Demand Charge	
Season	$/kW
Summer Peak	25.58
Summer Partial Peak	5.23
Summer Max Demand	21.08
Winter Peak	1.79
Winter Max Demand	21.08

BEV-2-S Subscription	
Block size	50 kW
Subscription charge	$95.56 / block
Overage fee	$3.82 / kW

B-10 Energy Charge	
Season	$/kWh
Summer Peak	0.26824
Summer Partial Peak	0.26824
Summer Off-Peak	0.17399
Winter Peak	0.19198
Winter Off-Peak	0.15650
Winter Super Off-Peak	0.12016

B-19 Energy Charge	
Season	$/kWh
Summer Peak	0.16285
Summer Partial Peak	0.13284
Summer Off-Peak	0.11162
Winter Peak	0.14379
Winter Off-Peak	0.11154
Winter Super Off-Peak	0.06826

BEV-1-S Subscription	
Block size	10 kW
Subscription charge	\$12.41 / block
Overage fee	\$2.48 / kW

TEST-EV-2-S Demand Charge	
Season	\$/kW
Summer	1.9112
Winter	1.9112

TEST-EV-2-1 Demand Charge	
Season	\$/kW
Summer	1.2410
Winter	1.2410

BEV/TEST-EV-2-S Energy Charge	
TOU period	\$/kWh
Peak	0.34630
Off-Peak	0.12740
Super Off-Peak	0.10413

BEV/TEST-EV-1-S Energy Charge	
TOU Period	\$/kWh
Peak	0.32431
Off-Peak	0.13230
Super Off-Peak	0.10564